Alma Mater Studiorum · Università di Bologna

School of Science
Department of Physics and Astronomy
Master Degree in Physics

Digital quantum simulations of Yang-Mills lattice gauge theories

Supervisore:
Prof. Elisa Ercolessi

Co-Supervisor:
Dott. Sunny Pradhan

Submitted by:
Luca Lumia

Academic Year 2019/2020

Sommario

I metodi di calcolo tradizionali per le teorie di gauge su reticolo risultano problematici in regioni di diagrammi di fase a grandi valori del potenziale chimico o quando sono utilizzate per riprodurre la dinamica in tempo reale di un modello. Tali problemi possono essere evitati da simulazioni quantistiche delle teorie di gauge su reticolo, le quali stanno diventando sempre più riproducibili sperimentalmente, grazie ai recenti progressi tecnologici. In questa tesi formuliamo una versione delle teorie di Yang-Mills su reticolo appropriata per risolvere il problema della dimensione infinita dello spazio di Hilbert associato ai bosoni di gauge. Questa formulazione è adatta per essere riprodotta in un simulatore quantistico e ne implementiamo una completa simulazione su un computer quantistico digitale, sfruttando il framework Qiskit. In questa simulazione misuriamo le energie del ground state e i valori di aspettazione di alcuni Wilson loop al variare dell'accoppiamento della teoria, per studiarne le fasi e valutare la prestazione dei metodi usati.

Abstract

The standard computational tools for lattice gauge theories encounter problems in regions of phase diagrams with large chemical potentials or when they are used to reproduce the real-time dynamics of a model. These issues can be avoided by performing quantum simulations of lattice gauge theories, which are becoming experimentally realizable thanks to recent technological advancements. In this thesis we formulate on a lattice a suitable version of Yang-Mills theories that solves the problem of the infinite dimensionality of the Hilbert space associated with the gauge bosons. This model is suited to be realized on a quantum simulator and we implement the full simulation on a digital quantum computer within the Qiskit framework. The ground state energy and the expectation values of some Wilson loops have been measured at several values of the coupling of the theory, in order to study its phases and to test the performance of our methods.

Contents

Introduction

The concept of gauge symmetry lies at the heart of our current understanding of many fundamental phenomena in nature, touching fields from condensed matter to high-energy physics. It was first introduced as an intrinsic redundancy in the description of the classical electromagnetic field through its potential $A^\mu = (\phi, \vec{A})$: different potential functions $\phi(x)$, $\vec{A}(x)$ generate to the same electric and magnetic fields $\vec{E}(x)$, $\vec{B}(x)$ if they are related by a particular relation called "gauge transformation". Hence, we have the freedom to choose different configurations that describe the same physical state. Gauge freedom is not an actual symmetry, nevertheless it strongly constraints the structure and the properties that the theory should have. For instance, in QED it has the key role of forbidding unitarity violations [65].

The gauge symmetry of QED can be constructed by promoting the global U(1) electric charge symmetry to a local one. Similarly also the other two fundamental interactions of the Standard Model of particle physics are formulated as Yang-Mills gauge theories, which can be seen as a generalization of QED to arbitrary non-abelian gauge groups, and gauge symmetries play an essential role also in the Higgs mechanism, which generates the mass of all fundamental particles. Besides the electroweak and strong interactions, also gravity can be thought of as a gauge theory, since when it is made local, the global Poincaré symmetry can lead to the diffeomorphism invariance typical of general relativity, even though some subtleties are involved [11].

Stepping aside from high-energy physics, gauge symmetries are important also in condensed matter models [29]. The simplest way to introduce them is to modify the Ising model in such a way that its $\mathbb{Z}_2$ symmetry becomes local, leading to a very interesting model that cannot magnetize but still shows a phase transition. Gauge symmetry is useful also to describe phenomena like superconductivity (whose explanation inspired the development of the Higgs mechanism), or to characterize topological phases like fractional quantum Hall effect states, which can be described as a Chern-Simons theory. In spite of their very constrained formulation, the behaviour of gauge theories is extremely rich, giving shape to the multi-colored variety of phenomena

that we observe in nature. This makes it extremely challenging to solve their dynamics from first principles and several approaches were tried. In continuum quantum field theory, interacting models are typically treated with perturbative expansions on the coupling constant, only meaningful as long as the coupling constant is small. However, it is well known that the physical couplings are not actually constants, but they run with the energy scale of the process under consideration. For Quantum Electrodynamics, the coupling constant (electric charge) is weak for low energies and the large scale electromagnetic phenomena that we observe can be treated with perturbation theory. Increasing the energy, the coupling constant grows and this effect can be interpreted in a very clear way as the screening of the electric charge due to a progressive production of virtual electron-positron dipoles. This interpretation is sensible until the energy scale of $\Lambda_{\text{QED}} = 10^{286}$ eV where QED has a Landau pole and the coupling constant diverges, meaning that perturbation theory has to break down at a scale $\Lambda < \Lambda_{\text{QED}}$ [65]. Nonetheless, for QED the Landau pole is not an actual phenomenological problem, since 10^{286} eV is a huge scale, far larger than Planck's mass, and we already expect something else to appear and change the physics before.

The same cannot be said for Quantum Chromodynamics, the SU(3) gauge theory describing the strong interaction between quarks. QCD is *asymptotically free* and the strong coupling vanishes when the energy scale is pushed to infinity; therefore, for small distance/high-energy processes, the coupling constant is finite but small and calculations can be done using perturbation theory. Instead, low energy QCD is characterized by a large coupling constant which diverges at a scale $\Lambda_{\text{QCD}} \approx 300$ MeV [65]. Unlike for QED, this is now a matter of concern: perturbation theory loses its meaning roughly at the scale of the mass of the hadrons, signaling that the degrees of freedom that we use to formulate small distance QCD probably are not best suited to describe large distance strong phenomena. One possibility could be to use effective field theories where the hadrons become the fundamental degrees of freedom, otherwise, we should find alternative non-perturbative approaches.

QCD is formulated in terms of quarks. The success of the quark constituent picture of hadrons, both for the interpretation of the systematics of their static properties and for the description of their dynamics, has always made very difficult to believe that quarks do not exist, even though they have never been seen as isolated fractional charges. This suggests the existence of a *confinement* mechanism, that prevents quarks from appearing as separate particles in a final state. Whatever non-perturbative approach we choose, we should take into account that confinement has to be explained somehow. The most important non-perturbative approach is probably lattice QCD, first studied by Ken Wilson in 1974 [90], in an paper where he

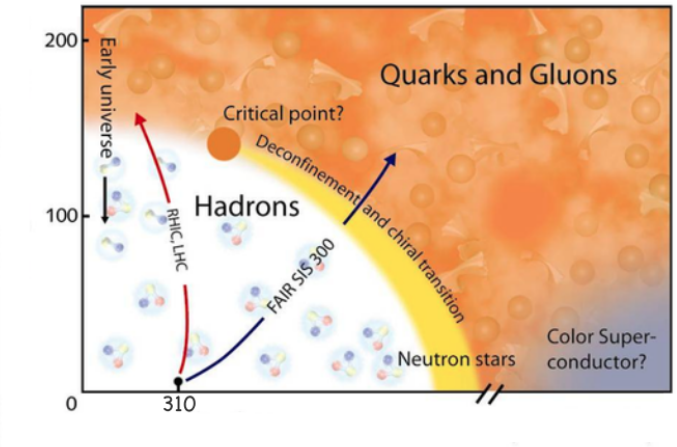

Figure 1: The proposed form of the QCD phase diagram, drawn with respect to the chemical potential on the x axis and the temperature on the y axis, both in MeV. This image is taken from [72].

introduced a hypercubic spacetime lattice as a gauge-invariant regulator of the ultraviolet divergences, with quark fields living on the lattice sites and gluons residing on the links between the nearest neighbour sites. If we work on a Wick-rotated euclidean spacetime and if we discretize it by formulating the theory on a lattice, QCD becomes a typical model of statistical mechanics. Wilson showed analytically that lattice QCD exhibits confinement in its strong coupling limit, suggesting also that it should be a phase transition what distinguishes the confined and deconfined regions of QCD. In addition to that, thanks to the connection between lattice gauge theories and statistical mechanics, particle physics profited enormously from the numerical methods used for condensed matter systems, such as Monte Carlo algorithms [32]. This approach made numerically accessible to classical computers several important quantities, such as masses and matrix elements of baryons and mesons, or properties at thermal equilibrium of the quark-gluon plasma, which is a phase of QCD that we expect to take place at sufficiently high temperatures and large values of the chemical potential.

The phase structure of QCD is not completely understood yet, either theoretically or experimentally, but it is suspected to resemble the phase diagram reported in Fig. 1. Close to the origin of the (T, μ) plane, we expect a *hadronic phase*, where quarks are confined and the relevant degrees of freedom are the hadrons. Increasing the temperatures, while keeping low values of the chemical potentials, we expect to get a gas of hadrons until we enter the *quark-gluon plasma* phase, where the relevant degrees of freedom

are well-separated deconfined quarks, antiquarks and gluons, forming the so-called "quark matter". Another form of quark matter is present in the *colour-flavour locked* phase, expected at ultra high-density regions, where quarks should show a colour-superconducting behaviour. Regions with high temperatures and small densities can be explored with high-energy hadron collisions, such as the ones studied with the ALICE experiment at LHC, whereas regions with high densities and lower temperatures might correspond to the phases of matter contained in the core of neutron stars. We expect the hadronic-confined and the quark matter-deconfined phases to be separated by a critical line along which there is the spontaneous symmetry breaking of the chiral symmetry. In the hadronic phase the chiral symmetry should break, because an unbroken (although approximate, since the quarks u and d are not exactly massless) symmetry is not compatible with the huge mass difference that we measure between parity partners such as the nucleon N with $m_N = 940$ MeV and N^* with $m_{N^*} = 1535$ MeV [32].

Monte Carlo calculations led to great results, but they are not able to explore the whole QCD phase diagram, since at high density regions the large values of the chemical potential cause the famous *sign problem*. We are typically interested in computing sums over configurations of the form

$$\langle A \rangle = \frac{\int \mathscr{D}\phi \; A(\phi)\, e^{-S(\phi)}}{\int \mathscr{D}\phi \; e^{-S(\phi)}} \,,$$

where A is some observable and ϕ a generic variable encoding the configuration. Sweeping over the whole configuration space with $\mathscr{D}\phi$ would be a computationally intensive operation and usually one relies on Monte Carlo importance sampling methods [1]: as long as the measure e^{-S} is positive definite, it can be interpreted as a probability distribution and we can simplifying the sum by considering only the most relevant contributions. However, this is the situation only at $\mu = 0$, since when a chemical potential is added the euclidean action becomes in general a complex number, which can be highly oscillating. In this regime, importance sampling algorithms fail because e^{-S} cannot be interpreted as a probability and, in general, the near-cancellations of positive and negative contributions to the integral introduce large errors in numerical methods. In addition to that, trying to reproduce the real-time dynamics has a similar kind of bottleneck, so that also out of equilibrium properties are hard to obtain using this approach [64].

The same issues arise in condensed matter systems and researchers started to study different approaches to tackle them. However it has been shown [87] that a general solution of the sign problem is *NP-hard*, meaning that any other NP problem can be mapped into it, so that a polynomial solution of

the sign problem would automatically provide a polynomial solution for all NP problems, therefore implying that P=NP. This is clearly a difficult task, so the attention was drawn by different methods and some of them were borrowed from the field of quantum information. The idea is to simulate quantum models with algorithms specifically tailored to encode the quantum properties of the system under attention. They usually require the theory to be formulated in the hamiltonian formalism (which is automatically free of the aforementioned sign problems) and, given an appropriate initial state $|\psi(0)\rangle$, they aim to simulate its time evolution $|\psi(t)\rangle = e^{-iHt}|\psi(0)\rangle$. However, when implemented on a classical computer, they meet the problem of the explosion of the dimension of the Hilbert space. A quantum system of 40 spins $|s = \pm 1/2\rangle$ has 2^{40} independent states and its hamiltonian will be represented by a $2^{40} \times 2^{40}$ matrix, which occupies 4 TB of memory by itself. Being the growth exponential, small increases of the number of lattice sites are enough to exceed the computational capabilities of even the most powerful supercomputers. Currently, the most common approach aims to optimize the computation on a classical computer, for instance by using particularly efficient algorithms like the DMRG (density matrix renormalization group) [8], or by exploiting the symmetries of the model to restrict its dynamics (and consequently the computation) to the physical Hilbert space, using e.g. a tensor network representation [57] of the gauge-invariant states.

A natural solution to this problem was proposed by Richard Feynman in 1982 [24], who suggested that we should use a *quantum simulator* to reproduce the behaviour of another quantum system, since only a truly quantum device might be able to encode all the quantum properties of the system under interest. Another advantage of quantum simulations is that many standard proposal using the DMRG and tensor networks are suited for 1d models and their generalization in other dimensions is far form trivial, whereas in principle the simulation approach can be employed in any dimension.

Today we have reached the technology sufficient to realize such quantum simulators: there are condensed matter systems, such as ultra-cold matter on optical lattices, superconducting qubits, nuclear spins or photon systems, whose interactions can be engineered with the freedom sufficient to represent wide classes of hamiltonians. The recent technological advancements fueled a vigorous interest on the topic and several projects have been proposed and realized by pioneering experiments with analog simulators. For instance, ultra-cold Fermi gases in optical superlattices can be used as quantum simulators of relativistic fermions on a D=3+1 lattice, allowing to realize a simulation of a 3d topological insulator [10] or to reproduce fractional quantum Hall states and non abelian anyons [35]. Cold atoms may be used to test also exactly solvable theories like the Thirring model or the Gross-Noveau model, that

can be used as a benchmark to demonstrate the ability of these simulators to reproduce important dynamical phenomena [15]. Another example is [93], where cold atoms are used to enforce gauge symmetry by taking advantage of the angular momentum conservation. These are only a few of many recent works of the field [8]: quantum simulations are becoming increasingly feasible and the number of proposals is growing. One could also try to encode the dynamics of a condensed matter system on digital quantum computers, which are still at a first development stage, but they are experiencing extremely fast improvements. Quantum computers are supposed to be universal, meaning that they have the potential of being able to reproduce the dynamics of any quantum system through purely digital methods.

The present thesis fits into this context, aiming to study a general method to simulate lattice gauge theories on a digital quantum computer and to implement a simple example. The simulation of lattice gauge theories using digital quantum computers is a young field of research and there are only a few studies in this direction, such as [21, 54, 56, 77]. Therefore this thesis is not meant to observe new physics, but rather our aim is to make a preliminary analysis of the performances of the methods we propose and to find out how to improve them, which is relevant since their generality suggests that one day they might be used to simulate any lattice gauge theory. We shall start by quickly discussing in Chapter 1 Yang-Mills theories in the continuum, putting our emphasis on the objects of primary importance when the theory is placed on a lattice. The general construction of a lattice gauge theory is explained both in the path integral formalism and in the hamiltonian formalism, which is crucial for the implementation of the theory on a quantum simulator. In Chapter 2 we move to the description of the general structure of quantum simulations and the problems that can be met when implementing one as well as some common approaches used to overcome them, before focusing on the finite group approximation for the rest of the thesis. Chapter 3 describes a possible definition of a hamitonian for a finite group lattice theory, relying on the mathematical structure of the well established theory for continuous gauge groups, and presents a quantum algorithm able to simulate the corresponding time evolution for an arbitrary gauge group. Finally we focus on $\mathbb{Z}_n$ lattice gauge theories, outlining their general behaviour in Chapter 4 and describing in Chapter 5 the implementation of our simulation of a pure $\mathbb{Z}_2$ model as well as its results.

CHAPTER I.

Yang-Mills theory on a lattice

The Standard Model of particle physics is based upon the formulation of gauge theories first given by Chen Nin Yang and Robert Mills in 1954 [?], who extended the local U(1) symmetry of QED to the non abelian group SU(2) in an attempt to describe the strong interactions in atomic nuclei as a consequence of a local isospin symmetry. Their work can be directly generalized to any non abelian group, allowing to formulate the $\mathrm{SU(2)_L}$ and $\mathrm{SU(3)_C}$ theories that describe weak and strong interactions. Quantum field theories are formulated in terms of continuous fields on a continuous spacetime, but if we want to reproduce them on any kind of computer, classical or quantum, we ought to discretize them, since computers have finite memory resources and an infinite amount of information cannot be represented. In this way, we get to a theory defined on a discrete lattice, ideally large but still finite. Lattice gauge theories, and in particular lattice QCD, were one of the first non perturbative approaches introduced to study properties such as quark confinement. This chapter aims at introducing lattice Yang-Mills theory and more specifically their hamiltonian formulation, which is fundamental for quantum simulations. We start by describing the continuum Yang-Mills theory, in order to set the notation and to underline some key points and then we give the standard path integral description of lattice gauge theories, before moving on to their hamiltonian formulation.

1.1 Continuum Yang-Mills theory

QED describes the interactions between a charged Dirac spinor ψ and the electromagnetic field A_μ where the interaction term is given by the minimal coupling, which can be interpreted in a geometrical setting by introducing the U(1) covariant derivative $D_\mu = \partial_\mu - iA_\mu$ [65]. A similar theory can be

constructed with different matter fields, such as complex scalars. Yang-Mills theories are defined by the choice of the gauge group G, usually supposed to be a compact Lie group, and by the choice of the matter fields plus the representation of G they belong to. Keeping in mind the example of QCD, we take G = SU(N) and matter made of Dirac spinors in the fundamental representation. The gauge fields A_μ are elements of the Lie algebra $\mathfrak{g} = \mathfrak{su}(\mathrm{N})$ and can be expanded as $A_\mu = A^a_\mu T_a$, if we introduce a set $\{T_a\}$, $a = 1, \ldots, \dim \mathrm{G}$ of hermitian generators of $\mathfrak{su}(\mathrm{N})$, usually chosen to satisfy

$$[T_a, T_b] = i\, f_{abc} T_c \tag{1.1}$$

$$\mathrm{tr}\,(T_a T_b) = \frac{1}{2}\delta_{ab}\,, \tag{1.2}$$

where f_{abc} are the completely anti-symmetric structure constants of SU(N). In these formulas we are employing Einstein's summation convention over repeated indices. If we take the Minkowski metric with signature $(+, -, \ldots, -)$, the action of the free matter field in $D = d + 1$ dimensions is

$$S_0[\psi, \bar{\psi}] = \int d^{d+1}x \;\; \bar{\psi}(i\partial\!\!\!/ - m)\psi \tag{1.3}$$

and it is invariant under global transformations $\psi(x) \mapsto g\,\psi(x)$, where g is any element of the gauge group SU(N). The symmetry can be promoted to local if we introduce the gauge field A_μ, interacting with the matter field ψ according to the *Yang-Mills action*

$$S_{YM}[A, \psi, \bar{\psi}] = \int d^{d+1}x \;\; \bar{\psi}(iD\!\!\!/ - m)\psi - \frac{1}{2g^2}\mathrm{tr}\,(F_{\mu\nu}F^{\mu\nu})\;, \tag{1.4}$$

where the covariant derivative is $D_\mu\psi = \partial_\mu\psi - iA_\mu\psi$ and the associated curvature tensor, also called field strength tensor, is

$$F_{\mu\nu} = i\,[D_\mu, D_\nu] = \partial_\mu A_\nu - \partial_\nu A_\mu - i\,[A_\mu, A_\nu] = F^a_{\mu\nu} T_a\,. \tag{1.5}$$

The symmetry is local, i.e. if we define a function $g(x) : \mathcal{M} \to \mathrm{SU(N)}$ on the spacetime $\mathcal{M}$, the simultaneous transformations

$$\psi(x) \;\mapsto\; g(x)\psi(x) \tag{1.6}$$

$$A_\mu(x) \;\mapsto\; g(x)A_\mu(x)g(x)^{-1} + ig(x)\partial_\mu g(x)^{-1} \tag{1.7}$$

leave S_{YM} invariant, as $D_\mu\psi(x) \to g(x)D_\mu\psi(x)$ and $F_{\mu\nu} \mapsto g(x)F_{\mu\nu}g(x)^{-1}$ so that, thanks to the ciclicity of the trace, $S_{YM} \mapsto S_{YM}^{'} = S_{YM}$. One should keep in mind that we are being a little sloppy here: since the group elements do not act directly on ψ but only through the chosen representation

ρ, we should have written $\rho(g(x))\,\psi(x)$. For instance, if the matter field is ϕ, belonging to the adjoint representation, the covariant derivative becomes $D_\mu\phi = \partial_\mu\phi - i[A_\mu, \phi]$. An equivalent formulation can be given by rescaling $A_\mu \to \tilde{A}_\mu = A_\mu/g$, so that $D_\mu = \partial_\mu - ig\tilde{A}_\mu$ and $\tilde{F}_{\mu\nu} = F_{\mu\nu}/g = \partial_\mu\tilde{A}_\nu - \partial_\nu\tilde{A}_\mu - ig\,[\tilde{A}_\mu, \tilde{A}_\nu]$; the kinetic term for $\tilde{A}_\mu$ becomes $-1/2g^2\,\mathrm{tr}\,F_{\mu\nu}F^{\mu\nu} = -1/2\,\mathrm{tr}\,\tilde{F}_{\mu\nu}\tilde{F}^{\mu\nu}$. In the following developments it will be convenient to split $F_{\mu\nu}$ into the chromoelectric field $E^i = F^{0i}$, $E_i = E_i^a\,T_a$ and into the chromomagnetic field $B^i = -\frac{1}{2}\epsilon^{ijk}F_{jk}$, $B_i = B_i^a T_a$. $\vec{E}$ and $\vec{B}$ are 3d objects so we take $E^i = E_i$, $B^i = B_i$ even though $A^i = -A_i$. The quantization of the theory is commonly performed in the path integral formalism, where

$$Z = \int \mathscr{D}A\mathscr{D}\bar{\psi}\mathscr{D}\psi \;\; e^{\,i\,S[A,\psi,\bar{\psi}]} \tag{1.8}$$

is the naive path integral. In the continuum formulation it is divergent as a result of the integration on the infinite redundant degrees of freedom [65] and it has to be taken care of using the Faddeev-Popov procedure and BRST quantization ⚠. On a lattice instead, the gauge redundancy does not pose a threat to the finiteness of Z [58], since the integral will be performed on the elements of the gauge group, which is compact, in place of the elements A_μ of the Lie algebra, that is an unbounded vector space.

This was a recap of the formulation of Yang-Mills theories on Minkowksi spacetime, however, lattice theories are often formulated on a euclidean spacetime. There are mainly two reasons for choosing to do so. One is that the Feynman's weight e^{iS} is mapped to a Boltzmann's weight e^{-S_E}, whose damped behaviour is easier to handle than the oscillations of e^{iS} and allows to exploit the traditional Monte Carlo methods. The second reason is that minkowskian quantum field theories have to be Lorentz invariant, but the non-compactness of SO(1,3) causes the residual symmetry to lose any remnant of the boosts [86]. Instead, SO(4) is a compact group and this symmetry of the euclidean theories leaves a well behaved discrete symmetry subgroup after the reduction of the continuous spacetime to a lattice.

In order to get the euclidean formulation, we have to analytically extend x^0 to imaginary times. The usual Wick rotation $x^0 \to -ix^D$ implies that a minkowskian action S_M transforms according to

$$i\,S_M \;\longrightarrow\; -S_E \;, \tag{1.9}$$

where the euclidean action S_E represents the energy of the system. If we consider e.g. D=4, since $d^4x_M \equiv dx^0 d^3x \to -i\,dx^4 d^3x \equiv -i\,d^4x_E$ we get

$$S_E = \int d^4x_E \; \mathscr{L}_E \tag{1.10}$$

$$i\, S_M = i \int d^4x_M \; \mathscr{L}_M \;\longrightarrow\; \int d^4x_E \; \mathscr{L}_M = -S_E \tag{1.11}$$

and we can identify the euclidean lagrangian with $\mathscr{L}_M \to -\mathscr{L}_E$. A vector field is supposed to transform consistently with $\partial/\partial x^\mu_M$, so the time component of the euclidean vector field A^E_μ is defined as $A^M_0 \to i\, A^E_4$. Substituting it into the definition of the field strength tensor, we get $F^M_{0k} \to i\, F^E_{4k}$, so that the gauge part of the lagrangian transforms as

$$\mathscr{L}_M \supset -\frac{1}{2g^2}\mathrm{tr}\,(F^M_{\mu\nu}F^{\mu\nu}_M) \;\longrightarrow\; -\frac{1}{2g^2}\mathrm{tr}\,(F^E_{\mu\nu}F^{\mu\nu}_E) \subset -\mathscr{L}_E\,. \tag{1.12}$$

Of course the euclidean objects do not distinguish between up and down indices and we have raised them only for aesthetic reasons. The matter part of the lagrangian contains spinors and we have to make use of euclidean Dirac matrices, which satisfy a euclidean Clifford algebra

$$\{\gamma^\mu_E, \gamma^\nu_E\} = 2\delta^{\mu\nu}\,. \tag{1.13}$$

Since $\mathscr{L}_M \supset \bar\psi(i\gamma^\mu_M\partial_\mu + \gamma^\mu_M A^M_\mu - m)\psi$ and $i\gamma^0_M\partial_0 \to -\gamma^0_M\partial_4$, we choose

$$\gamma^4_E = \gamma^0_M\;,\;\; \gamma^k_E = i\,\gamma^k_M\,, \tag{1.14}$$

so that $i\,\gamma^\mu_M\partial_\mu \to -\gamma^\mu_E\partial_\mu$ and $i\gamma^\mu_M \to i\,\gamma^\mu_E A^E_\mu$ and together they yield

$$\mathscr{L}_M \supset \bar\psi(i\gamma^\mu_M\partial_\mu + \gamma^\mu_M A^M_\mu - m)\psi \;\longrightarrow\; -\bar\psi(\gamma^\mu_E\partial_\mu - i\gamma^\mu_E A^E_\mu + m)\psi. \tag{1.15}$$

Then, if we set $D^E_\mu = \partial_\mu - iA^E_\mu$ and if we recall that $\mathscr{L}_M \to -\mathscr{L}_E$, the euclidean Yang-Mills lagrangian can be identified with

$$\mathscr{L}_E \;=\; \frac{1}{2g^2}\mathrm{tr}\left(F^E_{\mu\nu}F^{\mu\nu}_E\right) + \bar\psi(\gamma^\mu_E D^E_\mu + m)\psi\,. \tag{1.16}$$

1.2 Lattice regularization

Quantum field theories are disseminated of divergent integrals and the running of the parameters made necessary by renormalization calculations may cause perturbation theory to break down at some regimes, where a non-per-

turbative approach is needed [32]. We choose to discretize the spacetime by formulating the theory on a hypercubic oriented lattice

$$\Lambda = \Big\{ x \in m \;\Big|\; x = \sum_{\mu=1}^{D} n_\mu a\hat{\mu}\,,\;\; n_\mu = 0, 1, \ldots, L_\mu - 1 \Big\}\,,$$

where a is the spacing, $\hat{\mu}$ is a unit vector in the μ direction and L_μ is the extension of the lattice along μ. Let f be a function on Λ. The discretized version of the integral clearly is

$$\int_m d^D x \;\; \to \;\; a^D \sum_{x\,\in\,\Lambda} \;, \tag{1.17}$$

then we can define the lattice Fourier transform of f as

$$\tilde{f}(p) = a^D \sum_{x\,\in\,\Lambda} e^{-ip\cdot x} f(x)\,. \tag{1.18}$$

If we put periodic boundary conditions $f(x + a\hat{\mu}L_\mu) = f(x)$, we want the plane waves $e^{-ip\cdot x}$ to satisfy the same requirement [73]. This selects the set of allowed values for p_μ, which is the reciprocal lattice

$$\tilde{\Lambda} = \Big\{ p \in \mathbb{R}^D \;\Big|\; p_\mu = \frac{2\pi}{aL_\mu} k_\mu\,,\;\; k_\mu = -\frac{L_\mu}{2} + 1, \ldots, \frac{L_\mu}{2} \Big\}\,.$$

Denoting the size of the lattice with $|\Lambda| = L_1 \cdot \ldots \cdot L_D$, the previously defined Fourier transform can be inverted with the following formula:

$$f(x) = \frac{1}{a^D\,|\Lambda|} \sum_{p\,\in\,\tilde{\Lambda}} e^{ip\cdot x} \tilde{f}(p)\,. \tag{1.19}$$

All momenta can be restricted to the first Brillouin zone, therefore the presence of the lattice introduces a finite momentum cut-off, which regulates the divergences of the theory. We can discretize also ∂_μ as

$$\Delta_\mu f(x) = \frac{f(x + a\hat{\mu}) - f(x)}{a}\,. \tag{1.20}$$

This is the lattice forward derivative; a backward derivative can be analogously defined [58]. When we discretize the spacetime, any field $\phi(x)$ should correspondingly get restricted to the lattice. Let us consider a scalar field to begin with. The dynamics of the lattice field should be governed by a properly discretized action; suppose that the continuum action for ϕ in $D = 4$ dimensions takes the standard form

$$S[\phi] = \int d^4x \;\; \frac{1}{2}\big(\partial_\mu \phi(x)\big)^2 + \mathcal{V}\big(\phi(x)\big)\,. \tag{1.21}$$

Then, if we assume that the lattice field $\phi(x)$ is defined on the lattice sites $x \in \Lambda$ (as we are going to see in section 1.4, this assumption is correct only for matter fields), the naive discretization of $S[\phi]$ provides

$$S[\{\phi(x)\}] = a^4 \sum_{x \in \Lambda} \left[\frac{1}{2} \sum_{\mu=1}^{4} \left(\frac{\phi(x + a\hat{\mu}) - \phi(x)}{a} \right)^2 + \mathcal{V}\big(\phi(x)\big) \right]. \tag{1.22}$$

This naive lattice action can be considered correct only when ϕ is a scalar field, because also fermions are problematic [58]. If we are interested in the low-energy physics of the model, we can limit ourselves to consider

$$\mathcal{V}(\phi) = \frac{m_0}{2}\phi^2 + \frac{\lambda_0}{4!}\phi^4 \tag{1.23}$$

since all the other terms allowed by the symmetries are irrelevant in the sense of the RG flow [86]. Once the action is chosen, the euclidean path integral on the lattice can be defined as follows

$$Z = \int \mathscr{D}\phi \; e^{-S[\phi]} \equiv \int \left(\prod_{x \in \Lambda} d\phi(x) \right) e^{-S[\{\phi(x)\}]} . \tag{1.24}$$

It has the form of a partition function for a model of statistical mechanics, whose configuration is defined by the values of field $\{\phi(x)\}$, playing the role of one component real "spins" attached to each site $x \in \Lambda$. The path integral can be used to compute any correlation function. In particular, the 2-point correlator falls off exponentially within a scale given by the correlation length ξ, which is related to the mass gap $m = E_1 - E_0$ of the theory as [46]

$$m = \frac{1}{\xi\, a} . \tag{1.25}$$

Consequently an interesting continuum limit $a \to 0$ with a finite mass spectrum can only be found when $\xi \to \infty$, i.e. at a critical point. It is, therefore, crucial to study the phase diagram of lattice theories and the nature of their critical regions.

1.3 Parallel transport and Wilson loops

Before we describe the discretization procedure for the Yang-Mills field, it is convenient to pause and define some objects that will be crucial in the development of this thesis. Generally speaking, in order to "feel" gauge transformations, matter fields must have some internal degrees of freedom belonging

to a vector space V on which the gauge fields act through a representation $\rho : \mathrm{G} \to \mathrm{GL(V)}$. For instance, the quark fields of QCD are functions

$$q \,:\, \mathcal{M} \longrightarrow \mathbb{C}^3 \left(\otimes\, C^4\right), \quad q(x) = \begin{pmatrix} q_R(x) \\ q_G(x) \\ q_B(x) \end{pmatrix} .$$

where each $q_a(x)$ is a Dirac spinor belonging to $\mathbb{C}^4$. Here, the internal space of the *chromoelectric charge* is $\mathrm{V} = \mathbb{C}^3$, where the fundamental representation of SU(3) acts. The dynamics of these objects is governed by a covariant derivative, which, as it is well known in differential geometry, is related to a notion of parallel transport: it tells us how a chromoelectric charge vector $\vec{w} \in \mathrm{V}$ rotates when we drag it along a path on the spacetime $\mathcal{M}$.

Mathematically speaking, this parallel transport is defined on a vector bundle E which locally looks like $E \sim \mathcal{M} \times \mathrm{V}$ and the quark fields $q(x)$ can be seen as local sections of E [6] (neglecting the $\mathbb{C}^4$ part of spinors, which has no relevance here). The covariant derivative

$$D_\mu = \partial_\mu - iA_\mu$$

is the structure that we need to differentiate local sections on a fiber bundle. Being $A_\mu = A^a_\mu\, T_a \in \mathfrak{g}$, under the representation ρ to whom matters belongs, A_μ is realized as a matrix $A^{\,i}_{\mu j}$ belonging to End(V)

$$A_\mu = A^a_\mu\, T_a \quad \xrightarrow{d\rho} \quad A^{\,i}_{\mu j} = A^a_\mu\, (T_a)^i_j \,.$$

Let $\{\vec{e}_j\}$ be a basis for V. The Christoffel symbols for D_μ are given by

$$D_\mu \vec{e}_j = -iA^{\,i}_{\mu j}\, \vec{e}_i \tag{1.26}$$

Suppose that we want to drag a vector $\vec{w} \in \mathrm{V}$, defined a point $x_i \in \mathcal{M}$, along the path $\gamma(\tau)\,,\ \tau \in [\tau_i, \tau_f]$ s.t. $\gamma(\tau_i) = x_i$. The resulting vectors are found by imposing that their covariant derivatives along the tangent vector $v(\tau) = \gamma'(\tau)$ vanish, meaning that they are parallel transported. Expanding the covariant derivative on the bases $\vec{w} = w^i\, \vec{e}_i$ and $D_v = v^\mu D_\mu$, one finds

$$D_v \vec{w} = v^\mu \partial_\mu w^i \vec{e}_i - iA^{\,i}_{\mu j} v^\mu w^j \vec{e}_j \,. \tag{1.27}$$

Recalling that $v = \gamma'(\tau) = d/d\tau$, we see that $\vec{w}$ is parallel-transported along the path $\gamma(\tau)$ iff the *parallel transport equation* is satisfied

$$D_{\gamma'(\tau)}\, \vec{w} = \frac{d\vec{w}}{d\tau} - i \left[A_\mu \frac{d\gamma^\mu}{d\tau} \right] \vec{w} = 0 \,. \tag{1.28}$$

The second term $-i[A_\mu\, d\gamma^\mu/d\tau]\,\vec{w}$ is a rotation of $\vec{w}$, since $A = A_\mu dx^\mu$ is a one-form that acts on a vector $d\gamma^\mu/d\tau$, giving an element of the Lie algebra, that under ρ is represented by a matrix acting on V. The solution of the equation (1.28) can be expressed in the following way:

$$\vec{w}(\tau_f) = U[\gamma(\tau), A]\,\vec{w}(\tau_i)\,, \tag{1.29}$$

where $U[\gamma(\tau), A]$ is called *comparator*, parallel transporter or Wilson line and it can be expressed as the following path ordered exponential [6]:

$$U[\gamma(\tau), A] = \mathscr{P}\exp\left\{i\int_{\tau_i}^{\tau_f} d\tau\ \frac{d\gamma^\mu}{d\tau}\,A_\mu(\gamma(\tau))\right\} = \mathscr{P}\,e^{\,i\int_\gamma A}\,. \tag{1.30}$$

$A_\mu(\gamma(\tau))$ is the gauge field evaluated at the point $\gamma(\tau)$ and the path ordering $\mathscr{P}$ is analogous to the time ordering of quantum field theory, the only difference being that τ is a generic parameter of a curve and it may not be interpreted as a time variable. The comparator belongs to the gauge group, because it is the exponential of an element of its Lie algebra. If we apply a gauge transformation identified by the elements $g(x) \in \mathrm{G}$, then

$$\vec{w}'(\tau) = g(\gamma(\tau))\,\vec{w}'(\tau) \tag{1.31}$$

and $U[\gamma(\tau), A']$ is the linear transformation sending $\vec{w}'(\tau_i)$ to $\vec{w}'(\tau_f)$. Then, identifying $x_i = \gamma(\tau_i)$, $x_f = \gamma(\tau_f)$, the comparator transforms according to

$$U[\gamma(\tau), A] \;\longmapsto\; U[\gamma(\tau), A'] = g(x_f)\,U[\gamma(\tau),\, A]\,g(x_i)^{-1}\,. \tag{1.32}$$

When the path $\gamma(\tau)$ is a loop at a point x_0, $U[\gamma(\tau), A]$ becomes a linear map on the fiber V at x_0 (called holonomy by mathematicians) and we can use it to defines a gauge-invariant quantity called *Wilson loop*

$$\operatorname{tr} W[\gamma(\tau), A] = \operatorname{tr}\left(\mathscr{P}\,e^{\,i\oint_\gamma A}\right)\,. \tag{1.33}$$

This is clearly gauge-invariant, because when $x_i = x_f$ the two factors $g(x_f)$ and $g(x_i)^{-1}$ cancel thanks to the cyclicity of the trace. The simplest example one can give is about electromagnetism. When the gauge group is U(1), abelian, $\mathscr{P}$ is irrelevant and the vector potential A_μ is a real number, meaning that the comparator $U[\gamma, A]$ is a complex phase. If we drag a charged particle whose wavefunction is called ψ along a loop γ, we find

$$\psi(\tau_f) = e^{\,i\oint_\gamma A_\mu dx^\mu}\psi(\tau_i)$$

and the wavefunction will return to the initial point $\gamma(\tau_i) = \gamma(\tau_f)$ after having acquired a phase. This is the familiar Aharonov-Bohm effect [3]. The importance of these objects is due to the fact that Wilson was able to characterize

confinement using the behaviour of their expectation values [90]. Roughly speaking, the expectation values always decay exponentially according to the size of the loop, but how fast this decay is determines the presence of confinement. When the decay scales with the area of the loop, quark paths cannot separate macroscopically and the resulting phase is confined, while, if the decay scales with the perimeter, the final states of QCD processes can have well separated quarks and the theory is in a deconfined phase. Wilson loops and comparators are also the building blocks we need to give a general construction for the action and for the hamiltonian of a lattice gauge theory.

1.4 Gauge fields on a lattice

To see how gauge fields should be represented on a lattice, let us consider the coupling term with a scalar matter field ϕ. On the continuum, the minimal coupling is realized by the introduction of a connection $\partial_\mu \to D_\mu$. On geometrical terms, this is needed because the derivative of ϕ should be defined as a limit of the difference $\phi(x) - \phi(y)$ when x and y are infinitesimally close, but it is the connection what tells us how the two chromoelctrically charged vectors $\phi(x)$ and $\phi(y)$, defined at different points, should be compared.

On a lattice we do not have the limit anymore, but the problem of comparing fields at different points still persists. The lattice derivative should be defined at two nearest neighbours sites x, $x + a\hat{\mu}$, therefore we have to drag $\phi(x + a\hat{\mu})$ back to the site $\phi(a)$ using the equation (1.29). The link denoted $(x, \hat{\mu})$, connecting the sites x and $x + a\hat{\mu}$, is a path and we can consider the comparator defined on it; let this comparator be $U_\mu(x)$. $(x + a\hat{\mu}, -\hat{\mu})$ is $(x, \hat{\mu})$ but travelled along the opposite direction, therefore it is associated with the inverse comparator $U_\mu(x)^{-1}$. Then, the lattice covariant derivative is [58]

$$D_\mu \phi(x) = \frac{U_\mu(x)^{-1}\phi(x + a\hat{\mu}) - \phi(x)}{a}\,. \tag{1.34}$$

The intrinsic role of the gauge field is to tell matter how to evolve along a path and the truly important object is the comparator. A gauge potential $A_\mu(x)$ defined on a site and belonging to the Lie algebra will not be needed to formulate the theory (implying that lattice gauge theories can be defined also when the gauge group is discrete!), so we conclude that the lattice gauge variables are the comparators along elementary paths, i.e. links. The definition of a gauge transformation on a lattice clearly reduces to the choice of an element $g(x)$ attached to each site $x \in \Lambda$. Taking G=SU(N), it will act

on matter fields and on comparators according to

$$\phi(x) \;\mapsto\; g(x)\phi(x) \tag{1.35}$$

$$U_\mu(x) \;\mapsto\; g(x+a\hat{\mu})U_\mu(x)g^\dagger(x). \tag{1.36}$$

Like in the continuous case, lattice covariant derivative transforms as

$$D_\mu\phi\,(x) \mapsto g(x)\,D_\mu\phi\,(x) \tag{1.37}$$

and the lattice version of the gauge-invariant kinetic term for ϕ is

$$\begin{aligned} a^D \sum_{x\in\Lambda} |D_\mu\phi(x)|^2 = a^{D-2} \sum_{x\in\Lambda}\sum_{\mu=1}^{D} \Big[& 2\phi^\dagger(x)\phi(x) \\ & -\phi^\dagger(x)U_\mu(x)^\dagger\phi(x+a\hat{\mu}) - \phi^\dagger(x+a\hat{\mu})U_\mu(x)\phi(x)\Big]\,. \end{aligned} \tag{1.38}$$

The continuum form of the kinetic term for the gauge fields contains the square of the curvature tensor $F_{\mu\nu}F^{\mu\nu}$. The curvature tensor tells how much a vector changes when it is transported along an infinitesimal loop, so it is natural to build the action looking at the Wilson loops on the *plaquettes*, which are the elementary loops on a lattice. A plaquette, denoted as $\Box$, can be identified with a sequence of four links

$$(x,\mu) \;\to\; (x+a\hat{\mu},\nu) \;\to\; (x+a\hat{\mu}+a\hat{\nu},-\mu) \;\to\; (x+a\hat{\nu},-\nu)\,.$$

Then, the corresponding Wilson loop is given by the following equation

$$\operatorname{tr} W_\Box = \operatorname{tr}\left[U_\mu(x)U_\nu(x+a\hat{\mu})U_\mu(x+a\hat{\nu})^\dagger U_\nu(x)^\dagger\right]. \tag{1.39}$$

To compare it with continuum objects, we have to reintroduce the gauge potential $A_\mu(x)$. On an elementary path, the integral reduces to a multiplication by the spacing a. Therefore, we can identify

$$U_\mu(x) = e^{iaA_\mu(x)}\,. \tag{1.40}$$

Substituting it into $\operatorname{tr} W_\Box$, one finds [32] that up to higher order terms

$$\operatorname{tr} W_\Box = \operatorname{tr}\left[e^{ia^2F_{\mu\nu(x)}} + \dots\right] = \operatorname{tr}\left[\mathbb{I} + ia^2F_{\mu\nu} - \frac{a^2}{2}F_{\mu\nu}F_{\mu\nu} + \dots\right],$$

where the indices μ,ν are not summed on. $F_{\mu\nu}$ is traceless and, working in the fundamental representation of SU(N), $\operatorname{tr}\mathbb{I} = N$. Then it holds

$$\operatorname{tr} W_\Box = N + \frac{a^2}{2}\operatorname{tr} F_{\mu\nu}F_{\mu\nu} + \mathcal{O}(a^6)\,. \tag{1.41}$$

Notice that, since $F_{ij}F_{ij} = (\sum_k \epsilon_{ijk}B^k)^2$ and $F_{0i}F_{0i} = E_i^2$, when the plaquette $\square$ sits on two space directions i, j $\mathrm{tr}\, W_\square$ contributes to the magnetic term, while the electric term is given by plaquettes along a space direction i and the time direction 0. To get rid of the constant term we can use $\mathrm{tr}(\mathbb{I} - W_\square)$ instead. Then, we get an action that reduces to the continuum one in the limit $a \to 0$ if we sum on all plaquettes

$$S_W[\{U_\mu(x)\}] = \frac{2}{g^2 a^{4-D}} \sum_\square \mathrm{Re}\ \mathrm{tr}\left(\mathbb{I} - W_\square\right), \tag{1.42}$$

where Re has been added because the sub-leading order terms may not be real. This is the *Wilson action* and it is the simplest gauge-invariant lattice action for gauge fields one can write; other possibilities exist, but they differ only in higher order terms. An explicit labeling for $W_\square$ is $W_{\mu\nu}(x)$, where x is the origin of the plaquette and $\mu \neq \nu$ are the directions that identify the plane where it lies. Then, the sum on all plaquettes can be rewritten as a sum on all lattice sites $x \in \Lambda$ and on all directions $1 \leq \mu < \nu \leq D$, so that

$$S_W = \frac{2}{g^2 a^{4-D}} \sum_{x\in\Lambda} \sum_{\mu<\nu} \frac{a^4}{2} \mathrm{tr}\, F_{\mu\nu}F_{\mu\nu} = \frac{a^D}{2g^2} \sum_{x\in\Lambda} \sum_{\mu,\nu} \mathrm{tr}\, F_{\mu\nu}F^{\mu\nu}\,,$$

where a factor $1/2$ comes from the antisymmetry of $F_{\mu\nu}$. We have proved that the continuum limit is correct. An equivalent form of the action is

$$S_W[\{U_\mu(x)\}] = -\frac{1}{g^2 a^{-D}} \sum_\square \left(\mathrm{tr}\, W_\square + \mathrm{tr}\, W_\square^\dagger\right), \tag{1.43}$$

because the constant term is non-dynamical and it can be neglected. The lattice path integral for gauge fields is defined in the following way:

$$Z = \int \mathscr{D}U\, e^{-S_W[U]} \equiv \int \Big(\prod_{(x,\mu)} dU_\mu(x)\Big)\, e^{-S_W[\{U_\mu(x)\}]}\,. \tag{1.44}$$

Each integral with differential $dU_\mu(x)$ is done on the group manifold. The proper integration measure that defines them is the Haar measure [58]. Its main property is that it is both left and right invariant: given a function $f(U)$ on the group SU(N), $\forall g \in \mathrm{SU(N)}$ it holds that

$$\int_{SU(N)} dU\, f(g\cdot U) = \int_{SU(N)} dU\, f(U) = \int_{SU(N)} dU\, f(U\cdot g)\,, \tag{1.45}$$

meaning that the integral respects the gauge symmetry. Given an observable O, one is typically interested in computing the average

$$\langle O\rangle = \frac{1}{Z}\int \mathscr{D}U\ O(U)\, e^{-S_W[U]}\,. \tag{1.46}$$

A gauge transformation maps the right hand side of this equation to

$$\int \mathscr{D}U \; O(\{g(x+a\hat{\mu})U_\mu(x)g(x)^\dagger\})e^{-S_W[\{g(x+a\hat{\mu})U_\mu(x)g(x)^\dagger\}]} \,,$$

which is equal to the original integral thanks to left and right invariance. But the action is gauge-invariant, so it also equals

$$\int \mathscr{D}U \; O(\{g(x+a\hat{\mu})U_\mu(x)g(x)^\dagger\}) \, e^{-S_W[\{U_\mu(x)\}]}$$

for arbitrary functions $g(x)$, implying that the average of a local observable $\langle O \rangle$ can be different from zero only when O is gauge-invariant. The special importance of Wilson loops is underlined by the following fact: any gauge-invariant observable that depends continuously on the link variables can be approximated arbitrarily well by polynomials of the kind [58]

$$\sum_{n=0}^{\infty} \sum_{\gamma_1 \ldots \gamma_2} a(\gamma_1, \ldots, \gamma_2) \operatorname{tr} W[\gamma_1] \ldots \operatorname{tr} W[\gamma_n] \,. \tag{1.47}$$

Another consequence of this fact is the important statement known as *Elitzur's theorem*: gauge symmetries cannot be spontaneously broken [46].[1] If a system has a symmetry, the order parameter that signal its spontaneous breaking has to be non-invariant under the symmetry transformation. But this fact implies that their expectation value will always vanish, so an SSB cannot happen. We have considered here only a quantum statistical system at zero temperature, the fluctuations are only quantum, but if we added also thermal fluctuations the results would be the same.

Consider for instance a "gauged" version of the Ising model, that has been modified to promote its $\mathbb{Z}_2$ global symmetry to a local one. Its gauge symmetry cannot be broken, but nevertheless the phase diagram of this is non-trivial and it is an interesting issue to find an order parameter able to detect its transition. The key point is that we had assumed that O was a local function: on a gauge system phase transitions signaled by non-local order parameters can still happen.

1.5 Hamiltonian Yang-Mills theory

Path integrals are the standard tool used to study lattice gauge theories. However, the hamiltonian approach has some important advantages: truly

[1] It is often said that the Higgs mechanism corresponds to the SSB of a gauge symmetry. This is misleading, as it is forbidden by Elitzur's theorem: what is broken is only the global part of a local symmetry, while the redundancy still persists [28].

dynamical phenomena can be described only in a real-time hamiltonian setting, which avoids also the sign problem when a chemical potential is added [8], has we have already discussed in the introduction. Moreover, the interpretations of the variables is more transparent, since the observables are treated as the usual operators on a Hilbert space. Before formulating the lattice theory in its hamiltonian version, let us quickly review the continuum case. Matter does not need additional considerations with respect to the free case, so we shall consider only the gauge part.

The main issue we have to deal with is gauge invariance: the lagrangian is written with some redundant non-dynamical degrees of freedom. This is reflected into the fact that $\mathscr{L}_{YM}$ does not contain $\dot{A}_0$

$$\Pi_0 = \frac{\partial \mathscr{L}_{YM}}{\partial \dot{A}^0} = 0\,,$$

A_0 is not dynamical, since it has no conjugate momentum. Then we can isolate the A_0 dependent part of $\mathscr{L}_{YM}$, thus finding [49]

$$\mathscr{L}_{YM} = \frac{1}{g^2}\,\mathrm{tr}\left(\vec{E}^2 - \vec{B}^2\right) + \frac{1}{g^3}\,\mathrm{tr}\big(A_0 \mathscr{G}\big) \tag{1.48}$$

$$\mathscr{G}^a(x) = E_i^a(x) + f^{abc} A_i^b(x) E_i^c(x) = D_i\, E_i^a(x) \tag{1.49}$$

again with $\mathscr{G} = \mathscr{G}^a\, T_a$. A_0 is a Lagrange multiplier and its equation of motion corresponds to the phase space constraint $D_i\, E_i^a(x) = 0$: gauge theories are constrained systems. $D_i\, E_i^a(x) = 0$ is the generalization of the Gauss's law: when G is abelian, like for G=U(1), $[A_i, E_i] = 0$ and

$$D_i\, E_i(x) = \vec{\nabla} \cdot \vec{E}(x) = 0\,.$$

Instead, non-abelian gauge fields, carry a colour charge and a density term is added. The quantization can be simplified by imposing a gauge fixing condition from the start. We work in the *temporal gauge* $A_0 = 0$, in order to quantize only the dynamical degrees of freedom A_i. Now, the lagrangian is

$$\mathscr{L}_{YM} = \frac{1}{g^2}\mathrm{tr}\big(\vec{E}^2 - \vec{B}^2\big) = \frac{1}{2g^2}\big(E_a^i E_a^i - B_a^i B_a^i\big)$$

and using $E_a^i = -\dot{A}_a^i = \dot{A}_i^a$ we find the momentum conjugate to A_i^a

$$\Pi_a^i = \frac{\partial \mathscr{L}_{YM}}{\partial \dot{A}_i^a} = \frac{E_a^i}{g^2}\,. \tag{1.50}$$

The hamiltonian can be found from the Legendre transformation

$$\mathscr{H}_{YM} = \Pi_a^i \dot{A}_i^a - \mathscr{L}_{YM} = \frac{1}{2g^2}\big(E_a^i E_a^i + B_a^i B_a^i\big) \tag{1.51}$$

$$H_{YM} = \int d^D x\, \mathscr{H}_{YM} = \int d^D x\, \left(\frac{g^2}{2}\,\Pi_a^i \Pi_a^i + \frac{1}{2g^2} B_a^i B_a^i\right). \tag{1.52}$$

To quantize the theory, we have to promote the fields to operators that satisfy canonical equal-time commutation relations

$$[\hat{A}_i^a(x),\, \hat{A}_j^b(y)]_{x^0=y^0} = 0 = [\hat{\Pi}_a^i(x),\, \hat{\Pi}_b^j(y)]_{x^0=y^0} \tag{1.53}$$

$$[\hat{A}_i^a(x),\, \hat{\Pi}_b^j(y)] = i\delta_b^a \delta_i^j\, \delta^3(\vec{x}-\vec{y})\,. \tag{1.54}$$

The simplest representation of these relations is probably achieved on the space of wavefunctionals $\langle \vec{A}(x)\,|\,\psi\,\rangle = \psi[\vec{A}]$. Similarly to what happens in finite-dimensional quantum systems with $[\hat{x}_i,\, \hat{p}_j] = i\delta_{ij}$, $A_i^a(x)$ acts on $\psi[\vec{A}\,]$ multiplicatively while $\hat{\Pi}_a^i$ is the generator of translations

$$\hat{A}_i^a(x)\,\psi[\vec{A}\,] = A_i^a(x)\psi[\vec{A}\,] \tag{1.55}$$

$$\hat{\Pi}_a^i(x)\,\psi[\vec{A}\,] = -i\frac{\delta}{\delta A_i^a(x)}\,\psi[\vec{A}\,]\,. \tag{1.56}$$

However, the Hilbert space of all wavefunctionals $\psi[\vec{A}\,]$ is still too large. The temporal gauge keeps a residual gauge invariance for time independent gauge transformations $A_0 \;\mapsto\; gA_0g^{-1} + ig\partial_0 g^{-1}$, which is still vanishing if $A_0 = 0$ and $\partial_0 g = 0$. At the quantum level, it means that

$$\psi[\vec{A}\,] \sim \psi[g\vec{A}g^{-1} + ig\vec{\nabla}g^{-1}\,]\,, \tag{1.57}$$

the two wavefunctionals should identify the same physical state. Classically $D_iE_i(t,\vec{x}) = 0$, it is an integral of motion and it is promoted to a local operator $\hat{G}(\vec{x}) = D_i\hat{E}_i(\vec{x})$ (depending only on the spatial position, in the Schrödinger picture) that commutes with the hamiltonian

$$[\hat{H}_{YM},\, \hat{G}(\vec{x})] = 0\,. \tag{1.58}$$

It can be shown that $\hat{G}(\vec{x}) = D_i\hat{E}_i(\vec{x})$ is the quantum generator of time-independent gauge transformations [27]. For instance, in the simpler abelian case the commutation relations (1.54) imply

$$\hat{R}[\phi] = \exp\!\left\{\frac{i}{g^2}\int d^3x\,\phi(x)\vec{\nabla}\cdot\hat{\vec{E}}(\vec{x})\right\} \tag{1.59}$$

$$\hat{R}^\dagger[\phi]\,\hat{A}_j(\vec{x})\,\hat{R}[\phi] = \hat{A}_j(\vec{x}) + \partial_j\hat{\phi}(\vec{x})\,. \tag{1.60}$$

If we apply the quantum version of the Gauss's law constraint on the Hilbert space $\hat{G}|\psi\rangle = D_i\hat{E}_i(\vec{x})\,|\psi\rangle = 0$, the states that satisfy it are unchanged by (1.60), so it is equivalent to (1.57) and applying it removes the residual gauge redundancy. In conclusion, we can identify the *physical Hilbert space* with

$$\mathscr{H}_{phys} = \left\{\; |\mathrm{phys}\rangle \;\middle|\; \hat{G}(\vec{x})\,|\mathrm{phys}\rangle = 0 \;\right\}. \tag{1.61}$$

If we included charged matter fields, the constraint term would be modified by including matter density. For instance, in QED the traditional Gauss's law would be recovered as $(\vec{\nabla}\cdot\hat{\vec{E}} - q\,\hat{\psi}^\dagger\hat{\psi})|\text{phys}\rangle = 0$.

1.6 The Kogut-Susskind hamiltonian

The main difference between the path integral and the hamiltonian formalism for lattice theories is that for the hamiltonian one time can be kept real and continuous, while path integrals are formulated on a full spacetime lattice (with imaginary time). The hamiltonian should be the generator of time translations for all values of t on the real line. Two approaches can be followed to find the lattice hamiltonian.

One common approach to find the lattice hamiltonian is to use the transfer matrix formalism [46]. The idea is that for any lattice theory with discrete time, using the transfer matrix $T_{\tau',\tau}$, the partition function can be written as

$$Z = \sum_{n=0}^{N} \langle\, \phi(\tau_{n+1},\vec{x}) \,|\, \hat{T} \,|\, \phi(\tau_n,\vec{x}) \,\rangle = \operatorname{tr}\hat{T}^N\,, \tag{1.62}$$

as long as there are periodic boundary conditions on the time direction. Taking advantage of the fact that the euclidean action represents the energy of the system, we can interpret the transfer matrix can as the generator of an imaginary time evolution between the two time slices τ_n and τ_{n+1}. The duration of this time evolution equals the lattice spacing a, so that

$$\hat{T} = e^{-a\left[\hat{H}_a + \mathcal{O}(a)\right]}\,. \tag{1.63}$$

This defines the lattice hamiltonian, which is not a actual hamiltonian because of the discrete time. However, if we place the theory on an inhomogeneous lattice, with time spacing a_0 kept different from the spatial spacing a, we can perform the limit $a_0 \to 0$, which recovers a continuous time. Then

$$\hat{H} = \lim_{a_0\to 0} \hat{H}_{a_0}. \tag{1.64}$$

For point-like quantum system, whose path integral is defined only on a discrete time since they do not have a spatial extension, this limit recovers the correct quantum hamiltonian. Therefore this is a sensible definition also for field theories on a spatial lattice.

Instead of taking this route, we place directly a spatial lattice on the hamiltonian formulation of the continuum theory [57]. To recover the hamiltonian (1.52), we recognize that the chromoelectric term and the chromomagnetic are the same appearing in the lagrangian but with the opposite relative

sign: the former behaves as a kinetic term, while the latter as a potential one. We already know how to discretize the lagrangian. The magnetic part of the Wilson action is given by a sum on all spatial plaquettes of $\operatorname{tr} W_\square$ and this can be repeated straightforwardly for the hamiltonian. Instead, some problems appear for the electric term, which was obtained by summing $\operatorname{tr} W_\square$ on time-like plaquettes. Now the lattice is only spatial and time-like plaquettes do not exist anymore! We are not only unable to get the electric term like before, but also we cannot specify a group element $U_\mu(x)$ for $\mu = 0$, since there are no links in the time direction.

To avoid this issue, we perform again the quantization in the temporal gauge $A_0 = 0$, so that time-like links become associated with the identity and they do not affect comparators anymore [73]. Then, a classical configuration of the lattice pure-gauge theory is identified by the choice of a matrix $U \in \mathrm{SU(N)}$ for all spatial links at a fixed time. The system can be seen as a many-body model made of several links, each one with SU(N) as its configuration space. Correspondingly, the Hilbert space of a single link can be identified with the wavefunctions $\psi : SU(N) \to \mathbb{C}$, with the usual requirement of being square integrable. The full Hilbert space is given by the tensor product

$$\mathscr{H}_{N_L} = \bigotimes_{\ell=1}^{N_L} L^2\big(\mathrm{SU(N)}\big) = \underbrace{\mathrm{SU(N)} \otimes \cdots \otimes \mathrm{SU(N)}}_{\text{links}} . \tag{1.65}$$

The wavefunctions $\psi(U)$ take as input the group elements, which define the analog of the position basis. We can promote the "position" of a single link $U \in \mathrm{SU(N)}$ to a state $|U\rangle \in \mathscr{H}_1$. The set $\{\, |U\rangle \mid \forall U \in \mathrm{SU(N)}\}$ is a generalized basis of $\mathscr{H}_1 = L^2(\mathrm{SU(N)})$ satisfying the orthonormality relation $\langle U|V\rangle = \delta(U,V)$, similarly to what happens with $L^2(\mathbb{R})$ and $|x\rangle$ [57]. The physical (normalized) states will then be

$$|\psi\rangle = \int dU\, \psi(U)\, |U\rangle \ , \quad \psi \in L^2(\mathrm{SU(N)}) \tag{1.66}$$

where, as usual, dU represents the Haar measure on the gauge group. The single link Hilbert space we have just described is called by mathematicians the *group algebra* of SU(N); more details about it can be found in Appendix A. $|U\rangle$ is an eigenstate of the "position" operators $\hat{U}_{ij}$

$$\hat{U}_{ij}\, |U\rangle = |U\rangle\, U_{ij} \,, \tag{1.67}$$

associating to the link in the eigenstate $|U\rangle$ the corresponding matrix elements in the appropriate representation. Notice that $\hat{U}_{ij}$ is neither hermitian, since the eigenvalues U_{ij} are not necessarily real, nor unitary, because

the conjugate of (1.67) is $\langle U|(\hat{U}_{ij})^\dagger = U^*_{ij}\langle U|$, which implies

$$\langle U|\,(\hat{U}_{ij})^\dagger \hat{U}_{ij}\,|U\rangle = U^*_{ij}U_{ij}\,\langle U|U\rangle \neq \langle U|U\rangle\,.$$

The adjoint "position" $(\hat{U}_{ij})^\dagger$ acts also on kets as $(\hat{U}_{ij})^\dagger|U\rangle = |U\rangle\,U^*_{ij}$, since for all bras $\langle\psi| = \int dV\,\psi(V)^*\langle V|$ it holds that

$$\langle\psi|\Big((\hat{U}_{ij})^\dagger|U\rangle\Big) \equiv \Big(\langle\psi|(\hat{U}_{ij})^\dagger\Big)|U\rangle = \int dV\,\psi(V)^*\,V^*_{ij}\,\langle V|U\rangle = \psi(U)^*\,U^*_{ij}$$
$$\implies \quad \langle\psi|\Big((\hat{U}_{ij})^\dagger|U\rangle\Big) \;=\; \langle\psi|U\rangle\;U^*_{ij} \quad \forall\;\langle\psi|\,.$$

What prevents $\hat{U}_{ij}$ from being unitary is that this conjugation does not reverse the order of the indices i, j. We can define the matrix of operators $\hat{U}$ whose elements are $\hat{U}_{ij}$ s.t. $[\hat{U}]_{ij}\,|U\rangle = |U\rangle\,U_{ij}$. Being a matrix, its hermitian conjugate includes both a transposition and a Hilbert space adjunction

$$[\hat{U}^\dagger]_{ij} = (\hat{U}_{ji})^\dagger\,. \tag{1.68}$$

When the chosen representation is unitary, the previous equation implies

$$\langle U|\sum_j [\hat{U}^\dagger]_{ij}\hat{U}_{jk}|U\rangle = \sum_j U^{*,t}_{ij}\,U_{jk}\langle U|U\rangle = \langle U|U\rangle\,,$$

meaning that the matrix of operators $\hat{U}$ is the unitary object. At this point, we can define comparators on a path as Hilbert space operators [57]. Consider an elementary path e on a link ℓ and call $\hat{U}[e]$ the comparator on it. Comparators are matrices in the colour space which map charged fields on the origin of the path into charged fields on the endpoint of the path. Like we did in the path integral case, we identify the group element on the link ℓ with the comparator $\hat{U}[e]$ when the directions of e and ℓ coincide, otherwise they are the inverse of each other. So we have

$$\hat{U}[e] = \begin{cases} \hat{U}(\ell) & \text{if } e \parallel \ell \\ \hat{U}^\dagger(\ell) & \text{if } e \parallel -\ell \end{cases}\,, \tag{1.69}$$

denoting with ℓ the link where the "position" matrix is placed. The comparator on a general path $\gamma = e_1 \cdot ... \cdot e_n$, sequence of the elementary paths $e_1, ..., e_n$, is given by the composition

$$\hat{U}[\gamma] = \hat{U}[e_1] \cdot ... \cdot \hat{U}[e_n]\,. \tag{1.70}$$

If the path γ is closed, we can define the Wilson loop operator

$$\mathrm{tr}\,\hat{W}[\gamma] = \mathrm{tr}\,\Big(\hat{U}[e_1] \cdot ... \cdot \hat{U}[e_n]\Big) \tag{1.71}$$

For instance, when γ is a plaquette the previous equation yields

$$\operatorname{tr} \hat{W}_\square = \operatorname{tr} \hat{U}(x,i)\hat{U}(x+a\hat{i},j)\hat{U}(x+a\hat{j},i)^\dagger \hat{U}(x,j)^\dagger \tag{1.72}$$

We recover the magnetic part $\hat{H}_B$ by summing on all spatial plaquettes

$$\hat{H}_B = -\frac{1}{g^2 a^{4-d}} \sum_\square \Big(\operatorname{tr} \hat{W}_\square + \operatorname{tr} \hat{W}_\square^\dagger \Big) . \tag{1.73}$$

The trace is giving the missing 1/2 factor with respect to (1.52), while the power of a is now $d = D - 1$ because the lattice is only spatial.

To find the electric term, recall that in the continuum hamiltonian it is given by the square of $\hat{\Pi}_a^i = -i\ \delta/\delta A_i^a$, which generates translations on $\psi[\vec{A}]$. On a lattice we do not work with the potential $\vec{A}$ anymore and states are elements of the group algebra, i.e. square integrable functions $\mathrm{SU(N)} \to \mathbb{C}$, however, we can still write the electric term using the generator of translations. Translations on the group algebra are defined through the regular representation (cf. Appendix A) of the gauge group: U acts on $|V\rangle$ as

$$\hat{L}_U |V\rangle = |UV\rangle . \tag{1.74}$$

The corresponding action of U on the wavefunction $\psi(V)$ is given by

$$\hat{L}_U \psi(V) = \psi(U^{-1}V). \tag{1.75}$$

$\hat{L}$ is an infinite-dimensional unitary representations of SU(N) onto the space of wavefunctions $L^2(\mathrm{SU(N)})$ and it satisfies the relations

$$\hat{L}_U^\dagger \hat{L}_U = \mathbb{I} , \quad \hat{L}_U^\dagger = \hat{L}_{U^\dagger} . \tag{1.76}$$

Actually, this is only the *left* regular representation. One may also choose to work with the right regular representation $\hat{R}_U|V\rangle = |VU^{-1}\rangle$, which has analogous properties and would lead to the same results. The momentum operator is proportional to the generator of translations, therefore we need to find the Lie algebra representation $\hat{\ell}$ of $\mathfrak{su}(\mathrm{N})$ that corresponds to $\hat{L}$ [71],

$$\hat{\ell} : \ \mathfrak{su}(\mathrm{N}) \ \to \ \mathrm{End}\big(L^2(\mathrm{SU(N)})\big) .$$

Making use of the Lie exponential map, we can write any $U \in \mathrm{SU(N)}$ as $U = e^{iX}$, $X \in \mathfrak{su}(\mathrm{N})$. The compatibility of $\hat{\ell}$ and $\hat{L}$ is encoded into

$$\hat{L}_{e^{iX}} = e^{i\,\hat{\ell}(X)} .$$

Expanding on the Lie algebra generators $X = X^a T_a$, $\hat{L}_{e^{iX^a T_a}} = e^{i\,X^a \hat{\ell}_a}$. Here $\hat{\ell}_a \equiv \hat{\ell}(T_a)$ is the generator of $\mathfrak{su}(\mathrm{N})$ in the regular representation, which is the momentum operator we need. Being a representation, it satisfies

$$[\hat{\ell}_a, \hat{\ell}_b] = i\, f_{abc} \hat{\ell}_c \,. \tag{1.77}$$

Notice that $\hat{\ell}_a$ has only the Lie algebra index a, while the continuum momentum $\hat{\Pi}^i_a$ has also a spatial index i. The spatial direction is implicit on a lattice, because $\hat{\ell}_a$ is placed on a link (x, i), which is already characterized by a specific direction i. The electric term, then, can be identified as

$$\hat{H}_E = \frac{g^2}{2a^{d-2}} \sum_{(x,i)} \sum_a \hat{\ell}_a(x,i)^2 \,. \tag{1.78}$$

It contains the sum on all directions a of the squared generators of translations, giving a generalization of the laplacian operator on the gauge group, while the external sum is over all spatial links (x, i). $\hat{\ell}_a$ is a good choice for the momentum operator because it has the correct continuum limit, implying that also $\hat{H}_E$ is the right electric term of the hamiltonian. This follows from the lattice version of the canonical commutation relations [52]

$$[\hat{\ell}_a, \hat{U}_{ij}] = -(T_a \hat{U})_{ij} \tag{1.79}$$

$$[\hat{\ell}_a, \hat{U}^\dagger_{ij}] = (\hat{U}^\dagger T_a)_{ij} \,. \tag{1.80}$$

To derive them, consider the one-parameter subgroup $h(s) = e^{isX_a}$. Under the regular representation, $[\hat{L}_{h(s)}\psi](U) = [e^{is\hat{\ell}_a}\psi](U) = \psi(e^{-isX_a}U)$. Applying a derivative and evaluating it at $s = 0$, we find

$$[\hat{\ell}_a\, \psi](U) = -i \frac{d}{ds} \psi\Big(e^{-isX_a} U\Big)\Big|_{s=0} \,, \tag{1.81}$$

which is equivalent to $\hat{\ell}_a = -i \frac{d}{ds} \hat{L}_{e^{isX_a}}\big|_{s=0}$. One should apply this result to the straightforward equality $[\hat{L}_U, \hat{U}_{ij}]|V\rangle = (V_{ij} - (UV)_{ij})\hat{L}_U|V\rangle$, taking $U = h(s)$. This allows to prove (1.79) and the second one can be found similarly. (1.79) implies that the action of $\hat{\ell}_a$ on $\psi(U)$ can be represented as

$$\hat{\ell}_a = -(T_a U)_{ij} \frac{\partial}{\partial U_{ij}} \,. \tag{1.82}$$

After having reintroduced the potential $U = e^{iaA^a T_a}$, it can be shown [52] that if $a \to 0$ the expression above reduces to $\hat{\ell}_a(x,i) \to -a^{d-1}\hat{\Pi}^i_a(x)(1 + \mathcal{O}(a))$,

meaning that $\hat{\ell}_a$ is the correct lattice expression for the momentum operator. Putting together the two parts gives us the *Kogut-Susskind hamiltonian*

$$\hat{H}_{KS} = \frac{g^2}{2a^{d-2}} \sum_{(x,i)} \sum_a \hat{\ell}_a(x,i)^2 - \frac{1}{g^2 a^{4-d}} \sum_\square \Big(\operatorname{tr} \hat{W}_\square + \operatorname{tr} \hat{W}_\square^\dagger \Big) \tag{1.83}$$

which has to be though as the hamiltonian corresponding to the Wilson action in the temporal gauge [47]. Again, the $A_0 = 0$ condition leaves a residual freedom for time-independent gauge transformations. Gauge transformations act on the states of the system, that are now elements of a Hilbert space. On a single link (x,i), a gauge transformation is

$$|U(x,i)\rangle \;\mapsto\; |g(x + a\hat{i}\,)\, U(x,i)\, g(x)^\dagger\rangle \,. \tag{1.84}$$

If we call a link $e \equiv (x,i)$, $e_- = x$ the source site and $e_+ = x + a\hat{i}$ the target site, then the transformation is realized by the operator $\hat{\mathcal{G}}_e : \mathcal{H}_e \to \mathcal{H}_e$ s.t.

$$\hat{\mathcal{G}}_e\, |U(e)\rangle = |g(e_+)\, U(e)\, g(e_-)^\dagger\rangle = \hat{L}_{g(e_+)} \hat{R}_{g(e_-)}\, |U(e)\rangle \,. \tag{1.85}$$

Overall, $\mathcal{H} = \bigotimes_e \mathcal{H}_e$ and the states are generated by the basis $\big\{ \bigotimes_e |U(e)\rangle \big\}$. Since each factor of a tensor product of operators acts on its original space, the complete gauge transformation on the whole lattice is

$$\hat{\mathcal{G}} :\; \mathcal{H} \to \mathcal{H} \;,\quad \hat{\mathcal{G}} = \bigotimes_e \hat{L}_{g(e_+)} \hat{R}_{g(e_-)} \,. \tag{1.86}$$

One can check immediately that $[\hat{H}_B, \hat{\mathcal{G}}] = 0$ with a direct calculation. It is less obvious that $[\hat{H}_E, \hat{\mathcal{G}}] = 0$, but it also holds. The reason is that the electric term of each single link is proportional to the quadratic Casimir of the gauge group (see Appendix A), which acts trivially on each irreducible representation and the action of a gauge transformation is just a reshuffling of the states within the same representation. Together they yield

$$[\hat{H}_{KS},\, \hat{\mathcal{G}}] = 0 \tag{1.87}$$

and the Kogut-Susskind hamiltonian is gauge-invariant. The physical states will be selected by a Gauss's law, requiring their gauge invariance

$$\Big(\bigotimes_e \hat{L}_{g(e_+)} \hat{R}_{g(e_-)} \Big)\, |\text{phys}\rangle = |\text{phys}\rangle \,. \tag{1.88}$$

1.7 Phase structure of gauge theories

The interest in lattice gauge theories was raised by Wilson, who showed that lattice QCD exhibits confinement in the strong coupling phase [90]. In general, both continuum and lattice gauge theories provide interesting phase diagrams, whose behaviour is often driven by complex non-perturbative effects [66]. Notice that in the previous sections we have discussed only QFT at zero temperature. The lattice models we are considering have only quantum fluctuations and the transitions at $T = 0$ we encounter are quantum phase transitions. In order to outline a phase diagram, one usually studies some kind of order parameter. But remember the Elitzur's theorem: gauge symmetries cannot undergo a spontaneous symmetry breaking and the usual local order parameters are insensitive to their phase transitions.

Only gauge-invariant objects can have non-vanishing expectation values, so a plausible candidate for the order parameter can be the Wilson loop. Indeed, they are be able to show a phase transition thanks to their non-local nature, which allows them to feel changes in global properties of the system, such as the emergence of topological excitations and topological phase transitions [29]. However, other non-local order parameters do exist, such as the electric strings that will be described in the fourth chapter, or the 't Hooft loops that were introduced to characterize SU(N) theories exploiting their $\mathbb{Z}_n$ center symmetry [33, 38].

Let $\mathscr{C}_{R,T}$ be the closed rectangular path consisting of the links

$$\mathscr{C}_{R,T} = (0, \vec{x};\, 0, \vec{y}) \cdot (0, \vec{y};\, T, \vec{y}) \cdot (T, \vec{y};\, T, \vec{x}) \cdot (T, \vec{x};\, 0, \vec{x})\,,$$

where $R = |\vec{x} - \vec{y}|$, that is represented represented in Fig. 1.1. Let $\operatorname{tr} W[\mathscr{C}_{R,T}]$ be the Wilson loop along it and consider its expectation value e.g. in the path integral formalism. Then

$$\langle \operatorname{tr} W[\mathscr{C}_{R,T}] \rangle = \frac{1}{Z} \int \mathscr{D}A \;\; \operatorname{tr} W[\mathscr{C}_{R,T}]\, e^{-S_W} \underset{T\to\infty}{\sim} e^{-V(R)T}\,. \tag{1.89}$$

$V(R)$ is the so-called *static quark potential* and it represents the energy of a quark-antiquark pair which are kept fixed at a distance R [73].

A strong coupling expansion [32] allows to show that in lattice QCD $V(R) \sim \sigma R$ when $g \to \infty$ (and R is sufficiently large): the interaction between the two quarks is like a spring which keeps them tied. When the distance between the quark-antiquark pair is increased, the energy grows until it overcomes twice the mass of the quark and it becomes energetically favourable to break in halves the string and to produce another quark-antiquark pair. The two quarks cannot be separated, since, instead, we end

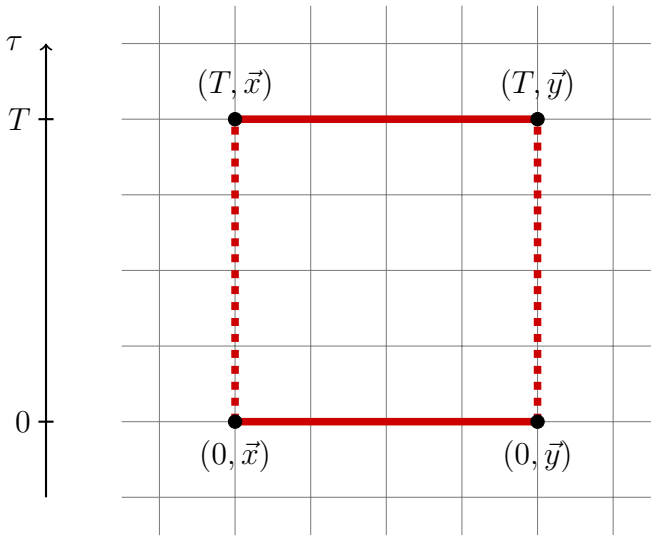

Figure 1.1: The loop $\mathscr{C}_{R,T}$ on a spacetime lattice. It represents the boundary of the worldsheet covered by the trajectory of a quark-antiquark pair fixed at positions $\vec{x}$, $\vec{y}$ linked by a string of the gauge field.

up with two quark-antiquark pairs. This dynamical process is called *string breaking mechanism* and it characterizes the confined phase. In this limit, Wilson loops satisfy the *area law*

$$\langle \operatorname{tr} W[\mathscr{C}_{RT}] \rangle \sim e^{-\sigma RT} = e^{-\sigma A[\mathscr{C}_{R,T}]}, \tag{1.90}$$

where $A[\mathscr{C}_{R,T}]$ is the area enclosed by $\mathscr{C}_{R,T}$. In the small coupling limit, instead, $V(R) \sim 1/R$, yielding a Coulomb potential. This is easy to see also in continuum QCD. Considering the rescaled potential $\tilde{A}_\mu$, $\tilde{F}^a{}_{\mu\nu} = \partial_\mu \tilde{A}^a_\nu + \partial_\nu \tilde{A}^a_\mu + g f^{abc} \tilde{A}^b_\mu \tilde{A}^c_\nu$: when $g \to 0$ it reduces to the QED field strength and it is natural to expect an electric-like interaction. This is the so-called Coulomb phase and it is deconfined, since we need a finite amount of energy to keet the two quarks infinitely distant. Of course, when R is large $V(R) \sim 1/R$ does not contribute to the exponential damping of the Wilson loop. Other terms dominate and what holds now is the *perimeter law* [58]

$$\langle \operatorname{tr} W[\mathscr{C}_{RT}] \rangle \sim e^{-\alpha\, p[\mathscr{C}_{R,T}]}, \tag{1.91}$$

where now $p[\mathscr{C}_{R,T}]$ indicates the perimeter of the loops $\mathscr{C}_{R,T}$. Another common possibility is a Higgs phase. It is still deconfined, but gauge fields develop a mass gap and Coulomb-like interactions undergo a screening, thus becoming short-ranged. Wilson loops in the Higgs phase satisfy again the perimeter law [28].

The proportionality constant σ is different from 0 if there is confinement, while it vanishes in decofined phases. Then, the *string tension* σ can be seen as an order parameter for the confinement-deconfinement transition. To see why (1.89) holds, let us switch to the hamiltonian formalism. Here, working in the temporal gauge, the Wilson loop operator $\mathrm{tr}\,\hat{W}[\mathscr{C}_{R,T}] = \mathrm{tr}\left(\hat{U}[0,\vec{x};\,0,\vec{y}]\,\hat{U}[0,\vec{y};\,T,\vec{y}]\,\hat{U}[T,\vec{y};\,T,\vec{x}]\,\hat{U}[T,\vec{x};\,0,\vec{x}]\right)$ becomes

$$\mathrm{tr}\,\hat{W}[\mathscr{C}_{R,T}] = \mathrm{tr}\left(\hat{U}[0,\vec{x};\,0,\vec{y}]\,\hat{U}[T,\vec{y};\,T,\vec{x}]\right). \tag{1.92}$$

Now consider a system with $\hat{H} = \hat{p}^2/2m + V(\hat{x})$ in a euclidean time $t = -iT$. Then, its propagator is given by

$$K(T,x';\,0,x) = \langle x'|e^{-\hat{H}T}|x\rangle \underset{m\to\infty}{\longrightarrow} \delta(x-x')e^{-iV(x-x')T}\,. \tag{1.93}$$

If the initial and final states are not eigenstates of the hamiltonian in the static limit $m \to \infty$, we can expand them on the eigenstates $|n\rangle$ and

$$K(T,\phi';\,0,\phi) = \sum_n \langle\phi'|n\rangle\langle n|\phi\rangle\, e^{-E_nT} \underset{T\to\infty}{\sim} \langle\phi'|0\rangle\langle 0|\phi\rangle\, e^{-E_0T}\,. \tag{1.94}$$

The static limit can be taken again, thus leaving only the potential part of the energy. Now we repeat this procedure for the lattice theory. Consider a static quark-antiquark pair as the initial state

$$|\Phi_0\rangle = \bar{\hat{\Psi}}(0,\vec{x})\,\hat{U}[0,\vec{x};\,0,\vec{y}]\,\hat{\Psi}(0,\vec{y})\,|0\rangle\,. \tag{1.95}$$

We had to include a Wilson line $\hat{U}$, connecting the two points $(0,\vec{x})$ and $(0,\vec{y})$, to make $|\Phi_0\rangle$ a gauge-invariant state: physically this means that two quarks are always connected by a flux line of the gauge field. Their propagator is

$$\begin{aligned} G(T,\vec{x}\,',\vec{y}\,';\,0,\vec{x},\vec{y}) = \langle 0|\,T\big[&\bar{\hat{\Psi}}(T,\vec{y}\,')\,\hat{U}[T,\vec{y}\,';\,T,\vec{x}\,']\,\hat{\Psi}(T,\vec{x}\,') \\ &\bar{\hat{\Psi}}(0,\vec{x})\,\hat{U}[0,\vec{x};\,0,\vec{y}]\,\hat{\Psi}(0,\vec{y})\big]\,|0\rangle \end{aligned} \tag{1.96}$$

In the same limits that we have considered above, this reduces to

$$G(T,\vec{x}\,',\vec{y}\,';\,0,\vec{x},\vec{y}) \underset{\substack{m\to\infty\\ T\to\infty}}{\sim} \delta^3(\vec{x}\,'-\vec{x})\delta^3(\vec{y}\,'-\vec{y})\,C(\vec{x},\,\vec{y})\,e^{-V(R)T}\,. \tag{1.97}$$

$V(R)$ is the static quark potential and it is the lowest energy contained into the quark-antiquark state whose overlap with the ground is non vanishing. $C(\vec{x},\,\vec{y})$ is a function describing this overlap. But the two probes are static and the energy $V(R)$ is only that of the gauge field, apart from self-energy terms. The static quarks can be decoupled from the dynamics and what

(1.96) does is essentially to compute (1.89), up to the trace which does not change the exponential damping.

This sketched proof holds for time-like Wilson loops, but the confinement criterion is correct also for Wilson loop that live on a fixed-time surface [86]. The reason is that a Wilson loop operator on a spatial closed path $\mathscr{C}$ can be seen as the creator of a loop of electric flux along $\mathscr{C}$. Then $\langle 0|\mathrm{tr}\,\hat{W}[\mathscr{C}]|0\rangle$ becomes the tunneling amplitude of the electric flux loop into the vacuum, which is highly suppressed in the confined phase because flux tubes are stable. Confinement is a property of the gauge field themselves and the transition is driven by a drastic change in the properties of their vacuum. In fact, it is typically seen as a condensation of magnetic monopoles, which is somehow dual to the Cooper pair condensation of superconductors [22]. For instance, consider a U(1) pure-gauge theory. Polyakov showed that in three dimensions it is always in a confined phase thanks to the contribution of the instantons, forming a gas of magnetic monopoles which produces the linearly confining force between quarks. Thankfully, in four dimensions it has also a familiar small coupling Coulomb phase, in addition to the strong coupling confined phase [67, 68], while in 1+1 dimensions is trivially confining, since the Coulomb potential is already $V(R) \sim R$.

In general, it has been proven that for all compact gauge groups, both continuous and discrete, the corresponding LGT in any spacetime dimension has a confined phase for sufficiently strong couplings [58]. The behaviour of pure U(1) LGTs traces the continuum one: in $D = 3$ it is always confined, while in $D = 4$ there is also the Coulomb phase. The group U(1) can be approximated by $\mathbb{Z}_n$. In $D = 3$, a $\mathbb{Z}_n$ LGT of course has a strong coupling confined phase, but at small couplings it exhibits a deconfined Higgs phase (that can exist also in the pure gauge case, provided that it is defined according to the behaviour of Wilson and 't Hooft loops [60, 26]), which shrinks and tends to disappear in the $n \to \infty$ limit. When $D = 4$ the structure with a shrinking Higgs phase is similar, but the Coulomb phase appears only for $\mathbb{Z}_{n\geq 5}$. We underline that the spatial Wilson loop criterion holds only at zero temperature: discrete group LGTs at a finite temperature have an additional deconfined phase with area law behaviour [12, 13]. For the SU(2) and SU(3) groups it is considerably harder to extract continuum analytical results, while Monte Carlo lattice simulations using finite groups tend to show confinement at all couplings [20], even though QCD at small coupling has to be deconfined.

CHAPTER II.

Quantum simulations for lattice gauge theories

The main interest of this thesis is to study the behaviour of lattice gauge theories and in particular their phase diagram. The rich interactions they involve make them challenging to study analytically and, during the last decades, the interest in computer simulations of lattice gauge theories received an important incentive. However, our focus is slightly shifted: we are interested in quantum simulations, instead of simulations on classical computers. The reader will find in this chapter some considerations on how quantum simulations work in general and the description of more specific examples for lattice gauge theories.

2.1 Analog and digital simulations

Physics is typically studied within a bottom-up approach: the description of a complex object is usually obtained by first studying separately its smaller components and, then, by putting them together to understand the behaviour of the original system. Sometimes, however, the starting object may be composed of too many parts and the elevated complexity prevents us from carrying on this project until its very end. We need to find alternative routes that may lead us anyway to a good and predictive description of the system. Among the various possibilities, one is to simulate the system: we artificially reproduce its properties and its dynamical evolution within an environment which is completely under our control, called the simulator. Generally speaking, a simulation is usually divided into three steps. First, we have to figure out how to encode the information we have about the system into the simulator; here "information" can refer to the variables that characterize its state, or

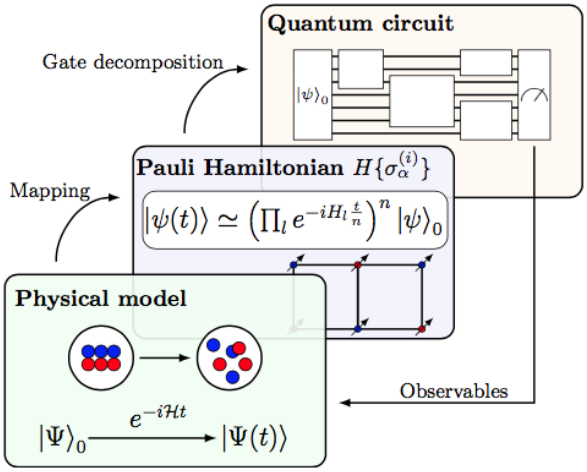

Figure 2.1: Representation of the steps of a digital quantum simulation. The model has to be encoded into the variables of the simulator, then its time evolution is decomposed into a collection of quantum gates and the outcome will be transformed back into an observable of the original system [81].

to the properties that we want to observe. After having given the simulator a proper initial state as the input, we have to elaborate it. This elaboration can be the time evolution of the properties of the system that we want to study and, in classical simulations of lattice gauge theories, this elaboration typically is the evaluation of path integrals with Monte Carlo techniques. The final step is the extraction of the output we need.

A straightforward example of a simulator may be a classical computer, but in principle any other well controlled physical system could be fine (and this is what allows us to overcome classical simulations when they run into trouble!). The examples can be many, but we are interested here in the case of quantum systems. When trying to simulate them, classical computers meet a few intrinsic problems that limit their usage, such as the previously mentioned sign problems that make the simulations of quantum many body systems difficult in a finite density region. Another fundamental issue is the exponential scaling of the dimension of the Hilbert space of the system with respect to its number of components, which causes an exponentially large request of storage resources. A possible solution was proposed by Feynman [24]: in 1982, he conjectured that using a controllable quantum device as a computing instrument would provide significant advantages in the simulation of quantum systems.

The Feynman's proposal is built upon the general idea that since nature ultimately behaves quantum mechanically, only a computing machine obeying quantum mechanical laws can be able to accurately simulate it. This quantum simulator has to be controllable, in the sense that we can adjust its degrees of freedom and we can freely modify its hamiltonian to mimic the ones of the original system under interest. It is clear that this approach will overcome the problem of the exponential scaling of memory demands, since also the dimension of the Hilbert space of the simulator will grow exponentially and we will be able to balance the requests with our new resources. Moreover, in the context of lattice gauge theories, the hamiltonian approach is known to be free of the sign problems, so if we realize the elaboration of the initial state as its time evolution we will be able to fully simulate it.

Quantum simulators may be both analog and digital [8]. Analog simulations represent the abstract system that we want to reproduce on a physical set-up under externally controlled conditions. The time evolution means actually letting the quantum system sit and evolve unperturbed (or else its state would collapse) for a chosen time interval and the extractions of the outputs are physical laboratory measurements. In a digital simulation, the system is encoded into a quantum computer, which aims to be a general purpose and programmable quantum device. The operations that we perform on the input state, like the time evolution, will be realized through the application of successive quantum gates. The computer should be universal in the sense that in this way we should be able to realize any operation. The figure 2.1 schematically represents the typical steps of a digital quantum simulation.

This difference between analog and digital simulators can be subtle, because in the end any quantum computer is a concrete quantum system and the extraction of the output will be a physical measurement. Today's quantum computers are mostly realized with superconducting qubits or with trapped ions trapped in an optical lattice: to realize a quantum gate we need to interact with the system, using proper circuits or through optical impulses! If we look inside the internal structure of a digital simulator of course we see an analog system, but the supposed universality of the digital simulators allows us to work without doing so. Usually analog simulators are specific purpose and their hamiltonians can be modified to reproduce a small class of quantum systems. Instead, universal computers can be used to simulate in principle any hamiltonian, independently of their internal structure. However, with the current technologies we should always be aware of what kind of quantum computer we are using, because different architectures have different advantages and drawbacks that need to be taken into account [81].

2.2 First step: encoding

In this section we describe more specifically how the steps sketched before work in the case of quantum simulations. Suppose that we want to simulate a system with hamiltonian H_0 and with Hilbert space $\mathcal{H}_0$. The first step was the encoding of the properties of the system within the degrees of freedom of the simulator, tha now is a quantum computer made of qubits. A qubit is an abstract two state quantum system, which can be represented in many ways: a spin 1/2 particle, or a two-level atom... Different physical realizations of a qubit provide different possible architectures of quantum computers.

Let $\mathcal{H}_{1/2} = \text{span}\{|0\rangle, |1\rangle\}$ be the Hilbert space of a single qubit. To encode the states of the system means to map its Hilbert space into the Hilbert space of an N-qubit quantum computer, which is $\mathcal{H} = \mathcal{H}_{1/2}^{\otimes N}$. This mapping should be an isomorphism $\mathcal{H}_0 \to \mathcal{H}$, or at least a 1-1 function, otherwise it could not be inverted and decoded in a univocal way. As a consequence, it holds the following fact: since $\dim \mathcal{H} = 2^N < \infty$, only finite dimensional systems can be exactly simulated. If $\dim \mathcal{H}_0 = \infty$, some kind of truncation of the Hilbert space must be involved and the quantum computer will necessarily simulate approximate properties of the system.

In addition to the states, we have to encode the observables into the ones of the quantum computer. On a single qubit, observables are hermitian operators, which can be represented in the Pauli basis as

$$A = \sum_{\mu=0}^{3} \lambda_\mu \sigma_\mu \ , \quad \sigma_\mu = (\mathbb{I}, \vec{\sigma}) \, ,$$

while quantum gates are by definition unitary and can be realized through their exponentials. Considering N qubits, each one will be associated to its set of Pauli matrices $\{\sigma_x^j, \sigma_y^j, \sigma_z^j\}$, $j = 1, \ldots, N$, satisfying an $\oplus_{j=1}^{N} \mathfrak{su}(2)_j$ algebra defined by the commutation and anticommutation relations

$$[\sigma_\mu^j, \, \sigma_\nu^k] = 2i\delta_{jk}\epsilon_{\mu\nu\lambda}\sigma_\lambda^j \ , \quad \{\sigma_\mu^j, \sigma_\nu^k\} = 2\delta_{\mu\nu}\delta_{jk}\mathbb{I} \, ,$$

where $\epsilon_{\mu\nu\lambda}$ is the totally antisymmetric Levi-Civita symbol. To encode the observables of the system into the quantum computer, we have to represent the hermitian operators A_0 on $\mathcal{H}_0$ in terms of Pauli matrices as $A = A(\{\sigma\})$ on $\mathcal{H}$, in such a way that the action of $A(\{\sigma\})$ on qubits is compatible with the one of A_0 on the abstract space $\mathcal{H}_0$. From a formal point of view, we have to build a *-algebra isomorphism $A_0 \to A = A(\{\sigma\})$ between the two operator algebras [78].

2.3 Second step: time evolution

After having understood how to digitalize the properties of the system respecting their quantum nature, we want to simulate its behaviour when we let it evolve under some specified external conditions. Of course, the first thing to do is to prepare the qubits in a properly chosen initial state. For example, if we want to simulate a fermionic many body system we may want the input state to reproduce a Slater determinant [64], or if we are studying a lattice gauge model the initial state may be better if chosen as gauge-invariant. Also the algorithms that we use to extract the final outputs may demand specific choices of initial states. The initial state preparation is a full fledged part of the computation, but we will not describe it in general since it strongly depends on the case under consideration.

Once we have prepared an appropriate initial state, we have to make it evolve forward in time by implementing the evolution operator $U(t) = e^{-iHt}$ (supposing that the hamiltonian H is time independent). Each quantum platform is endowed with its native set of unitary gates, which are the ones most easily realized on that kind of hardware [81]. For example, superconducting quantum computers have as their native set

$$\mathcal{S}_1 = \{R_\alpha(\theta), \text{CNOT}\} \ ,$$

where $R_\alpha(\theta) = \exp(-i\theta/2\sigma_\alpha)$ is a single qubit $\mathfrak{su}(2)$ rotation along the direction α and the CNOT is a two-qubit entangling gate that leaves always unchanged the first qubit (called the *control qubit*) while switching the second one when the control qubit is on (see Appendix B). Instead, trapped ions-quantum computers typically have as their native gates the set

$$\mathcal{S}_2 = \{T_1^{(1)}(\theta), \ \dots \ , T_1^{(N)}(\theta), T_2(\theta), T_3(\theta,\phi), T_4(\theta,\phi)\} \ ,$$

where

$$T_1^{(j)}(\theta) = \exp\big(-i\theta\sigma_z^j\big) \ ,$$
$$T_2(\theta) = \exp\Big(-i\theta\sum_{j=1}^{N}\sigma_z^j\Big) \ , \ T_3(\theta,\phi) = \exp\Big(-i\theta\sum_{j=1}^{N}\sigma_\phi^j\Big) \ ,$$
$$T_4(\theta,\phi) = \exp\Big(-i\theta\sum_{j<k}\sigma_\phi^j\sigma_\phi^k\Big)$$

and $\sigma_\phi = \sigma_x\cos\phi + \sigma_y\sin\phi$. The $T_1^{(j)}$'s are single qubit z rotations, T_2 and T_3 are collective non entangling gates, while T_4 is an entangling operation called Mølmer-Sørensen gate. These gates encode interactions of the kind

$\sigma_z^j \sigma_z^k$, where $j\,, k$ are not restricted to be neighbours, so trapped ions are best exploited to reproduce hamiltonians with non local multi-body interactions. Both $\mathcal{S}_1$ and $\mathcal{S}_2$ are universal, i.e. for any N-qubit unitary operator U there exists a combination of gates within each set whose composition realizes U exactly [81]. In particular, one can always find a quantum circuit that reproduces the evolution operator $U(t) = e^{-iHt}$, but nothing guarantees that this procedure will be efficient as the number of elementary operations required may blow up rapidly. Moreover, the decomposition in terms of elementary gates may be difficult to find. To avoid this issues, instead of trying to reproduce e^{-iHt} exactly, one usually implements an approximation based on the *Trotter formula* [61]: if the hamiltonian is a sum $H = \sum_l H_l$, then

$$\exp\left(-i \sum_l H_l\, t\right) = \lim_{n\to\infty} \left(\prod_l e^{-iH_l\, t/n}\right)^n . \tag{2.1}$$

In the finite dimensional case it is simply the Lie product formula, but it holds also for selfadjoint operators on infinite dimensional Hilbert spaces under proper assumptions. It can be shown that

$$\exp\left(-i \sum_l H_l\, t\right) = \prod_l e^{-iH_l\, t} \,+\, \mathcal{O}(t^2)\,, \tag{2.2}$$

which means that we can approximate the desired unitary operator by the independent application of the sequence of gates corresponding to the individual evolution operators $e^{-iH_l t}$, but this approximation will be increasingly worse when we want the system to evolve for a longer time t. When $H = \sum_l H_l$ is composed of locally interacting subsystems, the exponentials $e^{-iH_l t}$ will be substantially simpler to implement than the full operator e^{-iHt}, so to exploit this advantage also when t is longer we can divide it into n *Trotter steps* $\Delta t = t/n$ (with n sufficiently large) and iterate this approximation along each time slice Δt, thus realizing the evolution operator as

$$e^{-iHt} = \left(e^{-iH\Delta t}\right)^n \approx \left(\prod_l e^{-iH_l \Delta t}\right)^n . \tag{2.3}$$

Following this approach, Lloyd proved in 1996 [50] that we can simulate e^{-iHt} efficiently (i.e. with polynomial time and storage resources in the size of the target system) if H is a sum of *local* interaction terms H_l that act only on a small subsystem of the full Hilbert space.

The proof goes as follows [81]. A general unitary operator on N qubits acts on a 2^N dimensional space and it can be implemented with $\mathcal{O}(2N)$ elementary operations [61], which is, in general, inefficient. However, for a local system each component H_l acts on a small subspace. Let m_l be its dimension

(typically $m_l \ll 2^N$), hence H_l can be realized in $\mathcal{O}(m_l^2)$ operations. The system is characterized by some degree of locality p (e.g. the number of nearest neighbours, or next-to-nearest neighbours...). The number of local terms, then, scales polynomially with the number of qubits as $L \propto p \cdot N$. To compute the full product of the L elementary time evolutions, we need $\mathcal{O}(Lm_{max}^2)$ elementary operations, which is polynomial in the number of qubits as long as $L = \text{poly}(N)$. The more local are the interactions, the simpler will be to simulate them efficiently with this kind of approximation.

On one hand we are lucky, because physically meaningful interactions are typically local. But, on the other hand, the physical local hamiltonian is H_0, not H, and it has undergone an encoding procedure $H_0 \to H$ which in some cases happens to generate new non local interaction terms that increase the complexity. As already pointed out, when they arise, trapped-ions platforms allow to realize them in the simplest way.

Today we are in the so called "NISQ era" of quantum computation [69], meaning that state-of-the-art quantum devices are noisy and intermediate-scale. In practice, we don't have enough qubits to spare for error correction and a larger amount of gates will inevitably introduce a larger noise in the circuit, spoiling the precision of the computation. If we want to improve the precision of our simulation of the evolution for a time interval t, the Trotter decomposition requires to increase the number n of Trotter steps, correspondingly increasing the number of elementary evolutions we have to perform and the depth of the circuit. This attempt to improve the precision ends up worsening the noise, thus limiting the improvements that we can actually make. This results in a limit on the number of gates that we can use to trotterize the evolution which today is fewer than 10^3 gates [81], which, for instance, forces us to choose between a precise time evolution for a short time and an evolution for a longer time but with larger errors.

2.4 Third step: measurements

Once we have a codified version of the time-evolved initial state $e^{-iHt}|\psi_i\rangle$, we need to extract as outputs the observables we are interested in. To do so, in quantum computation we always assume that we are able to perform projective measurements in the computational basis. Any observable is encoded into a hermitian operator acting on N qubits, which is diagonalizable and by the spectral theorem there is a unitary transformation that maps the eigenvectors of the observable under interest into the computational basis. Suppose that, after the time evolution, we are left with the state $|\psi\rangle$ and that we are interested in measuring an observable A [18]. Let the eigenstates

of the operator A be $|A_j\rangle,\ j \in \mathbb{N}$. Then we can express

$$|\psi\rangle = \sum_j |A_j\rangle\, c_j, \tag{2.4}$$

for some constants c_j. There exists a unitary operator U_A such that it sends the jth A eigenstate $|A_j\rangle$ into the jth computational basis state, that we choose to denote $|j\rangle$. If we apply this rotation on $|\psi\rangle$ we find

$$U_A|\psi\rangle = \sum_{j=1}^{\infty} |j\rangle\, c_j \tag{2.5}$$

and now a projective measurement along the jth computational basis state will provide us the amplitude of the jth A eigenstate c_j. The unitary operator U_A will be implemented as a proper sequence of quantum gates, so also the measurement has to be considered as a part of the computation and it shall undergo the requirement of efficiency. The problem is that U_A is not an evolution operator generated by a physical hamiltonian and nothing guarantees that its realization will be efficient. Therefore to extract the observables one usually has to follow specific algorithms, each one tailored to extract a small class of them.

In the following, we will show some examples. The first one is a way to extract dynamical correlation functions [81] which are defined as

$$\mathcal{C}_{VW}(t) = \langle\psi|e^{iHt}V^\dagger e^{-iHt}W|\psi\rangle\,, \tag{2.6}$$

where V, W are two unitary operators and $|\psi\rangle$ is a state that we assume to be prepared in some way. The circuit that extracts $\mathcal{C}_{VW}(t)$ is shown in figure 2.2. We need an ancillary qubit that starts in the state $|+\rangle_a = (|0\rangle + |1\rangle)/\sqrt{2}$. Then, on the main register R prepared in the state $|\psi\rangle_R$ we apply first a controlled operator $c-W$, then $U(t) = e^{-iHt}$ and last a $c-V$ operator, controlled by the value $|0\rangle_a$ of the ancilla. This chain of operations produces

$$\begin{aligned} |\psi\rangle_R &\mapsto \frac{1}{\sqrt{2}}\Big(|0\rangle_a|\psi\rangle_R + |1\rangle W|\psi\rangle_R\Big) \\ &\mapsto \frac{1}{\sqrt{2}}\Big(|0\rangle_a U(t)|\psi\rangle_R + |1\rangle U(t)W|\psi\rangle_R\Big) \\ &\mapsto \frac{1}{\sqrt{2}}\Big(|0\rangle_a VU(t)|\psi\rangle_R + |1\rangle U(t)W|\psi\rangle_R\Big) \equiv |\Psi_{out}\rangle \end{aligned} \tag{2.7}$$

Then, a measurement of σ_x on the ancilla yields the expectation value

$$\langle\sigma_x^{(a)}\rangle = \mathrm{tr}\Big[|\Psi_{out}\rangle\langle\Psi_{out}|\left(\sigma_x^{(a)}\otimes\mathbb{I}\right)\Big] = \mathrm{Re}\left[\mathcal{C}_{VW}(t)\right], \tag{2.8}$$

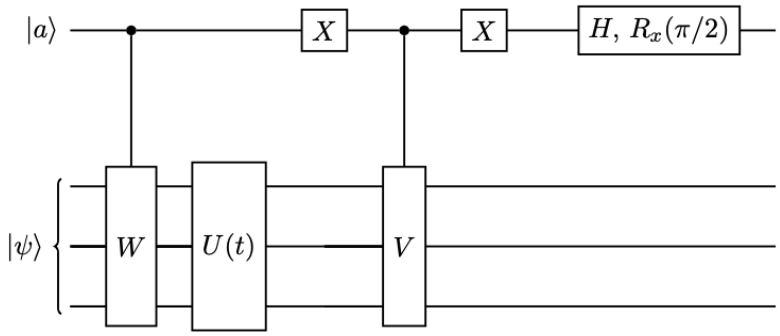

Figure 2.2: Quantum circuit for extracting dynamical correlators on a generic state $|\psi\rangle$, making use of an ancilla qubit $|a\rangle$. The last gate is H for its real part and the rotation gate measures its imaginary part.

while in a similar way it can be seen that measuring σ_y gives

$$\langle \sigma_y^{(a)} \rangle = \mathrm{tr}\Big[|\Psi_{out}\rangle\langle\Psi_{out}| \left(\sigma_y^{(a)} \otimes \mathbb{I}\right)\Big] = \mathrm{Im}\left[\mathcal{C}_{VW}(t)\right]. \tag{2.9}$$

Hence, through repeated measurements of the observables $\sigma_x^{(a)}$, $\sigma_y^{(a)}$ we can extract the complete value of $\mathcal{C}_{VW}(t)$. To measure them we use the procedure described before, that is we rotate their eigenvectors into the computational basis, using for σ_x a Hadamard gate H and for σ_y a $\pi/2$ rotation $R_x(\pi/2)$.

The second example exploits the procedure we have just described in a quantum-classical hybrid algorithm that extracts the spectrum of an arbitrary hermitian operator. Suppose that the time evolved operator V in $\mathcal{C}_{VW}$ is $V = \mathbb{I}$ and $W = U_{\mathcal{Q}}(\theta) \equiv e^{-i\mathcal{Q}\theta}$, $\mathcal{Q}$ being the hermitian operator we want to study. Then, the observable is just $\mathcal{C}_{\mathcal{Q}}(\theta) = \langle\psi|U_{\mathcal{Q}}(\theta)|\psi\rangle$ and the procedure described above extract the expectation value of the "evolution operator" $U_{\mathcal{Q}}(\theta)$ at a parametric "time" θ. Suppose that the initial state $|\psi\rangle$ where we compute $\mathcal{C}_U(\theta)$ is prepared in a linear combination of some eigenstates of $\mathcal{Q}$

$$|\psi\rangle = \sum_j |q_j\rangle\, \psi_j\,. \tag{2.10}$$

Then, using the method described before, we are able to measure

$$\langle\psi|U_{\mathcal{Q}}(\theta)|\psi\rangle = \sum_j |\psi_j|^2 e^{-iq_j\theta}\,, \tag{2.11}$$

where the number q_j is the eigenvalue of $\mathcal{Q}$ corresponding to $|q_j\rangle$. If we apply

a classical fast Fourier transform on eq. (2.11), it results in

$$\mathrm{FFT}\left(\langle U_{\mathcal{Q}}(\theta)\rangle\right) = 2\pi \sum_j |\psi_j|^2 \delta(q - q_j)\,, \tag{2.12}$$

meaning that we are able to extract the eigenvalues q_j contained in $|\psi\rangle$ by looking at the peaks of function resulting from the fast Fourier transform.

2.5 Simulating lattice gauge theories

Since our main goal is to simulate lattice gauge theories on a quantum computer, so let us specify the procedure that we have outlined before for this case. The first thing to do if we want to simulate a system is to encode its state into the one of the simulator and this has to be done through a Hilbert space isomorphism. Remember that an exact encoding is possible only for finite dimensional quantum systems. In our case, for instance, it implies that fermions can be exactly encoded, because their Hilbert space is kept finite dimensional by the Pauli exclusion principle. Instead, for an infinite order gauge group, $\dim L^2(G) = \infty$ and it is impossible to map via an injection all its states into the finite dimensional qubit Hilbert space. How can we overcome this issue? There are several approaches that allow us to solve it and the next subsections will be dedicated to some of them. Of course, in general these methods are approximations and apart from very specific cases an exact encoding remains unfeasible.

2.5.1 Hilbert space truncation

The first possibility is a direct truncation of the Hilbert space $\mathscr{H}_G$. The accuracy of this approximation will depend on how many states we remove but also on which are the states that we choose to remove. Let's consider the example of a $U(1)$ gauge theory without matter where, for definiteness we put $a = 1$. In this case the Kogut-Susskind hamiltonian becomes:

$$H = \frac{g^2}{2} \sum_{x,\mu} \ell^2(x,\mu) - \frac{1}{g^2} \sum_{\square} \left(W_\square + W_\square^\dagger\right) \tag{2.13}$$

$$W_\square = e^{iA(x,\mu)} e^{iA(x+\mu,\nu)} e^{-iA(x+\nu,\mu)} e^{-iA(x,\nu)}\,. \tag{2.14}$$

$U(1)$ is one dimensional, so the Lie algebra index disappears, moreover it is abelian and the order of the comparators in the Wilson plaquette operator

is irrelevant. If we define $U = e^{iA}$, the relations (1.79), (1.80) are

$$[\ell, U] = -U \tag{2.15}$$
$$[\ell, U^\dagger] = U^\dagger. \tag{2.16}$$

The Hilbert space of a single link may be generated by successive applications of U on the electric vacuum $|0\rangle$ [16], defined as the state satisfying

$$\ell(x,\mu)|0\rangle = 0 \quad \forall\, x, \mu\,. \tag{2.17}$$

The name "electric" comes from the fact that in the $g \to \infty$ limit the electric term dominates in the hamiltonian and the null eigenstate of ℓ is the ground state. Then, the states $|l\rangle \equiv (U)^l|0\rangle$ are orthogonal and they satisfy

$$\ell^2|l\rangle = |l\rangle\, l^2 \tag{2.18}$$
$$U|l\rangle = |l+1\rangle \tag{2.19}$$
$$U^\dagger|l\rangle = |l-1\rangle\,. \tag{2.20}$$

These states are the electric field eigenstates and they yield another basis for the single link Hilbert space, different from the group elements basis $\{|U\rangle\}$, which is made of eigenstates of the magnetic field. $|U\rangle$ is an eigenstate of H in the opposite limit $g \to 0$. The Hilbert space can be identified with $\text{span}\{|l\rangle \mid l \in \mathbb{Z}\}$ and it is clearly impossible to encode it into N qubits. One way to proceed is to perform a truncation of the allowed values of l

$$l \in \{-\infty, ..., +\infty\} \;\to\; l \in \{-l_{max}, ..., +l_{max}\}\,.$$

If we have N qubits available for a link, the maximum index allowed will correspond to $l_{max} = \lfloor (2^N - 1)/2 \rfloor$. Now the Hilbert space has become finite dimensional and it can be rewritten in the qubit spin language. The abstract state $|l\rangle$ becomes a state of the register $|l\rangle \to |l\rangle_{reg}$ and the operators of the equations (2.18)-(2.20) will be encoded into

$$\ell^2|l\rangle_{reg} = |l\rangle_{reg}\, l^2 \tag{2.21}$$
$$U^+|l\rangle_{reg} = |l+1\rangle_{reg} \qquad U^+|+l_{max}\rangle_{reg} = 0 \tag{2.22}$$
$$U^-|l\rangle_{reg} = |l-1\rangle_{reg} \qquad U^-|-l_{max}\rangle_{reg} = 0\,. \tag{2.23}$$

A simple (but inefficient) way to implement them using Pauli matrices is

$$\ell^2 = \sum_{l=-l_{max}}^{+l_{max}} l^2(\sigma_z^l + 1)/2 \tag{2.24}$$

$$U^+ = \sum_{l=-l_{max}}^{+l_{max}} \sigma_+^l \sigma_+^{l+1} \tag{2.25}$$

$$U^- = \sum_{l=-l_{max}}^{+l_{max}} \sigma_+^l \sigma_-^{l+a}\,, \tag{2.26}$$

where $\sigma_\pm = \sigma_x \pm i\sigma_y$ are the Pauli raising and lowering operators. These are all the ingredients needed to carry on the simulation; the only thing we have got to do is to choose a good value for l_{max}. Usually the most dominant terms are contained into $l_{max} \sim 5 - 10$ [16, 41]. A possible way to make the choice is to repeat the simulation a few times to extract values of the observables corresponding to different values of l_{max}, in order to analyze their convergence.

There are other possible choices that can be made to cut the dimensionality of the Hilbert space. One may choose to impose an energy cutoff in order to keep only the states closer to the ground, which are more likely to be occupied and they should be the dominant eigenstates of the time evolution operator. Another possibility is to work within the framework of the so-called "quantum link models" (cf. section 2.5.3), which represent all observables using spin s operators that preserve the abstract commutation relations but will act on a $2s + 1$ dimensional Hilbert space.

2.5.2 Gauge fields integration

This subsection is dedicated to a special but very interesting case where it is possible to carry on the simulation of the full theory, without the need of approximations to encode the states [54]. This case is the Schwinger model, i.e. a 1d $U(1)$ gauge theory with fermions. So far we have discussed the inclusion of matter only for scalar fields, because it was the simplest case and it was not necessary either to go deeper into that direction, since the original part of this work focuses on pure gauge theories. However, the inclusion of fermion fields on a lattice is not a trivial matter and a few words about it may be useful. We call "naive" the introduction of lattice fermions where we let the field $\psi(x)$ live on each site of the lattice $x \in \Lambda$ like it is done for scalar fields. This naive introduction leads to the famous *fermion doubling problem*: in the continuum limit, a single fermion field corresponds to several

particles, meaning that unphysical fermions called "doublers" have appeared. An important no-go theorem, called the *Nielsen-Ninomiya theorem*, states that any lattice action with fermions satisfying the usual requirements of locality, translational invariance, hermiticity of the corresponding hamiltonian and chirality (necessary to reproduce the Standard Model) will unavoidably meet the presence of doublers. Any sensible way to introduce fermions on a lattice has to break one of these assumptions. There are several ways to do it and, among them, a common one is the usage of *staggered fermions*, which break locality by spreading $\psi(x)$ on several sites by the introduction of another fermion field $\Psi(x)$. This method has been developed by Susskind [80] in the 70s and it has found several applications that have become standard in lattice gauge theories [58, 32]. Recently it has received a renovated attention in the field of quantum simulations [7, 23, 54]. In d=1 the lattice is a chain with sites labelled with $n = 1, ..., N$, so we can identify the links as $(n, n+1)$. On each site there is a staggered fermion Ψ_n, while the electric field operators $\ell_{n,n+1}$ and the comparators $U_{n,n+1}$ are defined on links. In this 1d theory with continuous time, the naive introduction of fermions causes the presence of one doubler for each physical particle and staggered fermions solve the problem by separating its particle and antiparticle degrees of freedom into two sites: on even sites Ψ_n is the positive energy part of ψ and on odd sites it corresponds to its negative energy part [51].

Being a one dimensional model, there is no magnetic field in this case. For convenience, we rescale $A \to A/g$, $\ell \to g\,\ell$, making the electric charge g disappear from the charge density term in (2.28) [23]. The hamiltonian is

$$H = J \sum_{n=1}^{N-1} \ell_{n,n+1}^2 - iw \sum_{n=1}^{N-1} \left(\Psi_n^\dagger U_{n,n+1} \Psi_{n+1} - h.c. \right) + m \sum_{n=1}^{N} (-1)^n \Psi_n^\dagger \Psi_n \quad (2.27)$$

where the first is the electric term, the second is the matter gauge-kinetic term and the last one is the mass term for the staggered fermion field. The constraint that determines the physical Hilbert space corresponds to the imposition of the generalization of the Gauss's law, which takes the form

$$\mathscr{G}_n \, |\text{phys}\rangle = 0 \ , \ \ \mathscr{G}_n = \Psi_n^\dagger \Psi_n - (\ell_{n,n+1} - \ell_{n-1,n}) + \frac{1}{2} \left[(-1)^n - 1 \right] \quad (2.28)$$

The special feature of this theory is the following: if we can restrict ourselves to the physical Hilbert space, the gauge bosons disappear completely and we avoid the problem of representing their infinite dimensional Hilbert space on a quantum computer. Let us start by encoding the fermions into the qubit Hilbert space. The fermion field operators Ψ_n can be mapped into

spin operators using a Jordan-Wigner transformation [64]

$$\Psi_n \rightarrow \prod_{l<n} \left[i\sigma_z^l \right] \sigma_-^n \tag{2.29}$$

and $U_{n,n+1} = e^{igA_{n,n+1}}$ can be removed by the gauge transformation

$$\sigma_-^n \rightarrow \prod_{l<n} \left[e^{-igA_{n,n+1}} \right] \sigma_-^n \,, \tag{2.30}$$

which transforms the hamiltonian into $H \rightarrow H'$, where

$$H' = J \sum_{n=1}^{N-1} \ell_{n,n+1}^2 + w \sum_{n=1}^{N-1} (\sigma_+^n \sigma_-^{n+1} + h.c.) + \frac{m}{2} \sum_{n=1}^{N} (-1)^n \sigma_z^n \,. \tag{2.31}$$

After the gauge transformation, the Gauss's law has taken the form

$$\ell_{n,n+1} - \ell_{n-1,n} = \frac{1}{2} [\sigma_z^n + (-1)^n] \tag{2.32}$$

and, assuming open boundary conditions, we can solve it by choosing an initial value $\ell_{1,2} = \epsilon_0$ and then solving for the successive ones, finding

$$\ell_{n,n+1} = \epsilon_0 + \frac{1}{2} \sum_{l=1}^{n} \left[\sigma_z^l + (-1)^l \right] . \tag{2.33}$$

Eventually, the hamiltonian becomes the following (if for simplicity $\epsilon_0 = 0$)

$$H'' = H_{ZZ} + H_{\pm} + H_Z \tag{2.34}$$

$$H_{ZZ} = \frac{J}{2} \sum_{n=1}^{N-2} \sum_{l=n+1}^{N-1} (N-l) \sigma_z^n \sigma_z^l \tag{2.35}$$

$$H_{\pm} = w \sum_{n=1}^{N-1} \left(\sigma_+^n \sigma_-^{n+1} + h.c. \right) \tag{2.36}$$

$$H_Z = \frac{m}{2} \sum_{n=1}^{N} (-1)^n \sigma_z^n - \frac{J}{4} \sum_{n=1}^{N-1} [1 - (-1)^n] \sum_{l=1}^{n} \sigma_z^l \,. \tag{2.37}$$

We see that all the gauge variables have completely disappeared. This means that we don't need to bother to find how to represent the infinite states of the electric fields, because its dynamics is already contained into the effective interaction terms among all fermions and if we need to recover the electric

fields we can always use eq. (2.33). Using this approach we have traded the problem of the infinite dimensions with the complexity of the hamiltonian and in particular of its term H_{ZZ}, which contains long distance interaction terms of the kind $\sigma_z^n \sigma_z^l$. As already pointed out, they are more difficult to treat but can be implemented on a trapped ions quantum computer using Mølmer-Sørensen gates [54, 81].

2.5.3 Quantum link models

The Kogut-Susskind hamiltonian of a lattice gauge theory is constructed using the comparator U, used to form the magnetic term, and the left translation operator ℓ, which is the surrogate for (minus) the electric field. Being the basic building blocks, their operator algebra identifies the abstract model we are studying. Considering again a pure U(1) theory for simplicity. The algebra of ℓ and U is encoded into the commutators

$$\begin{aligned} [\ell_{x,x+\hat{i}},\, U_{x',x'+\hat{i}'}] &= -\delta_{x,x'}\delta_{i,i'}\, U_{x,x+\hat{i}} \\ [\ell_{x,x+\hat{i}},\, U^\dagger_{x',x'+\hat{i}'}] &= \delta_{x,x'}\delta_{i,i'}\, U^\dagger_{x,x+\hat{i}} \\ [U_{x,x+\hat{i}},\, U^\dagger_{x',x'+\hat{i}'}] &= 0\,, \end{aligned} \tag{2.38}$$

where each operator is intended to be defined on the same link, since operators on different links simply commute. On a lattice, the generator of U(1) gauge transformations is $\mathscr{G}(x) = \sum_{i=1}^{d} \left(\ell_{x,x+\hat{i}} - \ell_{x-\hat{i},x}\right)$, the discrete version of $\vec{\nabla}\cdot\vec{E}$. Gauge invariance is guaranteed by $[H, \mathscr{G}(x)] = 0$ and this relation holds irregardless of the $[U, U^\dagger]$ commutator, which is never involved. Consider the 3d spin operators S^i, $i = 1, 2, 3$. Together with their corresponding ladder operators $S^\pm = S^1 \pm iS^2$, they satisfy $[S^3, S^\pm] = \pm S^\pm$: this reproduces the main part of (2.38), so under the replacements

$$\ell_{x,x+\hat{i}} \quad \to \quad S^3_{x,x+\hat{i}} \tag{2.39}$$

$$U_{x,x+\hat{i}} \quad \to \quad S^-_{x,x+\hat{i}} \tag{2.40}$$

$$U^\dagger_{x,x+\hat{i}} \quad \to \quad S^+_{x,x+\hat{i}}\,, \tag{2.41}$$

the algebra (2.38) is modified into the following one

$$\begin{aligned} [S^3_{x,x+\hat{i}},\, S^-_{x',x'+\hat{i}'}] &= -\delta_{x,x'}\delta_{i,i'}\, S^-_{x,x+\hat{i}} \\ [S^3_{x,x+\hat{i}},\, S^+_{x',x'+\hat{i}'}] &= \delta_{x,x'}\delta_{i,i'}\, S^+_{x,x+\hat{i}} \\ [S^-_{x,x+\hat{i}},\, S^+_{x',x'+\hat{i}'}] &= -2\delta_{x,x'}\delta_{i,i'}\, S^3_{x,x+\hat{i}} \end{aligned} \tag{2.42}$$

and the hamiltonian defines another kind of lattice theory, called *quantum link model*, which preserves the same gauge symmetry as the original model, because the only commutator that gets modified is $[U, U^\dagger]$. In contrast to (2.38), the new building blocks are finite dimensional spin operators and (2.42) can be realized on a finite number of qubits. The drawback of quantum link models is that the structure of the gauge coupling is altered: the new comparator is no longer unitary, since

$$(S^\pm)^\dagger S^\pm = S^\mp S^\pm \neq \mathbb{I}\,. \tag{2.43}$$

The commutators (2.42) are collection of copies of the $\mathfrak{su}(2)$ algebra and it has an infinite number of finite dimensional representations, each labelled by its spin s. The choice of s determines the dimension of the Hilbert space of a single link as $\dim \mathscr{H}_1 = 2s+1$, therefore we can expect to improve the approximation of the Kogut-Susskind theory by choosing larger values of s, ultimately recovering an infinite dimensional $\mathscr{H}_1$ for $s \to \infty$. Suppose that we have chosen a value of s to work with. In this context, the eigenstates of the electric field $|e\rangle$ correspond to states with a well-defined value of S^3. Then $S^3|e\rangle = |e\rangle\, e$, $e = -s, \ldots, +s$ and $\mathscr{H}_1 = \text{span}\{|e\rangle\}$. The comparators $S^\pm$ are ladder operators on these states: they increase or decrease the value of the electric flux by one unit, until we reach the boundary states $|-s\rangle$ and $|+s\rangle$, which get annihilated respectively by S^- and S^+. This is the main difference with Yang-Mills-like gauge theories, whose comparator is unitary and will never annihilate a charged physical state with finite norm.

We have considered here a simple pure-gauge U(1) QLM, but matter can be straightforwardly added, since fermions are untouched by the identification with spin operators. The only difference with the Schwinger model discussed in the previous subsection is that we have to replace $\ell \to S^3$ also in the Gauss's law (2.28). Quantum link models were first introduced by David Horn in 1981 [39] for SU(2) and they have been extended also for QCD [14] and other gauge groups [17]. Some explicit constructions for quantum simulations have been proposed, such as in [94].

2.5.4 Finite group approximation

In order to avoid the loss of unitarity typical of quantum link models, we will purse an alternative approach that consists in approximating the continuous gauge group with one of its finite subgroups. When G is finite, there are no convergence problems and $L^2(\mathrm{G})$ becomes the space of all functions on G, which is isomorphic to the free vector space generated by all elements of G (cf. Appendix A). Therefore $\dim L^2(\mathrm{G}) = |\mathrm{G}| < \infty$ and the gauge

bosons can be encoded into a qubit register. The subgroup has to be chosen properly to best reproduce the geometry of the original gauge group, for example a good choice for approximating $\mathrm{U}(1) \cong \{e^{i\theta} \,|\, \theta \in [0, 2\pi[\,\}$ may be $\mathbb{Z}_n \cong \{e^{2\pi i k/n} \,|\, k = 0, 1, ..., n-1\}$. For more complicated groups the choice becomes less trivial; let us consider the case of SU(2). It is well known that SU(2) and SO(3) are locally isomorphic via a double covering $\mathrm{SU}(2) \to \mathrm{SO}(3)$ and as a manifold $\mathrm{SU}(2) \cong S^3$. SO(3) contains as subgroups the symmetry groups of three dimensional polyhedra, e.g. the tetrahedral group T or the octahedral group O. These groups are a 3d generalization of the dihedral groups D_n, the symmetry groups of flat polygons. We can use the covering $\mathrm{SU}(2) \to \mathrm{SO}(3)$ to lift a subgroup $\mathrm{H} < \mathrm{SO}(3)$ to a subgroup $2\mathrm{H} < \mathrm{SU}(2)$ with twice the elements of H called "binary group". So a proper choices of finite subgroups for SU(2) might be the binary polyhedral groups like $2T$ or $2O$. This approach has been studied thoroughly in [20] in the context of Monte Carlo simulations, while we are interested in quantum simulations. The next chapter is dedicated to explain a general method that allows us to simulate any finite group pure-gauge theory.

CHAPTER III.

Simulating a general finite group LGT

We have already pointed out that with a finite gauge group the encoding of gauge bosons is possible, but of course the details on how to do it will depend on the specific case we choose. The simplest example probably is $G = \mathbb{Z}_2$, so that $\mathscr{H}_1 = L^2(G) \cong \text{span}\{|+1\rangle, |-1\rangle\}$: the Hilbert space of a link is a single qubit. We restrict our attention to pure finite group-gauge theories. Suppose that we have already mapped the states of the gauge bosons on each single link on a qubit register, whose basis states will be denoted as $|g\rangle$. A generic state is a function $f : G \to \mathbb{C}$, that in Dirac's notation can be expanded as

$$|f\rangle = \sum_{g \in G} |g\rangle\langle g|f\rangle = \sum_{g \in G} |g\rangle f(g)\,. \tag{3.1}$$

The Hilbert space is endowed with the discrete version of the L^2 inner product

$$\langle f|g\rangle = \sum_{h \in G} f(h)^* g(h)\,. \tag{3.2}$$

Then it is possible to define a set of "high level" gates into which the evolution can be decomposed:

1. inversion gate: $\mathfrak{U}_{-1}|g\rangle = |g^{-1}\rangle$ (3.3)
2. multiplication gate: $\mathfrak{U}_{\times}|g\rangle|h\rangle = |g\rangle|gh\rangle$ (3.4)
3. trace gate: $\mathfrak{U}_{tr}(\theta)|g\rangle = |g\rangle\, e^{i\theta\,\mathrm{Re}(\mathrm{tr}[g])}$ (3.5)
4. Fourier gate: $\mathfrak{U}_F \sum_{g \in G} f(g)|g\rangle = \sum_{\rho \in \hat{G}} \sum_{i,j=1}^{d_\rho} \hat{f}(\rho)_{ij}|\rho, ij\rangle\,.$ (3.6)

The first gate maps an element of the group to its inverse, the second realizes the group left multiplication, the third one is a multiplication to a phase related to the trace of the group element and the last gate is a group-theoretic generalization of the Fourier transform that we are going to discuss later. They are are all unitary transformation with respect to the inner product above defined. If one is able to realize these gates for the chosen gauge group using the native universal gates of the quantum computer at hand, then the time evolution can be implemented following the procedure that is given in Section 2. Before describing the algorithm in detail, we have to go back to the formulation of the hamiltonian theory, since the Kogut-Susskind hamiltonian is defined only for compact Lie groups and we want to extend it for finite groups. This is done in the first section, while we keep the second one for the description of the general simulation procedure.

3.1 Hamiltonian for a finite gauge group

We had already remarked a few times that lattice gauge theories make sense also with a finite gauge group, since the theory is constructed using only group-valued variables. This is clear in the path integral formalism, but looking at the hamiltonian it is less evident, as the electric field in the Kogut-Susskind hamiltonian for compact Lie groups (1.83) is a Lie algebra-valued object, ℓ_a, even on a lattice. One possibility to obtain an electric term for a finite group could be to work within the transfer matrix approach like we explained in the first chapter, since for path integrals everything is well defined [48]. Another more "intrinsic" way is possible if we take a better look at the Kogut-Susskind hamiltonian. We shall see that its structure is deeply related to the representation theory of the gauge group and their relationship is crucial to develop an algorithm able to simulate them.

3.1.1 Geometric interpretation of the hamiltonian

Let us recall for convenience the form of the Kogut-Susskind hamiltonian:

$$H_{KS} = H_E + H_B = \frac{g^2}{2a^{d-2}} \sum_{(x,i)} \sum_a \ell_a(x,i)^2 - \frac{1}{g^2 a^{4-d}} \sum_\square \Big(\operatorname{tr} W_\square + \operatorname{tr} W_\square^\dagger \Big) .$$

The Hilbert space associated to each link is the group algebra $\mathscr{H}_1 = L^2(\mathrm{G})$, so that globally the overall Hilbert space is given by the tensor product

$$\mathscr{H} = \bigotimes_{links} L^2(\mathrm{G}) .$$

As we have anticipated, the magnetic term is fine also when the gauge group G does not have a Lie algebra, therefore we shall focus on the electric part. As long as H_E is concerned, the dynamics of the links is decoupled: it is a sum on all links of the square of the operator ℓ_a, generator of left translations on the group algebra. More in detail, ℓ_a is a first order differential operator generating translations on the functions defined on the group along the direction a of the group itself (it drags the points along the integral curve of the generator T_a of G, seen as a left-invariant vector field). The interpretation for the electric hamiltonian of a single link is clear: it is (proportional to) the Laplace-Beltrami operator on the group manifold [58]

$$\sum_{a=1}^{\dim \mathfrak{g}} \ell_a^2 = -\Delta_G \,. \tag{3.7}$$

The metric with respect to which this laplacian is defined is the bi-invariant metric on G induced by its Killing form [36]. Since we are assuming to work with a compact gauge group, such as SU(N), the Killing form is negative definite [71] and if we put it in canonical form we get the minus sign written above. The electric term looks like a typical kinetic term, proportional to the laplacian operator acting on the wavefunction. In order to see better how it acts on the $L^2(\mathrm{G})$ wavefunctions, notice that this is also the expression of the quadratic Casimir operator in the regular representation Ω and it commutes with any other representation matrix within the regular representation:

$$[\Omega, L_g] = 0 \quad \forall\, g \in G \,. \tag{3.8}$$

By the Schur's lemma, it acts trivially on each irreducible subspace contained into $\mathcal{H}$. Therefore, our next step is to reduce the regular representation.

3.1.2 The representation basis

Up to now, we have always worked using the "position" basis of $\mathcal{H}$ made by the group elements $|g\rangle$. Generally speaking, in quantum mechanics there is another relevant basis which is the one made of momentum eigenstates and it can be extended also to this context. Remember that the elements of $\mathcal{H}$ are functions on the group. Any $|\psi\rangle \in \mathcal{H}$ can be expanded as

$$|\psi\rangle = \int_G dg\ \psi(g)\, |g\rangle \tag{3.9}$$

and the elements of the position basis are associated to Dirac delta functions: the basis vector $|g\rangle$ corresponds to the distribution

$$e_g(h) \equiv \langle h|g\rangle = \delta(g,h). \tag{3.10}$$

When the gauge group is continuous, we take as inner product the usual

$$\langle\varphi|\psi\rangle = \int_G dg\, \varphi^*(g)\, \psi(g)\,. \tag{3.11}$$

In order to define our "momentum" basis, we have to define a proper set of functions of the group G. Given a representation $\rho : \mathrm{G} \to \mathrm{GL}(\mathrm{V}_\rho)$, consider the group function

$$\bar{\rho}_{ij} :\ G \to \mathbb{C}\ \ , \quad \bar{\rho}_{ij}(g) \equiv \rho(g)^*_{ij}\ \in\ \mathbb{C}\,, \tag{3.12}$$

which maps each group element into its corresponding matrix elements. Let $\hat{\mathrm{G}}$ be the set of all irreducible inequivalent representations of G. An important result on the representation theory for compact Lie groups [76], known as the Peter-Weyl theorem (cf. Appendix A), ensures us that the functions $\bar{\rho}_{ij}$ form a basis of $\mathscr{H} = L^2(G)$ provided that we vary the representation ρ within $\hat{G}$ and $i, j = 1, \ldots, d_\rho \equiv \dim\rho$. This is called the *representation basis*. We introduce again the Dirac notation by defining the basis elements $|\rho, ij\rangle$ s.t.

$$\langle g|\rho, ij\rangle = \sqrt{\frac{d_\rho}{|G|}}\ \rho(g)^*_{ij}, \tag{3.13}$$

where |G| denotes the volume of G w.r.t. the Haar measure. The matrix elements of $\rho_\alpha,\ \rho_\beta \in \hat{G}$ satisfy the orthonormality relation

$$\int_G dg\, \rho_\alpha(g)_{ij}\rho_\beta(g)^*_{kl} = \ \frac{|G|}{d_\alpha}\, \delta_{\alpha\beta}\, \delta_{ik}\, \delta_{jl}\,, \tag{3.14}$$

which, thanks to the normalization factor above, translates into

$$\langle \rho_\alpha, ij|\rho_\beta, kl\rangle = \ \delta_{\alpha\beta}\, \delta_{ik}\, \delta_{jl}\,. \tag{3.15}$$

We shall see it later in a bit more detail, but we anticipate now that the basis $|\rho, ij\rangle$ is exactly the one that reduces the left regular representation. A simple way to understand it is to act on the basis elements with ρ_L:

$$[L_h\, \bar{\rho}(\cdot)_{ij}](g) = \rho(h^{-1}g)^*_{ij} = c_{ik}\, \rho(g)^*_{kj}\ \ , \ \ c_{ik} = \rho(h^{-1})^*_{ik}\,.$$

The block-diagonal structure is clear, because L acts on $\bar{\rho}(\cdot)_{ij}$ by producing a linear combination of the other matrix elements $\bar{\rho}(\cdot)_{kj}$, all within the same representation. Actually, the decomposition tells us that

$$L^2(G) \cong \bigoplus_{\rho\,\in\,\hat{G}} \left(\mathrm{V}^\star_\rho \otimes \mathrm{V}_\rho\right)$$

and the regular representation contains as blocks all the other irreducible representations of the group, each one appearing a number of times equal to its dimension. The set $\hat{\mathrm{G}}$ of all representations is discrete as long the group G is compact, like in our case [31]. At this point, recall that the electric term of the hamiltonian is proportional to the quadratic Casimir operator

$$[H_E, L_g] = 0 \quad \forall\ g \in G\,. \tag{3.16}$$

The Schur's lemma can be applied if the regular representation is restricted to its irreducible components $L = \bigoplus_{\rho \in \hat{G}} d_\rho\, \rho$, implying that H_E will act as a multiple of the identity on each of them, so that

$$H_E\,\big|_{V_\rho} = f(\rho)\, \mathbb{I}_{d_\rho} \quad \Rightarrow \quad H_E\,|\rho, ij\rangle = |\rho, ij\rangle\, f(\rho)\,. \tag{3.17}$$

Overall, if we introduce the projector P_ρ on the representation space V_ρ the electric term H_E can be written in its spectral expansion

$$H_E = \sum_{\rho \in \hat{G}} f(\rho)\, P_\rho\ , \quad P_\rho = \sum_{i,j=1}^{d_\rho} |\rho, ij\rangle\langle\rho, ij|\,. \tag{3.18}$$

To summarize, we have seen that there are two relevant bases. One is the group element basis $\{|g\rangle\}$, called also *magnetic basis* because it diagonalizes the magnetic term H_B, whose eigenvalues on a plaquette are related to the value of the magnetic flux. The other is the representation basis $\{|\rho, ij\rangle\}$, called also *electric basis* because it diagonalizes the electric term H_E and the eigenvalues λ_ρ are related to the value of the electric field on the link [57]. The relationship with the electric part of the hamiltonian and the quadratic Casimir of the gauge group allows us to see its gauge-invariance without any further calculation. Recall that a gauge transformation is represented by

$$\mathcal{G} = L_{g(e+)} R_{g(e-)}\,,$$

where $g(e+)$ and $g(e-)$ are the group elements associated to the target site and to the source site of the link e. The left and right regular representations share the same properties and both contain all irreducible representations as their irreducible components. V_ρ, where H_E acts trivially, is an invariant subspace for both of them and they clearly commute:

$$[H_E, \mathcal{G}] = 0. \tag{3.19}$$

We had already commented on the gauge-invariance of the magnetic term, which is manifest when working in the group element basis, so we have a hamiltonian divided into two parts that are separately gauge-invariant and this fact will also be useful for the simulation procedure.

3.1.3 The finite group electric term

With all the machinery introduced in the previous subsection, the electric part of the hamiltonian can be extended to the case of a finite gauge group. The basic requirement is that we want to preserve the structure

$$H_E = \sum_{\rho \in \hat{G}} \sum_{i,j=1}^{d_\alpha} |\rho, ij\rangle \, f(\rho) \, \langle \rho, ij|$$

and it can be done since finite groups and compact Lie groups share a lot of properties concerning their representations. What is left to fix are the eigenvalues $\lambda(\rho)$ and the different methods that provide us a possible H_E correspond to different choice of the eigenvalues. This freedom should not be seen as a limitation, but rather it is an opportunity: the choice of the gauge group does not fix completely the lattice theory and several models with different eigenvalues of the energy can be considered.

As far as we know, there is not a single best method in literature to determine this eigenvalues in general. For instance, in [63] a plausible expression of $f(\rho)$ for $G = \mathbb{Z}_N$ is chosen in order to match the correct continuum limit $\mathbb{Z}_N \to \mathrm{U}(1)$ for $N \to \infty$ (and assuming a unique ground state). Other works on non abelian groups focus on dihedral groups, which should recover a $\mathrm{O}(2)$ theory in the continuum limit, and [9] proposes the eigenvalues for D_N exploiting its similarities with cyclic groups, since it is a semi-direct product $\mathbb{Z}_N \rtimes \mathbb{Z}_2$ while [48] uses the transfer matrix method. Here, we shall review the method proposed in the thesis [52], referring to it for more details.

The idea is to enforce the similarity of the electric term with the laplacian on the Lie group and to keep defining it as a laplacian also when G is a finite group. Of course, when G is finite it is not associated to a manifold and a laplacian in the common sense cannot exist. In general, there is a whole class of differential operators that commute with the group algebra [84, 85]. Since a general conventional choice is lacking, we choose a simple possibility: we define the laplacian on a finite group as the laplacian of its Cayley graph. The Cayley graph encodes the structure of the group operation. To define it, let us consider a symmetric generating set Γ of the group G. Here symmetric means that $g^{-1} \in \Gamma \; \forall \, g \in \Gamma$. Γ is not unique and each choice of Γ leads in general to a different graph, so we denote it as $Cay(G, \Gamma)$. Now

1. the vertices of $Cay(G, \Gamma)$ are the elements of G;
2. $g, h \in G$ are connected by an edge if $\exists \gamma \in \Gamma$ s.t. $h = \gamma g \Leftrightarrow hg^{-1} \in \Gamma$.

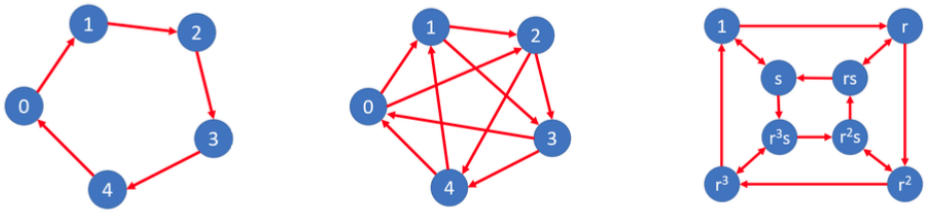

Figure 3.1: Some example of Cayley graphs, respectively for $\mathbb{Z}_5$ with generating set $\{s\}$, $\mathbb{Z}_5$ with generating set $\{s, s^2\}$ and D_4 with generating set $\{r, s\}$. This image is taken from [52].

Γ is symmetric, so it is irrelevant to definite it with gh^{-1} or hg^{-1}. In Fig. 3.1 there are some examples of a Cayley graph. Typically it is chosen also $1 \notin \Gamma$ so that the edges do not include loops on each site. We will choose also Γ to be closed under conjugation $\gamma \mapsto g\gamma g^{-1}$ The laplacian of a graph is its degree matrix minus its adjacency matrix [25]. The vector space on which it acts is the space of all functions on the sites of the graph, but since the sites of $Cay(G, \Gamma)$ are the group elements we are correctly working on the group algebra $\mathbb{C}[G] = \{f : \mathrm{G} \to \mathbb{C}\}$. Being a finite group, there are no convergence issues and we don't need the request of summability.

Let us define the two matrices in the group element basis. The *degree matrix* D of a graph is the diagonal matrix whose eigenvalues are the connectivities of the sites. For a Cayley graph, each site g is connected to $h = \gamma g \ \forall \gamma \in \Gamma$, so the connectivities are all equal to $|\Gamma|$. Therefore

$$D = |\Gamma| \, \mathbb{I} \,, \tag{3.20}$$

it is proportional to the identity and it is diagonal on every basis. Instead, the *adjacency matrix* A has matrix element $A_{gh} = 1$ if the vertices g and h are linked by an edge. Hence, it acts on $|f\rangle = \sum_g f(g)|g\rangle$ as

$$[Af](g) = \langle g|A|f\rangle = \sum_{h \in G} A_{gh} f(h) \tag{3.21}$$

Following [25], in this case $A_{gh} = 1$ iff $h = \gamma g$ and we can rewrite A as an operator using the definition of the left regular representation

$$[Af](g) = \sum_{\gamma \in \Gamma} f(\gamma g) = \sum_{\gamma \in \Gamma} L_\gamma f(g) \quad \Rightarrow \quad A = \sum_{\gamma \in \Gamma} L_\gamma \,. \tag{3.22}$$

If Γ is closed under conjugation, the adjacency matrix commutes with the left regular representation, since

$$AL_g = \sum_\gamma L_\gamma \, L_g = \sum_\gamma L_{\gamma g} = \sum_{\gamma'} L_{(g\gamma' g^{-1})g} = \sum_{\gamma'} L_g L_{\gamma'} = L_g A \tag{3.23}$$

The Schur's lemma implies that also A acts trivially on each irreducible component of L and

$$A = \sum_{\rho \in \hat{G}} a(\rho)\, P_\rho \,. \tag{3.24}$$

Notice that it has the exact block-diagonal structure that we need for the electric term. By making use of the familiar decomposition of the regular representation, we can express it also as

$$A = \sum_{\gamma \in \Gamma} L_\gamma = \sum_{\gamma \in \Gamma} \bigoplus_{\rho \in \hat{G}} d_\rho \rho(\gamma) = \bigoplus_{\rho \in \hat{G}} d_\rho \sum_{\gamma \in \Gamma} \rho(\gamma) \tag{3.25}$$

if we equate them and if we compute the trace within each block we get

$$a(\rho)\, d_\rho = \sum_{\gamma \in \Gamma} \chi_\rho(\gamma) \,, \tag{3.26}$$

where χ_ρ is the character associated to the representation ρ. This expression fixes the eigenvalue $a(\rho)$. Then, we define the laplacian as

$$\Delta = D - A \tag{3.27}$$

and its spectral decomposition follows from (3.20) and (3.24)

$$\Delta = \sum_{\rho \in \hat{G}} \sum_{i,j=1}^{d_\alpha} f(\rho)\, P_\rho \;\;, \quad f(\rho) = |\Gamma| - \frac{1}{d_\rho} \sum_{\gamma \in \Gamma} \chi_\rho(\gamma) \,. \tag{3.28}$$

The laplacian of a graph is positive-semidefinite and the trivial representation corresponds to the ground state. It has dimension $d_0 = 1$ and it maps every element $g \in G$ to the identity matrix, so that $\chi_0(\gamma) = \operatorname{tr} \mathbb{I}_{d_\rho} = 1 \;\; \forall\, \gamma \in \Gamma$, implying that $f(\rho_0) = 0$. For non-abelian groups, where irreducible representations with more than one dimension are allowed, the states $|\rho, ij\rangle$ are all associated to the same eigenvalue and some degenerations in the spectrum are guaranteed. We conclude this section by giving our definition for the complete hamiltonian in the finite group case:

$$H = H_E + H_B = \frac{g^2}{2a^{d-2}} \sum_{(x,i)} \Delta_{(x,i)} - \frac{1}{g^2 a^{4-d}} \sum_{\square} \left(\operatorname{tr} W_\square + \operatorname{tr} W_\square^\dagger \right) . \tag{3.29}$$

3.2 Duality and generalized Fourier transforms

In the first part of this chapter, we have introduced the representation basis, whose key role is manifest since it is the generalization of the electric

field basis. However, its properties have not been fully discussed yet, as we postponed some important comments in order to avoid losing the train of thought while we were constructing the hamiltonian for a finite gauge group. In particular, this section is dedicated to analyze the duality that holds between the representation basis and the group element basis, which is crucial for quantum simulations. In a similar way to what happens in quantum mechanics with the usual position and momentum basis, they are related by a Fourier transform, which in this case has to be properly generalized in order to act on the functions defined on a group. This kind of Fourier transform is also extremely useful in many algorithms of quantum computation, for instance regarding the famous hidden subgroup problem [34].

We shall present their duality starting from the compact Lie group case, but for finite groups it is equivalent and it will extend straightforwardly. The representation basis is composed by the kets $|\rho, ij\rangle$, corresponding to the matrix elements that realize each group element in an irreducible representation

$$\langle g|\rho, ij\rangle = \sqrt{\frac{d_\rho}{|G|}}\,\rho(g)^*_{ij}\,.$$

Being a basis, for any function $f \in L^2(G)$ there are some constants $c_{\rho,ij}$ s.t.

$$f(g) = \sqrt{\frac{d_\rho}{|G|}} \sum_{\rho\in\hat{G}} \sum_{i,j=1}^{d_\rho} c_{\rho,ij}\,\rho(g)^*_{ij} \tag{3.30}$$

and these coefficients can be shown (cf. Appendix A) to be the following

$$c_{\alpha,ij} = \hat{f}(\rho)_{ij} \quad , \quad \hat{f}(\rho) = \sqrt{\frac{d_\rho}{|G|}} \int_G dg\, f(g)\rho(g)\,. \tag{3.31}$$

The object $\hat{f}(\rho)$ is the Fourier transform of $f : G \to \mathbb{C}$ computed on the representation ρ and, being a linear combination of matrices $\rho(g) \in \mathrm{GL}(V_\rho)$, it is an element of $\mathrm{End}(V_\rho)$. This realizes an isomorphism $L^2(G) \cong \oplus_{\rho\in\hat{G}}\mathrm{End}(V_\rho)$.

But why is (3.31) a generalization of the Fourier transform? To see it, take a look at the usual Fourier series. It is defined for periodic functions, that can be regarded as functions on the circle. Given $f : [0, 2\pi[\to \mathbb{C}$, then

$$f(\theta) = \sum_{n\in\mathbb{Z}} \hat{f}(n)\, e^{in\theta} \ , \ \ \hat{f}(n) = \frac{1}{2\pi}\int_0^{2\pi} d\theta\, f(\theta)\, e^{-in\theta} \tag{3.32}$$

and it is related to the group U(1), as the function $f(\theta)$ that we are expanding can be seen as $f : \mathrm{U}(1) \cong S^1 \to \mathbb{C}$. The inequivalent representations of U(1)

are $\rho_n(e^{i\theta}) = e^{in\theta}$, which are exactly the elements of the Fourier plane wave basis, and the sum labelled by the index $n \in \mathbb{Z}$ is a sum on all inequivalent representations of U(1). Analogously, the r.h.s. of eq (3.30) has a sum on $\hat{\mathrm{G}}$, the set of all inequivalent representations of the group G. The second sum is on the matrix elements $i, j = 1, ..., d_\rho$ of the representative matrices in the representation ρ. This second sum disappears in the usual Fourier series, since U(1) is abelian and all its irreducible representations are one dimensional. Also (3.31) reduces to the usual Fourier coefficients. The reason why we are actually comparing to the Fourier series and not to the Fourier transform is that we have chosen to work with a compact gauge group, whose irreducible representations $\hat{G}$ form a countable set. If we had considered $\mathbb{R}$, instead, $\hat{\mathbb{R}} \cong \mathbb{R}$ and, coherently, it yields the usual Fourier transform [74].

The representation basis is useful because it diagonalizes the electric part of the hamiltonian as a consequence of reducing the left regular representation. We shall see here better why. In our context it is convenient to work with Dirac's notation. Using (3.13), the Fourier transform is rewritten as

$$\hat{f}(\rho)_{ij} = \sqrt{\frac{d_\rho}{|G|}} \int_G dg\, f(g)\rho(g) = \int_G dg\, \langle \rho, ij|g\rangle\langle g|f\rangle \,. \tag{3.33}$$

Using the completeness relation of the group element basis, it becomes simply

$$\hat{f}(\rho)_{ij} = \langle \rho, ij|f\rangle \,, \tag{3.34}$$

and the Fourier expansion of eq. (3.30) takes the form of a completeness relation for the representation basis $|\rho, ij\rangle$:

$$\langle g|f\rangle = \sum_{\rho\in\hat{G}} \sum_{i,j=1}^{d_\rho} \langle g|\rho, ij\rangle\langle \rho, ij|f\rangle \,. \tag{3.35}$$

It should be clear now that the Fourier transform is just a change of basis, moving the vector from the group element basis, where it is expanded like in (3.9) to the representation basis, where its expansion is the Fourier series

$$|f\rangle = \sum_{\rho\in\hat{G}} \sum_{i,j=1}^{d_\alpha} \hat{f}(\rho)_{ij}\, |\rho, ij\rangle \,. \tag{3.36}$$

To find the abstract expression for the Hilbert space operator associated to the Fourier transform, let us consider first the structure of a change of coordinates for simplicity in the finite dimensional case. A coordinate change operator is just an identity operator expanded with two different basis on

domain and codomain. Suppose that we want to go from the orthonormal basis $|e_i\rangle$ of a general vector space to another orthonormal basis $|f_i\rangle$. Using their completeness relations, we can define the coordinate change operator

$$M = \mathbb{I} \cdot \mathbb{I} = \sum_{i,j} |f_i\rangle \Big(\langle f_i | e_j \rangle \Big) \langle e_j | \,. \tag{3.37}$$

When acting on a vector $|v\rangle = \sum_k v_k |e_k\rangle$, it produces $M|v\rangle = \sum_i |f_i\rangle\langle f_i|v\rangle$, that is again the vector $|v\rangle$ but expanded in the new basis $|f_i\rangle$. One can also define a basis change matrix N that maps the two sets of basis vectors as

$$|f_i\rangle = \sum_j |e_j\rangle N_{ji} \,. \tag{3.38}$$

Notice that this is a row by column multiplication only if we gather the basis vectors into a row vector. A straightforward calculation shows that the matrix associated with M is the inverse of N. In our context, the two bases are $|g\rangle$ and $|\rho, ij\rangle$ and the change of coordinates operator is given by

$$\mathfrak{U}_F = \sum_{\rho,\, ij} \int_G dg \; |\rho, ij\rangle \Big(\langle \rho, ij | g \rangle \Big) \langle g | \tag{3.39}$$

and when it acts on a generic element $|f\rangle$ expanded in the group element basis it produces exactly the relation written above in eq. (3.6). Moving the sum on representations inside the integral, the operator takes the form

$$\mathfrak{U}_F = \int_G dg \, |\hat{g}\rangle\langle g| \;, \quad |\hat{g}\rangle = \sum_{\rho \in \hat{G}} \sum_{i,j=1}^{d_\rho} \sqrt{\frac{d_\rho}{|G|}} \, \rho(g)_{ij} \, |\rho, ij\rangle \tag{3.40}$$

This expression can be used to prove that the left regular representation is block diagonal. Since $L_g \, |h\rangle = |gh\rangle$, it can be rewritten as

$$L_g = \int dh \; |gh\rangle\langle h| \,. \tag{3.41}$$

By changing the basis from the group elements to the matrix elements

$$\hat{L}_g = \mathfrak{U}_F \, L_x \, \mathfrak{U}_F^\dagger = \int dx dy \int dh \; |\hat{x}\rangle\langle x|gh\rangle\langle h|y\rangle\langle \hat{y}'| = \int dh \; |\widehat{gh}\rangle\langle \hat{h}| \,,$$

substituting the definitions, it can be expressed as

$$\hat{L}_g = \int dh \sum_{\rho,\rho'} \sum_{ij,i'j'} \frac{\sqrt{d_\rho d'_\rho}}{|G|} \, \rho(gh)_{ij} \rho(h)^*_{i'j'} \, |\rho, ij\rangle\langle \rho, i'j'| \,.$$

Now, if we expand $\rho(gh)_{ij} = \rho(g)_{il}\rho(h)_{lj}$ we can compute the integral using the completeness relation of the $|h\rangle$ basis, therefore finding [18]

$$\hat{L}_g = \sum_{\rho \in \hat{G}} \sum_{i,j,l} |\rho, ij\rangle \, \rho(g)_{il} \, \langle \rho, lj| \, . = \sum_{\rho \in \hat{G}} \left(\rho(g) \otimes \mathbb{I}_{d_\rho} \right) \, , \tag{3.42}$$

As it can be easily checked by computing the matrix elements of $\rho(g) \otimes \mathbb{I}_{d_\rho}$ onto the states $|\rho, r\rangle|\rho, s\rangle \equiv |\rho, rs\rangle$, it is exactly to the tensor product

$$\hat{L}_g = \sum_{\rho \in \hat{G}} \left(\rho(g) \otimes \mathbb{I}_{d_\rho} \right) \, , \tag{3.43}$$

with the block-diagonal structure that we have claimed before. The finite group case is completely analogous, up to minor differences. The first one it that when G is finite the Hilbert space $L^2(\mathrm{G})$ becomes the set of all functions on the group, since there are no convergence problems anymore. The elements $|g\rangle$ correspond to

$$e_g : G \to \mathbb{C} \, , \;\; e_g(h) = \delta_{g,h} \, ,$$

where $\delta_{g,h}$ is a proper Kronecker delta, so that now e_g is a function instead of a distribution and $|g\rangle$ is a basis for $L^2(G)$ in the proper sense, implying that $\dim L^2(\mathrm{G}) = |\mathrm{G}|$. For a finite group the set $\hat{G}$ of all inequivalent irreducible representations is finite instead of countable [31]. Then, the formulas that we gave for compact groups can be repeated if we make the replacement

$$\frac{1}{|G|} \int_G dg \; \longrightarrow \; \frac{1}{|G|} \sum_{g \in G} ,$$

interpreting now $|G|$ as the order of the group. For reference, we repeat here some formulas. The Fourier transform operator of (3.40) becomes

$$\mathfrak{U}_F = \sum_{g \in G} |\hat{g}\rangle\langle g| \, , \;\; |\hat{g}\rangle = \sum_{\rho \in \hat{G}} \sum_{i,j=1}^{d_\rho} \sqrt{\frac{d_\rho}{|G|}} \, \rho(g)_{ij} \, |\rho, ij\rangle \tag{3.44}$$

And when it acts on $|f\rangle = \sum_g f(g)|g\rangle$ it reproduces exactly the Fourier gate that we have given in the beginning of this chapter

$$\mathfrak{U}_F \sum_{g \in G} f(g)|g\rangle = \sum_{\rho \in \hat{G}} \sum_{i,j=1}^{d_\rho} \hat{f}(\rho)_{ij} |\rho, ij\rangle \, .$$

To see better how it works, we conclude this subsection by giving a simple but important example of this transform. Consider $G = \mathbb{Z}_2 = \{e, s\}$, so that

$$L^2(G) = \text{span}\{e_e,\, e_s\}\,, \tag{3.45}$$

where $e_e(g) = \delta_{e,g}$ and $e_s(g) = \delta_{s,g}$. $\mathbb{Z}_2$ is self-dual in the sense of the Pontryagin duality [74], meaning that $\hat{\mathbb{Z}}_2 \cong \mathbb{Z}_2$: its set of inequivalent irreducible representations is still a group and it is isomorphic to the initial group. So $\mathbb{Z}_2$ has only two inequivalent irreps:

- the trivial representation ρ_1, s.t. $\rho_1(e) = 1$, $\rho_1(s) = 1$;
- the roots of unity representation ρ_2, s.t. $\rho_1(e) = 1$, $\rho_1(s) = -1$.

Both are 1d representations and the two functions of the Fourier basis are

$$\frac{1}{\sqrt{2}}\rho_1(g) = \frac{1}{\sqrt{2}}\Big(e_e(g) + e_s(g)\Big) \tag{3.46}$$

$$\frac{1}{\sqrt{2}}\rho_2(g) = \frac{1}{\sqrt{2}}\Big(e_e(g) - e_s(g)\Big)\,. \tag{3.47}$$

We can immediately identify the matrix N introduced above by looking at

$$(|\rho_1\rangle,\, |\rho_2\rangle) = (|e_e\rangle,\, |e_s\rangle) \begin{pmatrix} 1/\sqrt{2} & 1/\sqrt{2} \\ 1/\sqrt{2} & -1/\sqrt{2} \end{pmatrix} \equiv (|e_e\rangle,\, |e_s\rangle)\, N\,. \tag{3.48}$$

The change of coordinates is $M \equiv \mathfrak{U}_F$, so that N corresponds to $\mathfrak{U}_F^\dagger$

$$\mathfrak{U}_F = \begin{pmatrix} 1/\sqrt{2} & 1/\sqrt{2} \\ 1/\sqrt{2} & -1/\sqrt{2} \end{pmatrix} = \mathfrak{U}_F^\dagger\,. \tag{3.49}$$

This procedure can be easily generalized to any cyclic group $\mathbb{Z}_n$, finding that our group-theoretical Fourier transform reduces to the usual discrete Fourier transform. Consider $\mathbb{Z}_n = \{e,\, s\,, ..., s^{n-1}\}$. All cyclic groups satisfy $\hat{\mathbb{Z}}_N \cong \mathbb{Z}_n$ and their irreps (all 1d, being $\mathbb{Z}_n$ abelian) can be identified as

$$\rho_j(s^k) = e^{\frac{2\pi i}{n} jk}\ , \quad j = 0, ..., n-1\,.$$

If we denote with $|\rho_j\rangle$ the representation basis, the Fourier transform of f is

$$\hat{f}(j) = \langle \rho_j | f \rangle = \sqrt{\frac{d_j}{|\mathbb{Z}_n|}} \sum_{g \in \mathbb{Z}_n} f(g)\rho_j(g) \quad \Rightarrow \quad \hat{f}(j) = \frac{1}{\sqrt{n}} \sum_{k=0}^{n-1} f(s^k)\, e^{\frac{2\pi i}{n} jk} \tag{3.50}$$

which is a discrete Fourier transform. Instead, the operator $\mathfrak{U}_F$ is the usual quantum Fourier transform [61]. Being $\mathfrak{U}_F$ linear, in order to characterize it it is enough to see how it acts on a basis, then let us specify eq. (3.6) for the basis vectors $f = e_h$, so that $f(g) = e_h(g) = \delta_{h,g}$. Let $g = s^k$, $h = s^{\tilde{k}}$, then

$$\widehat{e_h}(j) = \frac{1}{\sqrt{n}} \sum_{k=0}^{n-1} e_h(s^k)\rho_j(s^k) = \frac{1}{\sqrt{n}} \sum_{k=0}^{n-1} \delta_{s^k,s^{\tilde{k}}}\, e^{\frac{2\pi i}{n}kj} = \frac{1}{\sqrt{n}} e^{\frac{2\pi i}{n}\tilde{k}j}\,, \qquad (3.51)$$

and, using this explicit form of the Fourier transform, eq. (3.6) becomes

$$\mathfrak{U}_F|\, s^{\tilde{k}}\rangle = \sum_{j=0}^{n-1} \frac{1}{\sqrt{n}} e^{\frac{2\pi i}{n}\tilde{k}j}|\, \rho_j\rangle\,. \qquad (3.52)$$

If we rename $\tilde{k} \equiv k$, $|s^{\tilde{k}}\rangle \equiv |k\rangle$ and $|\rho_j\rangle \equiv |j\rangle$ we see that it is just the quantum Fourier transform, whose implementation as a quantum circuit is well known [61]

$$|k\rangle \quad \longmapsto \quad \frac{1}{\sqrt{n}} \sum_{j=0}^{n-1} e^{\frac{2\pi i}{n}kj}|j\rangle\ . \qquad (3.53)$$

It is straightforward to verify that in the $\mathbb{Z}_2$ case the matrix associated to this transformation coincides with the one given in eq. (3.49). Notice that our choice of normalization for the states $|\rho, ij\rangle$ ensures their orthonormality, so that $\mathfrak{U}_F <$ represents a change of basis between two orthonormal sets of states and it is therefore unitary. Unitary operators are the kind of operations that are allowed on qubits in a quantum computer! This operator is a generalization of the quantum Fourier transform, often abbreviated QFT, which is of extreme importance for the field of quantum computing, because it is one of the few operations that have a well-known quantum algorithm whose advantage with respect to the classical counterpart (the fast Fourier transform) is exponential [61]. Moreover, many computational problems reduce to algebraic questions, so that group-theoretical properties become fundamental in the algorithm design phase. Some examples of applications of the quantum Fourier transform and its generalization, together with procedures to implement them in circuits can be found in [34, 40, 59, 70].

3.3 Time evolution algorithm

Finally, we are ready to describe a procedure able to implement the time evolution operator $U(t) = e^{-iHt}$ for a generic finite group lattice gauge theory, using the gates introduced by [48]. We shall assume that an initial state $|\psi_i\rangle$

that is physical (i.e. it satisfies the gauge invariance condition $G|\psi_i\rangle = 0$) has already been prepared. Then, being H gauge-invariant, $[G, H] = 0$ and $[G, e^{-iHt}] = 0$, implying that the evolved state will remain physical, since it satisfies $G\, e^{-iHt}|\psi_i\rangle = 0$. Now, in order to realize the time evolution we need to implement as a quantum circuit $U(t) = e^{-iHt}$, where $H = H_E + H_B$. Let us recall the form of the Hamiltonian:

$$H = H_E + H_B = \lambda_E \sum_{(x,i)} \Delta_{(x,i)} - \lambda_B \sum_{\square} \left(\operatorname{tr} W_{\square} + \operatorname{tr} W_{\square}^{\dagger} \right) .$$

Where we have generalized the coefficients of the two terms as λ_E and λ_B. First, we assume that for every link there is a qubit register which encodes its the state, identifying the states on the register with the group element/magnetic basis of the system. Then we proceed by following the trotterization procedure described in Section 2.3. First, divide t into n Trotter steps $\Delta t = t/n$, so that

$$U(t) = \prod_{j=1}^{n} e^{-i(H_E + H_B)\Delta t} . \tag{3.54}$$

Then, use the Trotter approximation on the operators H_E, H_B to decompose

$$U(t) \approx \prod_{j=1}^{n} e^{-iH_E \Delta t} e^{-iH_B \Delta t} . \tag{3.55}$$

Notice that now we are not time evolving along the original hamiltonian, but along an approximation and in general it may lose gauge invariance. In this occasion we do not have this problem, as both H_E and H_B are separately gauge-invariant and time evolving with eq. (3.55) will not break the physicality of the initial state. At this point, we can realize the two electric and magnetic parts of the time evolution taking advantage of the previous discussion, where we have come to the conclusion that H_B is diagonal in the group element basis and H_E is diagonalized by the Fourier transform gate.

Let us start from H_B. Wilson loops of different plaquettes are commuting, so we can separate exactly the exponentials on different plaquettes as

$$e^{-iH_B \Delta t} = \prod_{p} U_B^{(p)}(\Delta t) . \tag{3.56}$$

Now we can consider individually each plaquette; suppose that we want to implement the evolution generated by Re tr W = Re tr$[U_0 U_1 U_2^{\dagger} U_3^{\dagger}]$, where

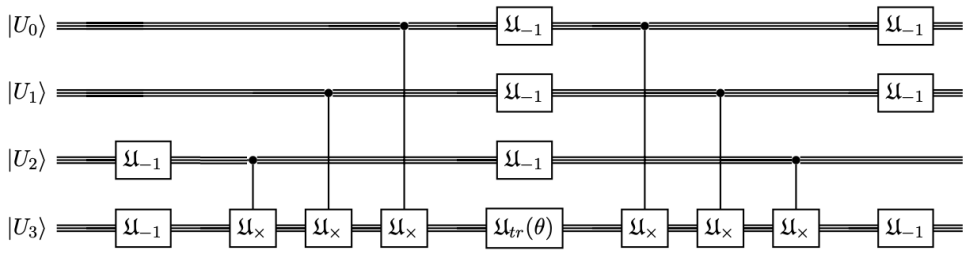

Figure 3.2: Quantum circuit realizing the time evolution of a single plaquette generated by the magnetic term of the hamiltonian.

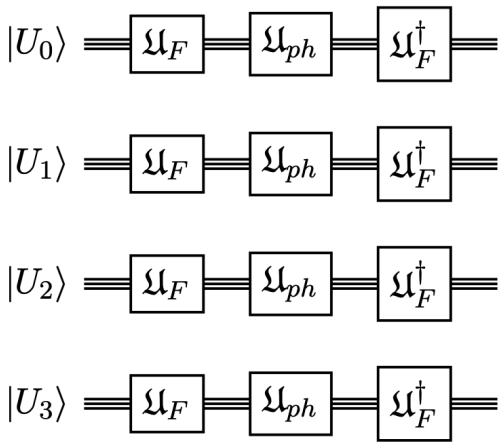

Figure 3.3: Circuit realizing the time evolution of 4 links generated by H_E.

$0, 1, 2, 3$ label the four links of a plaquette. This operator acts on a single plaquette Hilbert space $\mathcal{H} = L^2(G)_0 \otimes L^2(G)_1 \otimes L^2(G)_2 \otimes L^2(G)_3 \ni |U_0\rangle|U_1\rangle|U_2\rangle|U_3\rangle$. Re W is diagonal on the $|U\rangle$ basis and

$$U_B^{(p)}(\Delta t)\,|U_0\rangle|U_1\rangle|U_2\rangle|U_3\rangle = |U_0\rangle|U_1\rangle|U_2\rangle|U_3\rangle\, e^{-i(-2\lambda_B \Delta t)\mathrm{Re}\,\mathrm{tr}\,W}\,. \qquad (3.57)$$

The factor 2 comes from $\mathrm{tr}\,W_\Box + \mathrm{tr}\,W_\Box^\dagger$, which returns two times the real part of the Wilson loop operator. The circuit that implements eq. (3.57) is depicted in figure 3.2, where a triple line represents a qubit register that encodes a single link state. First we choose one of the registers to transform it into the sequence of group elements of the plaquette $W = U_0 U_1 U_2^\dagger U_3^\dagger$; a simple choice is to start from $|U_3\rangle$, since our multiplication gate is a left multiplication. This step uses the two gates $\mathfrak{U}_\times$, $\mathfrak{U}_{-1}$: first act with $\mathfrak{U}_{-1}$ on the qubits that have to be reversed, then realize the product on $|U_3\rangle$ Now $|U_3\rangle \mapsto |U_0 U_1 U_2^\dagger U_3^\dagger\rangle$ and acting on it with $\mathfrak{U}_{\mathrm{tr}}(\theta)$ produces in the $L^2(G)_3$

register the phase factor of eq. (3.57) if we choose

$$\theta = 2\lambda_B \, \Delta t \tag{3.58}$$

To reproduce completely the final state, we just have to undo the first transformation on $L^2(G)_3$, so that $|U_0 U_1 U_2^\dagger U_3^\dagger\rangle \mapsto |U_3\rangle$.

Now let us turn to the electric part $e^{-iH_E \Delta t}$. Again, terms on different links commute and we can separate the exponentials in the following way

$$e^{-iH_E \Delta t} = \prod_l U_E^{(l)}(\Delta t) \, . \tag{3.59}$$

The implementation of $U_B^{(p)}(\Delta t)$ was straightforward because it was already diagonal, now we choose to diagonalize $U_E^{(l)}(\Delta t)$ to simplify its realization. Suppose to have the operator T expanded in the basis $\mathscr{E} = \{|e_i\rangle\}$ and that M is the coordinate change operator between $\mathscr{E}$ and $\mathscr{F} = \{|f_i\rangle\}$, which diagonalizes T. The diagonal expansion of T in the new basis $\mathscr{F}$ is given by

$$[T]_{\mathscr{F}} = M [T]_{\mathscr{E}} M^{-1} \, . \tag{3.60}$$

In our case, $M = \mathfrak{U}_F$ and we denote $U_E^{(l)}(\Delta t)$ in the new basis and it will be a diagonal phase gate that is simple to realize. We get

$$U_E^{(l)}(\Delta t) = \mathfrak{U}_F^\dagger \, \mathfrak{U}_{ph} \, \mathfrak{U}_F \, . \tag{3.61}$$

In figure 3.3 there is represented the circuit that realizes the electric part of the time evolution operator, that is just eq. (3.61) implemented link by link. We cannot specify further the structure of $\mathfrak{U}_{ph}$ because it will be highly dependent on the model considered and it has to be studied case by case.

CHAPTER IV.

$\mathbb{Z}_n$ gauge models

Approximating the gauge group with one of its finite subgroups is a possible path that can lead to accurate simulations of lattice Lie-group gauge theories. To start this program regarding quantum simulations, we consider the case of the approximation of the group U(1) with $\mathbb{Z}_n$. We have focused on a simple case, in order to better analyze the performance of this approach. If we added matter fields, our model would become a finite group approximation of QED in an arbitrary number of dimensions. Even if this is the simplest case it is not a trivial one, since, as we have outlined in the first chapter, also abelian gauge theories can have very interesting phase diagrams.

4.1 Pure $\mathbb{Z}_n$ lattice hamiltonian

We start by specifying the construction of the previous chapters to the group G=$\mathbb{Z}_n$. The single link Hilbert space is $L^2(\mathbb{Z}_n)$ and it is generated by $|g\rangle\,, \forall\, g \in \mathbb{Z} = \{e, s, \ldots, s^{n-1}\}$. The electric term is most easily written in the representation basis, made of the elements $|\rho_j\rangle$, $j = 1, \ldots, n$, which satisfy the duality relation

$$\langle s^k|\rho_j\rangle = \frac{1}{\sqrt{n}}\rho_j(s^k)^* = \frac{1}{\sqrt{n}}\, e^{-\frac{2\pi i}{n}\, jk}\,.$$

We need the laplacian of the group $\mathbb{Z}_n$. Let us choose the generating subset of the Cayley graph as $\Gamma = \{s,\, s^{-1}\}$, so that $|\Gamma| = 2$. The irreducible representations ρ_j are all one dimensional, so the characters are

$$\chi_j(s^{\pm 1}) = \rho_j(s^{\pm 1}) = e^{\pm\frac{2\pi i}{n} j}.$$

The resulting laplacian for $\mathbb{Z}_n$ can be expressed by the following equation

$$\Delta = \sum_{j=0}^{n-1} f(\rho_j)\, P_j \ , \quad f(\rho_j) = 2\left[1 - \cos\left(\frac{2\pi j}{n}\right)\right] = 4\sin^2\left(\frac{\pi j}{n}\right) \tag{4.1}$$

and the electric term is proportional to the sum of the laplacians on all links

$$H_E = \lambda_E \sum_{(x,i)} \Delta_{(x,i)} \, . \tag{4.2}$$

The magnetic term instead is diagonal on the magnetic/group element basis $|s^k\rangle$. If we work within the representation $j = 1$ of the roots of the unity, $s^k \sim e^{\frac{2\pi i}{n} k}$ and the "position" operator is U such that

$$U\,|s^k\rangle = |s^k\rangle\, e^{\frac{2\pi i}{n} k} \, . \tag{4.3}$$

The operator U is used to build the magnetic term of the hamiltonian:

$$H_B = -\lambda_B \sum_{\square} \left(W_\square + W_\square^\dagger\right) = -2\lambda_B \sum_{\square} \operatorname{Re} W_\square$$
$$W_\square = U_{\ell_1} U_{\ell_2} U_{\ell_3}^\dagger U_{\ell_4}^\dagger \, ,$$

where we have called $\ell_1, \ldots, \ell_4$ the oriented links of the plaquette $\square$. The trace is irrelevant here, since we are working with a one dimensional representation. Recall that the two bases are related by the quantum Fourier transform (3.52). Furthermore $\mathfrak{U}_F$ is just an identity operator expanded in two different bases, so that we can actually identify the abstract vectors as

$$|s^k\rangle = \frac{1}{\sqrt{n}} \sum_{j=0}^{n-1} e^{\frac{2\pi i}{n} kj}\, |\rho_j\rangle \, .$$

It can be interesting to see how the operator U acts on the electric/representation basis. Acting with conjugate of the equation (4.3) on the ket $|\rho_j\rangle$, one finds

$$\langle s^k|\, U\, |\rho_j\rangle = \frac{1}{\sqrt{n}}\, e^{-\frac{2\pi i}{n} k(j+1)} = \langle s^k | \rho_{j+1 \,(\mathrm{mod}\, n)}\rangle \, ,$$

where $\mathrm{mod}\, n$ means that we are identifying $n+1 \sim 1$, $n+2 \sim 2$ etc. As long as this identification is understood, it can be rewritten as

$$U\,|\rho_j\rangle = |\rho_{j+1}\rangle \, . \tag{4.4}$$

The states $|\rho_j\rangle$ have a definite value of the electric field and the operator U acts as a ladder operator, raising the electric field on the link where it

is defined. Clearly, $U^\dagger$ is the corresponding lowering operator. Recall our quick discussion of quantum link models in section 2.5.3. QLM also had U and $U^\dagger$ represented as ladder operators, but they where spin operators and they annihilated the states with maximum or minimum value of the third component of the spin. Now, instead of annihilating the extremal states, we get a cyclic action able to preserve the unitarity of the model.

In this context, the electric field is represented by an operator V somewhat dual to the magnetic field operator U. V is diagonal on the representation basis and its eigenvalues are the same that also U has, because $\hat{Z}_n \cong \mathbb{Z}_n$:

$$V\,|\rho_j\rangle = |\rho_j\rangle\, e^{\frac{2\pi i}{n} j} \tag{4.5}$$

and it will act by cyclically permuting the eigenstates of the magnetic term $|s^k\rangle$. A computation [53] shows that they satisfy the *Schwinger-Weyl algebra*

$$VU \;=\; e^{\frac{2\pi i}{n}}\, VU\,, \tag{4.6}$$

which can be taken as the starting point to build these $\mathbb{Z}_n$ models along another path [53, 63]. The Schwinger-Weyl group is the discretization of the Weyl group, generated by the commutator of a coordinate with its conjugate momentum $[q, p] = i$ and this fact can be used to perform a controlled continuum limit $\mathbb{Z}_n \to \mathrm{U}(1)$ [53].

4.2 Ising gauge theory

Today, quantum computers are still at a first development stage. As we have already pointed out, apart from the intrinsic quantum uncertainties, they suffer from noise-related problems, decoherence and we don't have a large amount of qubit at our disposal. In order to keep the circuits as simple as possible, we focus on the $\mathbb{Z}_2$ case, which happens to be a relevant model by itself: it is related to the first lattice gauge theory introduced by Wegner [89] in 1971 promoting the global symmetry of the Ising model to a local one.

4.2.1 Formulations of the model

When G=$\mathbb{Z}_2$, each element is the inverse of itself: $g = g^{-1}$. Working within the unitary representation $\rho_1(s^k) = e^{\frac{2\pi i}{2} k}$, the elements of $\mathbb{Z}_2$ are $e \sim +1$, $s \sim -1$ and they satisfy $g^\dagger = g$. As a consequence, the operator U becomes hermitian and so does any Wilson loop $W_\square$, therefore we do not need to add its conjugate to the magnetic hamiltonian, that becomes

$$H_B = -\lambda_B \sum_\square W_\square = -\lambda_B \sum_\square \mathrm{Re}\, W_\square\,. \tag{4.7}$$

With this convention, there is a lacking factor 2 with respect to the original Kogut-Susskind term. The U operator acts as

$$U\,|e\rangle = |e\rangle\,(+1)$$
$$U\,|s\rangle = |s\rangle\,(-1)\,,$$

therefore on the magnetic basis it is represented by the Pauli matrix σ^z

$$U = |e\rangle\langle e| - |s\rangle\langle s| \quad \Rightarrow \quad U = \begin{pmatrix} 1 & 0 \\ 0 & -1 \end{pmatrix} = \sigma^z \tag{4.8}$$

and the magnetic term takes the following form:

$$H_B = -\lambda_B \sum_{\square} \sigma^z_{\ell_1}\sigma^z_{\ell_2}\sigma^z_{\ell_3}\sigma^z_{\ell_4}\,. \tag{4.9}$$

The eigenvalues of the laplacian are now $f(\rho_0) = 0$ and $f(\rho_1) = 4$, so that on the electric basis it can be expressed as

$$\Delta = |\rho_0\rangle\, 0\, \langle\rho_0| + |\rho_1\rangle\, 4\, \langle\rho_1|\,. \tag{4.10}$$

hence the electric term becomes

$$H_E = \lambda_E \sum_{\ell} \Delta_\ell\,. \tag{4.11}$$

The original Wegner's model had the same structure, the only difference being that the electric term had eigenvalues -1, $+1$, so that its diagonal form was given by the matrix $-\sigma^z$. The magnetic and electric bases are related by a $\mathbb{Z}_2$ quantum Fourier transform, which is represented by

$$\mathfrak{U}_F = \frac{1}{\sqrt{2}}\begin{pmatrix} 1 & 1 \\ 1 & -1 \end{pmatrix} = \mathfrak{U}_F^\dagger\,.$$

More explicitly, the representation basis eigenstates can be found as

$$|\rho_0\rangle = \frac{|e\rangle + |s\rangle}{\sqrt{2}}\,, \quad |\rho_1\rangle = \frac{|e\rangle - |s\rangle}{\sqrt{2}}\,. \tag{4.12}$$

Performing this change of basis on $-\sigma^z$ shows that it is represented by $-\sigma^x$ on the magnetic basis, so the hamiltonian of Wegner's $\mathbb{Z}_2$ gauge theory was

$$H_W = -\lambda_E \sum_{\ell} \sigma^x_\ell \; - \lambda_B \sum_{\square} \sigma^z_{\ell_1}\sigma^z_{\ell_2}\sigma^z_{\ell_3}\sigma^z_{\ell_4}\,. \tag{4.13}$$

The same model can be found also as a suitable limit of a deformed toric code, as it is explained in [82]. We shall stick to our form of the electric term, but what we are going to say can be repeated also for Wegner's model, since the only difference is a rescaling of the electric eigenvalues and it does not change the general behaviour of the system.

4.2.2 Structure of the Hilbert space

Consider a 2d $N \times N$ lattice with periodic boundary conditions, which contains N^2 plaquettes and $2N^2$ links. In the magnetic basis, a single link Hilbert space is $\mathcal{H}_1 = \text{span}\{|\sigma^z = +1\rangle, |\sigma^z = -1\rangle\} \cong \mathbb{C}^2$. The full Hilbert space of the model is $\mathcal{H} \cong (\mathbb{C}^2)^{\otimes 2N^2}$. In this case, a transformation can only change the state of a link by flipping it and, in the magnetic basis we are working in, it is exactly what σ^x does:

$$\sigma^x = \begin{pmatrix} 0 & 1 \\ 1 & 0 \end{pmatrix} \quad \Rightarrow \quad \sigma^x |\sigma^z = \pm 1\rangle = |\sigma^z = \mp 1\rangle \,.$$

The plaquette operator, renaming in counterclockwise direction the plaquette links from 1 to 4 starting from the bottom, is now A gauge transformation is defined by choosing a group element $g(x)$ at each site of the lattice. A link will transform under the action of the element at its source and of the element of its target point. Overall, each site acts on its four neighbouring links (see Fig. 4.3); if $g(x) = e$ the action will be trivial, while if $g(x) = s$ the states of the four links will be reversed. If we denote $\ell \supset x$ the set of links that contain the site x, given any site $x \in \Lambda$ we can define

$$A(x) = \bigotimes_{\ell \supset x} \sigma^x_\ell \,, \tag{4.14}$$

which is sometimes called *star operator* and it encodes the action of a $\mathbb{Z}_2$ gauge transformation. It clearly commutes with the electric term, since they are diagonal in the same (representation) basis and a straightforward calculation shows that it commutes also with the magnetic term. Hence, the full hamiltonian is gauge-invariant as it should be and it satisfies

$$[A(x), H] = 0 \quad \forall\, x \in \Lambda \,. \tag{4.15}$$

gauge-invariant states should satisfy the constraint $A(x)\,|\text{phys}\rangle = |\text{phys}\rangle \;\forall\, x$.

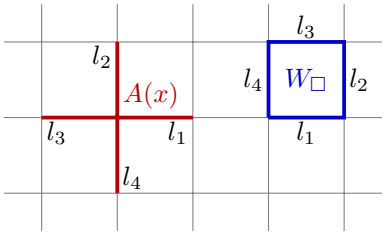

Figure 4.1: Example of how a star operator and a plaquette operator act.

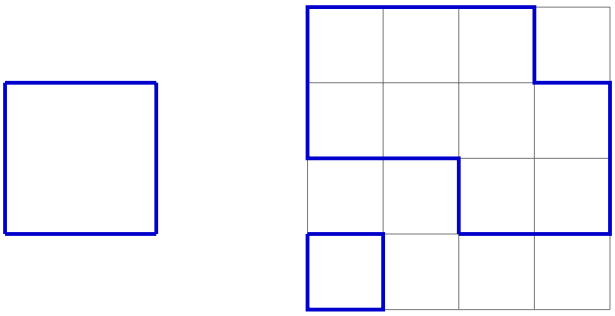

Figure 4.2: Some examples of gauge-invariant electric loops on a single plaquette and on a 4×4 lattice with open boundary conditions.

The two eigenstates of the single link electric term are also eigenstates of σ^x

$$|\rho_0\rangle = \frac{|\sigma^z = +1\rangle + |\sigma^z = -1\rangle}{\sqrt{2}} = |\sigma^x = +1\rangle$$
$$|\rho_1\rangle = \frac{|\sigma^z = +1\rangle + |\sigma^z = -1\rangle}{\sqrt{2}} = |\sigma^x = -1\rangle\,.$$

The *electric vacuum* is the overall state $|\rho_0\rangle^{\otimes 2N^2}$, where all links are in the state $|\rho_0\rangle$. It is gauge-invariant and it is the ground state of the electric term. Consider now the state where all the links are in $|\rho_0\rangle$ but one, that is taken in the state $|\rho_1\rangle$. Let that link be ℓ, connecting the points $\ell-$ and $\ell+$. It is an eigenstate of all star operators, but $A(\ell-)$ and $A(\ell+)$ have eigenstate -1. This is the state of the gauge field corresponding to the presence of two electric charges in the sites $\ell-$ and $\ell+$ [29, 53]: it is not a gauge-invariant state but it is nevertheless meaningful, since it would become gauge-invariant if we added matter. A straightforward generalization of this state is the one where, instead of a single link, we have switched on to $|\rho_1\rangle$ all the states along a path $\mathscr{C}_{xy}$ from a site x to another site y. In this case it represents the string that links two electric charges in the sites x and y.
To get a gauge-invariant state, each $A(x)$ must act on an even number of $|\rho_1\rangle$ states. Consequently, the gauge-invariant Hilbert space is generated by the states where the links in $|\rho_1\rangle$ form a closed path, such as the ones represented in Fig. 4.2. We call this basis for the gauge-invariant Hilbert space the basis of the *electric loops* and it will be denoted $\mathscr{B}$. The electric loops of arbitrary shape and size are exactly the states generated by acting on the electric vacuum with arbitrary products of plaquette operators $W_\square$, which behave like creation operators for the physical Hilbert space.

4.2.3 The $\mathbb{Z}_2$ confined phase

It is simple to see that in the strong coupling limit the behaviour of this model is confined. Recall that in our hamiltonian

$$H = \lambda_E \sum_\ell \Delta_\ell - \lambda_B \sum_\square W_\square \,,$$

the coefficients λ_E and λ_B are proportional to g^2 and $1/g^2$, so that in the strong coupling limit $g \to \infty$ the electric term dominates. In this limit, at the leading order the ground state is the electric vacuum

$$|E_0\rangle_\infty = \bigotimes_\ell |\rho_0\rangle_\ell \,,$$

which is the ground state of the electric term. This fact is general for any gauge group, since $|\rho_0\rangle$ is always the ground state of the laplacian on each link and it is a gauge-invariant state. The first excited states are the short electric loops along each plaquette. Each link carries energy $E = 4\lambda_E$, so that the state has energy $E = 16\lambda_E$. The basis of gauge-invariant states described before covers exactly the set of eigenstates of the electric term: a generic eigenstate is an electric loop along L links, whose energy is $E = 4\lambda_E\, L$.

Other states typical of the this phase are the confined quark-antiquark pairs. As we have seen, in the $\mathbb{Z}_2$ case there are only two possible values for the charge: 0, absence of charge, and -1, presence of a charge, so that the distinction between particles and antiparticles is lost. Consequently, here a quark-antiquark pair becomes the state with two electric charges linked by a gauge string that has already been introduced. Also this state can be realized by acting on the electric vacuum with a suitable operator. Notice that the Pauli matrix σ^z becomes σ^x in the basis of the eigenstates of σ^x, implying that $\sigma^z|\sigma^x = 1\rangle = |\sigma^x = -1\rangle$. Therefore, going back to the magnetic basis, the state with two electric charges at x and y is

$$W[\mathscr{C}xy]\,|E_0\rangle_\infty = \bigotimes_{\ell\,\in\,\mathscr{C}_{xy}} \sigma^z_\ell\,|E_0\rangle_\infty \,. \tag{4.16}$$

$W[\mathscr{C}_{xy}]$, that we can call the *Wilson string operator*, creates two electric charges at the endpoints of the string $\mathscr{C}_{xy}$. In abstract, it takes the form

$$W[\mathscr{C}xy] \;=\; \bigotimes_{\ell\,\in\,\mathscr{C}_{xy}} U_\ell \,. \tag{4.17}$$

To see that it is a confined phase, let us compute the string tension on this state with two electric charges, that we take for simplicity along the same

direction and with distance $R = |x - y|$. As we have already argued, the corresponding state of the gauge field is a string connecting x and y, whose energy is $E = 4\lambda_E L$. The string tension is computed with the minimum energy eigenstate contained into the trial state with two charges, consequently L has to be the length of the shortest string from x to y and we get

$$E(R) = \sigma R + \mathcal{O}(1/g^2) \ , \quad \sigma = 4\,\lambda_E \, . \tag{4.18}$$

As we have claimed, there is a finite string tension and the phase is confined and, furthermore, this proves that time-like Wilson loops satisfy the area law. With a bit more work it is possible to prove that also space-like Wilson loop satisfy the area law [30, 39]. At the leading order, $W[\mathscr{C}]\,|E_0\rangle_\infty$ switches on the links along the loop $\mathscr{C}$ and ${}_\infty\langle E_0|\,W[\mathscr{C}]\,|E_0\rangle_\infty = 0$: the states are orthogonal. Treating the magnetic term as a small perturbation of the hamiltonian, it can be shown that the first order in perturbation theory at which the perturbed ground $|E_0\rangle$ overlaps with the state $W[\mathscr{C}]\,|E_0\rangle$ is n, where n equals to the number of plaquettes surrounded by $\mathscr{C}$ [29]. Therefore n is proportional to the area of the loop $\mathscr{C}$ and the resulting behaviour is

$$\langle E_0|\,W[\mathscr{C}]\,|E_0\rangle = const \cdot \left(\frac{1}{g^2}\right)^n = const \cdot e^{-\mu(g)\,A[\mathscr{C}]} \, . \tag{4.19}$$

More in detail, it is possible to prove [46] that the strong coupling expansion has a finite radius of convergence and this implies the existence of a critical coupling g_c at which a quantum phase transition takes place, since the analyticity breaks down. The ground state can be written as a different superposition of electric loops at any coupling, since it must be a gauge-invariant state. In the limit $g \to \infty$ all links are turned off and getting closer to g_c increases the size and the number of the electric loops contributing to the ground, so that at the quantum critical point g_c the electric loops proliferate. The correlation length ξ is related to the size of the electric loops and it diverges as $g \to g_c$

$$\xi(g) \sim (g - g_c)^{-\nu} \, , \tag{4.20}$$

where ν is the corresponding critical exponent. Like it is typical in quantum phase transitions, the energy gap Δ shrinks at the critical point and the first excited state becomes degenerate with the ground [44, 75]

$$\Delta \sim (g - g_c)^{z\,\nu} \sim \xi^{\,z} \, . \tag{4.21}$$

Here z is another critical exponent. The correlation length at a given coupling is sometimes taken as a measurement of the characteristic length of confinement at that scale.

4.2.4 The $\mathbb{Z}_2$ deconfined phase

In the weak coupling limit, instead, the phase of the model turns out being deconfined and it has a non-trivial topological structure. When $g = 0$ the hamiltonian contains only the magnetic term and its ground state has on each link $|\sigma^z = 1\rangle$, the eigenstate of σ^z with eigenvalue $+1$ (and not -1, because of the minus in front of the magnetic term). In abstract the eigenstates of σ^z form the group element basis and, in particular, $|\sigma^z = 1\rangle$ corresponds to the identity element. The overall ground state is then

$$|E_0\rangle_0 = \bigotimes_{\ell} |e\rangle_\ell \,. \tag{4.22}$$

This state is not gauge invariant: $|e\rangle = |\sigma^z = 1\rangle$ and the action of the star operator flips to $|\sigma^z = -1\rangle$ the states of the links where it acts. Gauge invariant states are most easily described in the electric basis, where gauge-invariant states have only loops of switched on links. $|\sigma^z = 1\rangle$ satisfies

$$|\sigma^z = 1\rangle = \frac{|\sigma^x = 1\rangle + |\sigma^x = -1\rangle}{\sqrt{2}} \,,$$

then a gauge invariant ground state can be written as a uniform superposition of all gauge-invariant states in the basis of electric loops $\mathcal{B}$ [29, 44]

$$|E_0\rangle_0 = \sum_{|\psi\rangle \in \mathcal{B}} |\psi\rangle \,. \tag{4.23}$$

This is a manifestly gauge-invariant form for $|E_0\rangle_0$ and it shows the proliferation of electric loops in the deconfined case. A spatial Wilson loop is a product of σ^z operators, so that at the leading order obviously

$${}_0\langle E_0| \, W[\mathscr{C}] \, |E_0\rangle_0 = 1 \,.$$

A similar kind of reasoning to the one we have outlined in the confined case using perturbation theory [28] shows that only the plaquettes along $\mathscr{C}$ contribute to corrections, resulting in the perimeter law

$$\langle E_0| \, W[\mathscr{C}] \, |E_0\rangle = e^{-f(g)\, p[\mathscr{C}]} \,. \tag{4.24}$$

In the confined phase the excited states were electric charges, now there are excitation corresponding to magnetic charges, or *magnetic vortices*. Under the action of the star operator, a state $|\psi\rangle$ having an electric charge in the position x satisfies

$$A(x) \, |\psi\rangle = -|\psi\rangle \,. \tag{4.25}$$

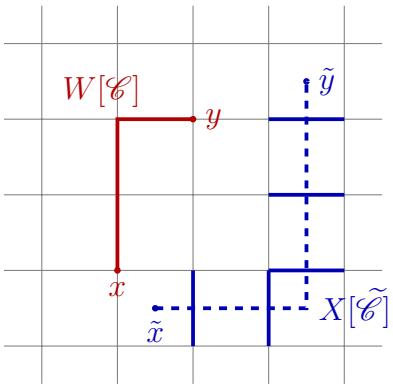

Figure 4.3: The Wilson line operator $W[\mathscr{C}]$ acts on the links where the path $\mathscr{C}$ lies, while the 't Hooft loop operator $X[\widetilde{\mathscr{C}}]$ acts on the links crossed by the path on the dual lattice $\widetilde{\mathscr{C}}$.

Similarly, $|\psi\rangle$ contains a magnetic vortex in the plaquette $\square$ iff

$$U_{\square}\,|\psi\rangle = -|\psi\rangle\,. \tag{4.26}$$

Consider the dual lattice $\tilde{\Lambda}$, whose sites lie in the middle point of each plaquette in the 2d case. Let $\widetilde{\mathscr{C}}$ be a path on $\tilde{\Lambda}$ joining two sites $\tilde{x}$, $\tilde{y}$ and therefore their corresponding plaquettes. A with two magnetic vortices can be created if we act on the deconfined vacuum $|E_0\rangle_0$ with a *'t Hooft string operator*

$$X[\widetilde{\mathscr{C}}] = \bigotimes_{\ell\cap\widetilde{\mathscr{C}}} V_\ell = \bigotimes_{\ell\cap\widetilde{\mathscr{C}}} \sigma^x_\ell\,, \tag{4.27}$$

where by $\ell\cap\widetilde{\mathscr{C}}$ we mean the links that intersect the path on the dual lattice $\widetilde{\mathscr{C}}$. The second expression is its realization in the magnetic basis, showing that it flips the state of the links where it is acting on. The figure 4.3 shows a pictorial representation of these two operators. In contrast to $W[\mathscr{C}]$, $X[\widetilde{\mathscr{C}}]$ is a product of σ^x operators and it is gauge-invariant, so it is allowed to have a non-vanishing expectation value. This enables another interpretation of the confinement transition: Wegner's model is dual to the 2D quantum Ising model and under this duality the operator that creates magnetic charges maps to the magnetization. Deep in the confined phase, where the ground state is close to having $|\sigma^x = 1\rangle$ on each link, the expectation value of $X[\widetilde{\mathscr{C}}]$ is clearly of the order of the unity and the confined phase maps to the ferromagnetic phase, while in the thermodynamic limit it is 0 in the whole deconfined phase [82]. Therefore, the transition from deconfinement to confinement can be seen as a condensation of magnetic monopoles [29].

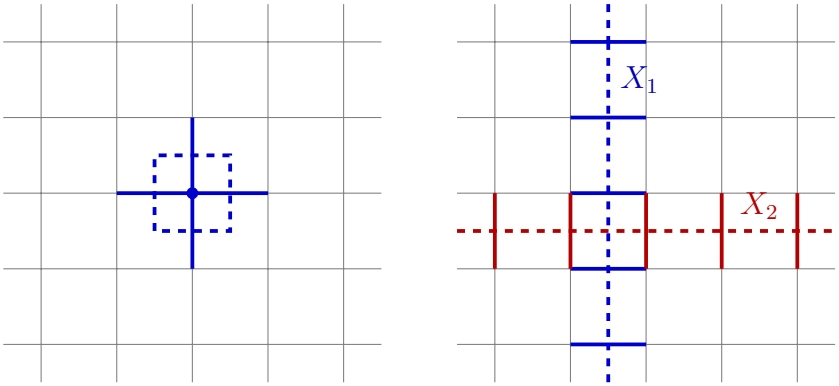

Figure 4.4: On the left the simplest visual example of how contractible 't Hooft lines are not independent of star operators. On the right, two non-contractible 't Hooft lines are shown.

4.2.5 Boundary conditions and the $\mathbb{Z}_2$ topological fluid

We have yet to consider the effects of the boundary conditions on the model. What has been said up to know holds irrespectively from them, but the periodic boundary conditions embed the $\mathbb{Z}_2$ lattice on a torus and it earns a non-trivial topological structure. Consider the operator $X[\widetilde{\mathscr{C}}]$. Obviously it commutes with the electric part of the hamiltonian, but, using the algebra of Pauli matrices $\sigma^i\sigma^j = \delta^{ij} + i\epsilon^{ijk}\sigma^k$, a direct calculation shows that it commutes also with the magnetic term when the path $\widetilde{\mathscr{C}}$ is a loop, owing to the fact that each plaquette is intersected 0 or 2 times by $\widetilde{\mathscr{C}}$ if it is closed

$$[X[\widetilde{\mathscr{C}}], H] = 0\,. \tag{4.28}$$

Since these 't Hooft strings are gauge-invariant operators, there seems to be a wealth of other symmetries of the model. This is actually incorrect, because on a contractible loop $X[\widetilde{\mathscr{C}}]$ can be expressed as a product of star operators, as it is represented in 4.4, so (4.28) does not provide any further information that is not already contained in the gauge invariance of the hamiltonian. However, our model lives on a torus and there are two non-contractible loops on the dual lattice $\widetilde{\mathscr{C}}_1$ and $\widetilde{\mathscr{C}}_2$, along which the 't Hooft loop cannot be a product of star operators: the theory on a torus has two additional independent symmetries, generated by the 't Hooft loop operators

$$X_\mu \equiv X[\widetilde{\mathscr{C}}_\mu] = \bigotimes_{\ell \cap \widetilde{\mathscr{C}}_\mu} V_\ell\,, \tag{4.29}$$

with $\mu = 1, 2$. The other relevant gauge-invariant operator, i.e. Furthermore, when $g = 0$ the hamiltonian has another interesting symmetry. Let $\mathscr{C}_\mu$ be

a non-contractible loop that wraps around the μ direction of the toroidal lattice. Then we define the Wilson loop operator along it

$$W_\mu \equiv W[\mathscr{C}_\mu] = \bigotimes_{\ell \in \mathscr{C}_\mu} U_\ell \tag{4.30}$$

and it clearly commutes with H at $g = 0$ because the hamiltonian has only the magnetic term $\sim \sigma^z$. Putting everything together, these operators satisfy the following commutation relations [21]

$$[X_\mu, H] = 0 \tag{4.31}$$
$$[W_\mu, H] = 0 \text{ if } g = 0 \tag{4.32}$$
$$\{X_\mu, W_\nu\} = 0 \text{ if } \mu \neq \nu\,, \tag{4.33}$$

trivially completed by $[W_\mu, W_\nu] = 0$ and $[X_\mu, X_\nu] = 0$. As always, the presence of a (true) symmetry implies degeneration: X_μ and H commute and there is a common basis of eigenstates $|x_1 x_2, E\rangle$. W_ν maps an eigenstate of X_μ into another one with opposite eigenvalue due to their anticommutation:

$$X_\mu\big(W_\nu|x_\nu\rangle\big) = -W_\nu X_\mu\,|x_\mu\rangle = \big(W_\nu\,|x_\mu\rangle\big)(-x_\mu)\,.$$

As we shall see soon, the eigenvalues of X_μ are ± 1. So if we start with the eigenstate of X_1, X_2 (but not yet of H) $|++\rangle$ we get the quadruplet:

$$|++\rangle \tag{4.34}$$
$$W_1\,|++\rangle = |+-\rangle \tag{4.35}$$
$$W_2\,|++\rangle = |-+\rangle \tag{4.36}$$
$$W_1 W_2\,|++\rangle = |--\rangle\,. \tag{4.37}$$

The model has four symmetry sectors that are called *topological sectors*, since their presence is determined by the topological global structure of the lattice. Now, if the initial state is chose as an eigenstate also of H $|++, E\rangle$, the states where the operators W_μ send it may have a different energy, but at $g = 0$ $[W_\mu, H] = 0$ and the four topological sectors $|++, E\rangle$, $|+-, E\rangle$, $|-+, E\rangle$, $|--, E\rangle$ are degenerate.

Consider the electric vacuum $|E_0\rangle_\infty$, on which all links occupy the state $|\sigma^x = 1\rangle$. Then, clearly $|E_0\rangle_\infty$ belongs to the $(+,+)$ sector. The ground state always belongs $(+,+)$. In general, it is possible to prove that the splitting of the topological sectors in the deconfined phase is suppressed exponentially by the length of the torus and in the thermodynamical limit the four sectors become degenerate on the whole deconfined phase [29]. Suppose now to flip from $|\sigma^x = 1\rangle$ to $|\sigma^x = -1\rangle$ all the links on a non-contractible loop along the

direction $\hat{1}$ on the lattice. The state has become a non-trivial electric loop along $\hat{1}$ and it is an eigenstate of X_2 with eigenvalue -1. In general, it is immediate to see that X_μ measures the parity of the number of non-contractible electric loops along $\hat{\nu}$, making clear their topological nature. More in general, the topological sectors are related to the "handles" of the surface we are working in: if the surface has genus g, the ground state degeneracy is 4^g. This degeneracy that is present only in one phase and not in the other is not related to a loss of symmetry, but it depends on the different topological properties of the ground states: in one case the electric loops proliferate and wrap around the handles, in the other case only short trivial loops are present and the ground has to be in the $(+,+)$ sector. The deconfined phase of this model is a topological phase called $\mathbb{Z}_2$ *topological fluid*. This structure can be extended to all $\mathbb{Z}_n$ models. General 't Hooft and Wilson loops are

$$X_\mu = \bigotimes_{\ell \cap \widetilde{\mathscr{C}}_\mu} V_\ell \ , \quad W_\mu = \bigotimes_{\ell \cap \mathscr{C}_\mu} U_\ell \tag{4.38}$$

and they satisfy again $[X_\mu, H] = 0$ and $[W_\mu, H] = 0$ if $g = 0$, but $\{X_\mu, W_\nu\} = 0$ is replaced by the Schwinger-Weyl algebra commutation relation (4.6). Each X_μ operator has n eigenvalues corresponding to the representations of $\mathbb{Z}_n$, which result in n topological sectors for each dimension, each one counting the number of non-trivial loop along the other directions $\mathrm{mod}\, n$. In general, a $\mathbb{Z}_n$ model of this kind in d dimensions will show n^d topological sectors.

CHAPTER V.

Implementation of the quantum algorithm

Now that we have described how our $\mathbb{Z}_n$ models are constructed and what behaviour should be expected, all there is left to do is to realize the digital quantum simulation using the methods that have been discussed so far. For our simulation we have chosen to focus on the simplest case, that is $n = 2$, for mainly two reasons. One is that the number of qubits demanded is proportional to the order of the gauge group, hence with more complicated groups the requirements would quickly exceed the current hardware availabilities. The second reason is that this is a rather young field of study and, to our knowledge, the published works where the simulations have actually been implemented on a digital quantum computer are not many [8, 21, 77, 56]; consequently, working with a relatively simple and well-known model can serve as a benchmark to test the performance of the methods employed. In Appendix B a few basics of quantum computing are quickly discussed. After having specified the $\mathfrak{U}$ gates for G=$\mathbb{Z}_2$ we describe our simulation, which consists in the preparation of the ground states at several values of the coupling and in the measurements of the corresponding expectation values of the energy and of some Wilson loops. These observations can be used to study the phases of the system.

5.1 The gate-set for $\mathbb{Z}_2$

In the third chapter we have introduced four unitary operations, $\mathfrak{U}_{-1}$, $\mathfrak{U}_{\times}$, $\mathfrak{U}_{\mathrm{tr}}$ and $\mathfrak{U}_F$, which can be used to decompose the time evolution generated by the hamiltonian of a lattice gauge theory with an arbitrary gauge group. In this section we see how to represent them for $\mathbb{Z}_2$, where they turn out being

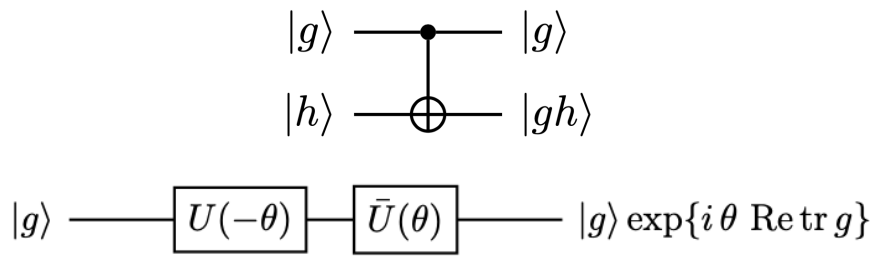

Figure 5.1: Quantum circuits that implement the $\mathbb{Z}_2$ multiplication (above) and the $\mathbb{Z}_2$ trace gate (below).

particularly simple. We can express the group $\mathbb{Z}_2$ as

$$\mathbb{Z}_2 = \{e,\, s \,|\, s^2 = e\}\,. \tag{5.1}$$

It is a group of order 2, so $\dim L^2(\mathrm{G}) = |\mathbb{Z}_2| = 2$ and a register of single qubit is enough to encode the Hilbert space of a single link. We choose to identify the computational basis with the group element basis and in particular $|0\rangle \equiv e$ and $|1\rangle \equiv s$. To implement the $\mathfrak{U}$ gates, we should see first how they act on the group element basis and then realize the corresponding transformation on the states of the computational basis.

1. **Inversion gate** $\qquad \mathfrak{U}_{-1}|g\rangle = |g^{-1}\rangle$

In this case it is trivial: since $e^{-1} = e$, $g^{-1} = g$, we can conclude that $\mathfrak{U}_{-1} = \mathbb{I}$.

2. **Multiplication gate** $\qquad \mathfrak{U}_{\times}|g\rangle|h\rangle = |g\rangle|gh\rangle$

The table of all products of $\mathbb{Z}_2$ is $e \cdot e = e$, $e \cdot g = g$, $g \cdot e = g$, $g \cdot g = e$. The identifications above allow us to translate it into a truth table for $\mathfrak{U}_{\times}$.

g	h	g	$g \cdot h$
0	0	0	0
0	1	0	1
1	0	1	1
1	1	1	0

We immediately see that on $|g\rangle$ it is an identity, while it acts on $|h\rangle$ as a CNOT controlled by $|g\rangle$, so $\mathfrak{U}_{\times}$ can be realized as the circuit in figure 5.1.

3. **Trace gate** $\mathfrak{U}_{\rm tr}(\theta)|g\rangle = |g\rangle\, e^{\,i\theta\,\mathrm{Re\ tr}[g]}$

To define a trace on $\mathbb{Z}_2$ we have to work within a specific representation, so now we should identify $e = 1$ and $g = -1$. Therefore $\mathfrak{U}_{\rm tr}(\theta)$ acts as

$$|0\rangle \mapsto |0\rangle\, e^{i\theta}$$
$$|1\rangle \mapsto |1\rangle\, e^{-i\theta}\,.$$

A phase gate $U(\phi)$ maps $|0\rangle \mapsto |0\rangle$, $|1\rangle \mapsto |1\rangle\, e^{i\phi}$ and it is represented by

$$U(\phi) = \begin{pmatrix} 1 & \\ & e^{i\phi} \end{pmatrix}\,. \tag{5.2}$$

We can revert its action by applying an $X \equiv \sigma_x$ gate before and after it:

$$\bar{U}(\phi) = XU(\phi)X = \begin{pmatrix} e^{i\phi} & \\ & 1 \end{pmatrix}\,, \tag{5.3}$$

that produces the transformation $|0\rangle \mapsto |0\rangle\, e^{i\phi}$, $|1\rangle \mapsto |1\rangle$. In the end, $\mathfrak{U}_{\rm tr}(\theta)$ can be realized as $\bar{U}(\theta)U(-\theta)$, as depicted in figure 5.1.

4. **Fourier gate** $\mathfrak{U}_F \sum_{g\in G} f(g)|g\rangle = \sum_{\rho\in\hat{G}} \sum_{i,j=1}^{d_\rho} \hat{f}(\rho)_{ij}|\rho, ij\rangle\,.$

As it was described in Section (3.5), on $\mathbb{Z}_n$ this gate is the usual quantum Fourier transform and its implementation as a quantum circuit is well known. Here it happens to be a single Hadamard gate, as it can be see in Eq. (3.49).

5. **Phase gate** $U_E^{(l)}(\Delta t) = \mathfrak{U}_F^\dagger\, \mathfrak{U}_{ph}\, \mathfrak{U}_F\,.$

A precise expression for $\mathfrak{U}_{ph}$ is given once we specify the electric term H_E. As we have already said, we choose the Yang-Mills like electric term defined by the $\mathbb{Z}_n$ laplacian (4.1), that in the electric basis takes the form

$$\mathfrak{U}_F H_E \mathfrak{U}_F^\dagger = \lambda_E \sum_{links} \sum_{\rho_j} f(\rho_j)\hat{P}_{\rho_j}\ ,\ \ f(\rho_j) = 4\sin^2\left(\frac{\pi j}{N}\right)\,. \tag{5.4}$$

Specifying it for $\mathbb{Z}_2$, $j = 0, 1$ and then $f(0) = 0$, $f(1) = 4$, which implies

$$\mathfrak{U}_F H_E \mathfrak{U}_F^\dagger = \lambda_E \sum_{links} \Big(|\rho_0\rangle\, 0\, \langle\rho_0| + |\rho_1\rangle\, 4\, \langle\rho_1|\Big)\,. \tag{5.5}$$

Taking the exponential of each single link term we find $\mathfrak{U}_{ph} = \mathfrak{U}_F^\dagger e^{-iH_E\,\Delta t}\mathfrak{U}_F = e^{-i\,\mathfrak{U}_F^\dagger H_E \mathfrak{U}_F\,\Delta t}$, that is associated to the matrix

$$\mathfrak{U}_{ph} = \exp\left\{-i\lambda_E \Delta t \begin{pmatrix} 0 & 0 \\ 0 & 4 \end{pmatrix}\right\} = \begin{pmatrix} 1 & 0 \\ 0 & e^{-4i\lambda_E \Delta t} \end{pmatrix} \tag{5.6}$$

and it can be directly implemented as the phase gate $U(\phi = -4\lambda_E \Delta t)$. Given an arbitrary initial state encoded into a suitable set of qubits, the corresponding evolved states given by the applications of $e^{-iH_E \Delta t}$ and $e^{-iH_B \Delta t}$ are obtained by applying these gates in the combinations described in the section 3.3. This is the gate $\mathfrak{U}_{ph}$ appearing in the electric time evolution (3.61), while $\mathfrak{U}_{-1}$, $\mathfrak{U}_{\times}$ and $\mathfrak{U}_{\rm tr}(\theta)$ are used to build the magnetic evolution (3.57). The only difference to what is described in the third chapter is that now the parameter θ has to be chosen as

$$\theta = \lambda_B \Delta t\,, \tag{5.7}$$

which does not have the factor 2 of the equation (3.58), because the $\mathbb{Z}_2$ magnetic term given in (4.7) is already self-adjoint without needing to sum its conjugate.

5.2 Preparation of the initial state

Our aim is to compute the expectation of values of some operators on the ground state of the hamiltonian, which is a different state $|E_0\rangle_g$ depending on the value of the coupling g. We have to find a way to prepare the ground state at any given value of g and this will be the first part of the computation, as it has been described in the second chapter. There are two possible ground states that are particularly simple to describe and, hopefully, to implement: the electric vacuum $|E_0\rangle_\infty$ and the magnetic vacuum $|E_0\rangle_0$, that are respectively the grounds in the two limits $g \to \infty$ and $g \to 0$

$$|E_0\rangle_\infty = \bigotimes_\ell |\sigma^x = 1\rangle \;\;, \quad |E_0\rangle_0 = \bigotimes_\ell |\sigma^z = 1\rangle\,.$$

A possible approach that can be followed to prepare $|E_0\rangle_g$ is to employ the protocol of *adiabatic quantum computation*. The idea is to exploit the adiabatic theorem of quantum mechanics [55], which, roughly speaking, consists in the following statement. Consider a time dependent hamiltonian $H(t)$ and its ground state at $t = 0$ $|E_0(t = 0)\rangle$. If the hamiltonian were time independent, the state would be unchanged by time evolution, which would be realized by the operator e^{-iHt}. Now the hamiltonian is time-dependent, but, if its evolution is sufficiently slow, the time-evolved state will remain very close to the instantaneous ground state at the time t $|E_0(t)\rangle$. This statement can be made more precise and we shall see in a while what controls

the accuracy of this approximation. A review on the topic is [4]. As a consequence, if we encode the time dependence of the hamiltonian into a slow evolution of the coupling $g(t)$, we should be able to get an approximation of the ground state $|E_0\rangle_{g(t)}$ by time-evolving the ground state at a fixed value of the coupling $g(t=0)$ with the methods described before.

Which of the two limiting ground states is more convenient to take as the initial state? This question probably does not have a single best answer, as each choice has its advantages and drawbacks. The most immediate advantage of the electric vacuum is its simplicity: it is already gauge invariant and it can be immediately realized by applying a Hadamard gate on each link, because $|\sigma^x = 1\rangle = (|\sigma^z = 1\rangle + |\sigma^z = -1\rangle)/\sqrt{2}$. Furthermore this procedure can be straightforwardly generalized to any other gauge group and it can be always implemented with the gate-set introduce before, since the state $|\rho_0\rangle$ of the representation basis can be prepared with the aid of the Fourier gate. A gauge invariant vacuum in the $g \to 0$ limit is less immediate to prepare. The article [21] describes a possible implementation of this state, but it involves projection operators, that are not unitary and cannot be inserted as a part of an actual quantum computation. Projections can be simulated by performing measurements on the system, but it turns out being only a probabilistic realization of the desired projector and this would decrease the efficiency of the procedure on a real quantum device. The authors of [21] were able to circumvent this issue because they had employed a classical simulator of a quantum computer, so, for the sake of the general spirit of this thesis (i.e. to keep the methods used as general and as "quantum" as possible) we shall stick to the first possibility. We are going to see this point better, but the disadvantage of this choice is that it increases the range of values of the coupling that has to be covered, which results in worse uncertainties.

After all these comments, let us describe in detail the first part of the simulation algorithm. We start the procedure with each qubit on the state $|0\rangle = |\sigma^z = 1\rangle = |e\rangle$. Then, we apply on each of them a Hadamard gate that produces the electric vacuum with

$$|+\rangle = \frac{|\sigma^z = 1\rangle + |\sigma^z = -1\rangle}{\sqrt{2}} = |\sigma^x = 1\rangle$$

on every link. If we plan to produce the ground state at any other coupling with an adiabatic evolution that starts from the confined electric vacuum, it is convenient to rewrite the hamiltonian as follows:

$$H = \sum_{\ell} \Delta_\ell + h \sum_{\square} U_{\ell_1} U_{\ell_2} U_{\ell_3} U_{\ell_4} \,. \tag{5.8}$$

We have placed a single coupling constant h in front of the magnetic term, so that in the limit $h \to 0$ the electric term dominates and the ground state is our desired initial state. The adiabatic evolution that prepares the ground state at any other coupling h can be implemented with a slight modification of the Trotter algorithm presented in the second chapter: we reproduce the time evolution generated by an evolving hamiltonian by letting the coupling vary in each Trotter step, starting from $h_{j=0} = 0$ to a large enough value $h_{j=N_s} = h_f$, where N_s is the total number of Trotter steps. If the evolution of h_j is sufficiently slow, i.e. if the steps Δh at which h is increased are sufficiently small, the adiabaticity should be preserved. At each step j, the hamiltonian is

$$H_j = H_E + h_j\, H_B = \sum_{\ell} \Delta_\ell + h_j \sum_{\square} U_{\ell_1} U_{\ell_2} U_{\ell_3} U_{\ell_4} \;\;, \quad h_j = \Delta h \cdot j \tag{5.9}$$

where the magnetic term has been renamed with the coupling extracted for convenience. If each Trotter step lasts for t_s, $h_j = \Delta h \cdot j$ is the coupling $h_j \equiv h(t_j)$ at the time $t_j = t_s \cdot j$, so we are effectively realizing a linear growth of the coupling $h(t_j) = \Delta h / t_s \cdot t_j$. The evolution we implement is

$$\prod_{j=1}^{N_s} e^{-iH_j\, t_s} = \prod_{j=1}^{N_s} e^{\,-iH_E\, t_s - ih_j H_B\, t_s} \tag{5.10}$$

and the electric and magnetic evolution terms are decoupled by making use of the Trotter approximation

$$\prod_{j=1}^{N_s} e^{-iH_j\, t_s} \approx \prod_{j=1}^{N_s} \left(e^{-iH_E\, t_s}\, e^{-ih_j H_B\, t_s} \right). \tag{5.11}$$

Since the electric part and the magnetic part of the hamiltonian are separately gauge invariant, this decomposition will preserve the gauge invariance of the initial state. Furthermore, they also separately commute with the two non-contractible 't Hooft loops X_μ, $\mu = 1, 2$, so that the state will remain in the $(+,+)$ topological sector throughout all the evolution. For each step, the error introduced by this approximation is estimated by the operator norm of their difference [77], which is bounded by the commutator

$$\left|\left| e^{-i(H_E + h_j\, H_B)\, t_s} - e^{-iH_E\, t_s}\, e^{-ih_j H_B\, t_s} \right|\right| \;\leq\; \frac{t_s^2}{2} \left|\left| \left[H_E, h_j H_B \right] \right|\right|. \tag{5.12}$$

Recall that our single link electric term, in the representation basis, is given by the laplacian $\Delta_{\mathbb{Z}_2} = \mathrm{diag}\,(0, 4)$. In the same basis, $V = \mathrm{diag}\,(-1, 1)$,

implying that $\Delta_{\mathbb{Z}_2} = 2V + 2\mathbb{I}$. Consider the magnetic term on a plaquette in the group element basis, where it is represented by $\sigma^z_{\ell_1}\sigma^z_{\ell_2}\sigma^z_{\ell_3}\sigma^z_{\ell_4}$. It does not commute only with the electric terms on the links of the plaquette, with V being represented by a σ^x matrix in this basis. The Pauli algebra implies

$$\left|\left|\left[\, 2\sigma^x_{\ell_1} + 2\mathbb{I},\, h_j\, \sigma^z_{\ell_1}\sigma^z_{\ell_2}\sigma^z_{\ell_3}\sigma^z_{\ell_4}\,\right]\right|\right| = \left|\left|-4h_j i\, \sigma^y_{\ell_1}\sigma^z_{\ell_2}\sigma^z_{\ell_3}\sigma^z_{\ell_4}\right|\right| = 4h_j$$

since the norm of a tensor product of operators is the multiplication of their norms and Pauli matrices have a unitary norm [5]. Taking into account the 4 links for each plaquette whose operators σ^x do not commute with the magnetic term and the overall N_p plaquettes, the error on a single step is

$$\delta_{T,j} \leq \frac{t_s^2}{2}\, 16 N_p\, h_j = 8\, N_p t_s^2\, h_j \tag{5.13}$$

and it should be propagated on all steps. Since $h_j = \Delta h \cdot j$, we have

$$\delta_T = \sum_{j=0}^{N_s} \delta_{T,j} \;\leq\; 8\, N_p t_s^2\, \Delta h \sum_{j=0}^{N_s} j = 8\, \Delta h\, N_p t_s^2\; \frac{N_s(N_s-1)}{2}\,.$$

Recall that $\Delta h = h_f/N_s$. Then, apart from the factor 4, approximation $N_s(N_s-1) \approx N_s^2$ yields the scaling law of the error

$$\delta_T \approx h_f\, N_p N_s\, t_s^2\,. \tag{5.14}$$

It is important to keep track also of the conditions under which the adiabatic theorem provides a good approximation of the exact vacuum. The adiabatic theorem is exact if the evolution is infinitely long and infinitesimally slow, but this is of course impracticable. The standard quantitative version of the theorem states that the adiabatic approximation is good as long as the rate at which the matrix elements of the hamiltonian vary is slow compared to the time scale set by the inverse of the energy gap Δ between the ground and the first excited state [4]. If t_f is the total evolution time, the adiabatic condition can be expressed as

$$\max_{t\,\in\,[0,t_f]} \frac{|\langle E_1(t)|\, \partial H/\partial t\, |E_0(t)\rangle|}{|\Delta(t)|^2} \;\ll 1\,. \tag{5.15}$$

The approximation is spoiled if the state of the system gets soiled by unwanted transitions in higher energy states and the transitions that are more likely are on the states with closest energies. This is why often it is enough to restrict the attention to the first excitation. The energy eigenvalues also vary with t, so one should make sure that the condition is satisfied in the worst

case, when the gap $\Delta(t)$ is the smallest and spurious transitions are more likely to happen. There seems to be a problem here: by varying the coupling this model should cross a critical point, where the correlation length becomes infinite and the gap shrinks like in Eq. (4.21). If $\Delta = 0$, the corresponding time scale $1/\Delta$ becomes infinite and the adiabatic approximation inevitably fails. The way-out is that the gap actually shrinks only in the thermodynamic limit and we are going to implement the simulation only for small lattices, so that with a sufficiently slow evolution this issue can be avoided. Yet another difficulty has to be overcome: as we have explained in the section 4.2, the four topological sectors become degenerate in the deconfined case. Again this would break the adiabaticity of the evolution, but this problem too can be avoided. The reason is that this is a symmetry protected transition: there are symmetry operators X_μ commuting with the hamiltonian for all the values of the coupling h_j

$$[X_\mu, H_j] = 0$$

which implies that the population transfers between states belonging to different symmetry sectors are exactly forbidden [92], so the gap that has to be considered is between the ground and the first excitation in the (+,+) sector. The time dependence of the hamiltonian is contained only in the coupling, that increases of Δh in a time step t_s, so a rough estimate of the parameter that governs the adiabatic approximation can be given by the ratio

$$r = \frac{\Delta h}{t_s} = \frac{h_f}{N_s\, t_s}\,, \tag{5.16}$$

which has to be compared with the squared gap at any coupling [21]. We see a non-trivial interplay between these two error sources: the Trotter approximation works better if the evolution time is shorter, but a variation of the coupling occurring in a very short time may result in a quench that spoils the adiabaticity. Consequently, the choice of the parameters N_s, t_s will be a delicate matter.

5.3 Measurement of physical observables

After having realized an approximation of the ground state at a given coupling h with the methods described in the previous section, we measure some quantities which help us characterizing the state that we have prepared. We have chosen to measure the ground state energy and the expectation values of contractible Wilson loops, whose behaviour can be used to characterize the

phases of the model, as explained in the fourth chapter. The hamiltonian is

$$H = \sum_{\ell} \Delta_{\ell} - h \sum_{\square} U_{\ell_1} U_{\ell_2} U_{\ell_3} U_{\ell_4}$$

and a generic Wilson loop operator along a path $\mathscr{C}$ is defined as

$$W[\mathscr{C}] = \bigotimes_{\ell \in \mathscr{C}} U_{\ell} \, .$$

The hamiltonian is always hermitian, but in the $\mathbb{Z}_2$ also Wilson loops are hermitian operators due to the self-adjointness of $U_{\ell} = U_{\ell}^{\dagger}$. To measure them, we employ a slightly modified version of the algorithm for dynamical correlation functions (2.6) presented in the second chapter.

Let Q be an hermitian operator that we want to measure. If we replace the unitary operators in (2.6) with $V = \mathbb{I}$, $W = e^{-iQt}$ the previously described procedure allows us to measure $\mathcal{C}(t) = \langle \psi | \, e^{-iQt} \, | \psi \rangle$ on any state $|\psi\rangle$, that in our case consists in the approximate ground state $|E_0\rangle_h$. Then, to extract the expectation value of Q we make the estimate

$$\langle \psi | Q | \psi \rangle \; = \; i \frac{d}{dt} \langle \psi | \, e^{-iQt} \, | \psi \rangle \, \Big|_{t=0} \; \approx \; i \, \frac{\mathcal{C}(\epsilon) - \mathcal{C}(0)}{\epsilon} \, , \tag{5.17}$$

Where ϵ is some small time interval that has to be chosen. If we expand the state $|\psi\rangle$ into the basis of the eigenstates $|q\rangle$ of Q, we get

$$\mathcal{C}(\epsilon) = \sum_{q} e^{-iq\,\epsilon} \langle \psi | q \rangle \langle q | \psi \rangle = \sum_{q} e^{-iq\,\epsilon} \, p_{\psi}(q) \, . \tag{5.18}$$

Actually, it is enough to measure only the imaginary part of $\mathcal{C}(\epsilon)$. To see it, let us expand at the first order the equation above

$$\mathcal{C}(\epsilon) = \sum_{q} \Big(\cos(q\epsilon) \, p_{\psi}(q) - i \sin(q\epsilon) p_{\psi}(q) \Big) =$$

$$= \sum_{q} p_{\psi}(q) - i \sum_{q} q\epsilon \, p_{\psi}(q) + \mathcal{O}(\epsilon^2) = 1 - i \sum_{q} q\epsilon \, p_{\psi}(q) + \mathcal{O}(\epsilon^2)$$

because all probabilities add up to one. Then $\mathcal{C}(0) = 1$, so (5.16) implies

$$\langle \psi | Q | \psi \rangle \approx i \frac{-i\epsilon \sum_q q p_{\psi}(q) + \mathcal{O}(\epsilon^2)}{\epsilon} = i \frac{i \, \mathrm{Im} \, \mathcal{C}(\epsilon) + \mathcal{O}(\epsilon^2)}{\epsilon} \, .$$

In conclusion, we can measure the expectation value of an operator Q as

$$\langle \psi | Q | \psi \rangle \approx - \frac{\mathrm{Im} \, \mathcal{C}(\epsilon)}{\epsilon} \, . \tag{5.19}$$

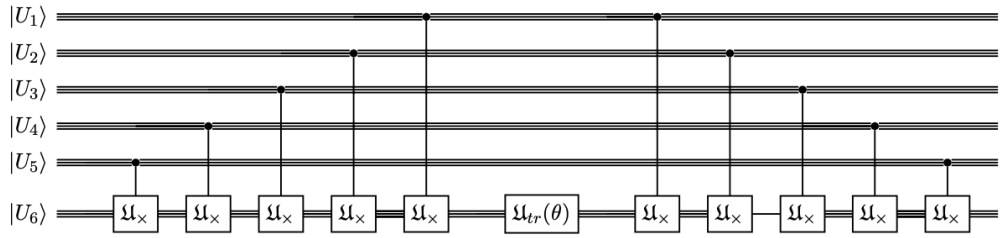

Figure 5.2: Circuit measuring the expectation value of a $\mathbb{Z}_2$ Wilson loop along the links ℓ_1, ℓ_2, ℓ_3, ℓ_4, ℓ_5, ℓ_6, on the state encoded by the registers on the left.

We apply this method to the operators $Q = H$ and $Q = W[\mathscr{C}]$. To do it we only need to know how to implement the unitary evolutions generated by them and this is very simple. For the energy we have to realize e^{-iHt}, which is the ordinary time evolution operator and we have already explained how to implement it. $W[\mathscr{C}]$ is a product of independent U_ℓ operators, so it has exactly the same structure of the magnetic term of the hamiltonian. For instance, if the loop along which we are studying the Wilson loop consists of the links ℓ_1, ℓ_2, ℓ_3 travelled in the positive direction and ℓ_4, ℓ_5, ℓ_6 travelled in the negative direction, the corresponding Wilson loop operator is

$$W[\mathscr{C}] = U_{\ell_1} U_{\ell_2} U_{\ell_3} U_{\ell_4}^\dagger U_{\ell_5}^\dagger U_{\ell_6}^\dagger = U_{\ell_1} U_{\ell_2} U_{\ell_3} U_{\ell_4} U_{\ell_5} U_{\ell_6} \tag{5.20}$$

and $e^{-iW[\mathscr{C}]t}$ can be implemented with the circuit in Fig. 5.2, that is analogous to the circuit which realize the magnetic part of the time evolution, apart from the adaptation of the number of links and a modification of the parameter θ of the trace gate $\mathfrak{U}_{\mathrm{tr}}(\theta)$, which now has to be chosen as

$$\theta = -t_s \,. \tag{5.21}$$

If the gauge group were something different from $\mathbb{Z}_2$ and $W[\mathscr{C}]$ were not hermitian, we should have measured separately the real part and the imaginary part of the expectation value. This measurement can be carried on with the circuit represented in Fig. 2.2. We only need the imaginary part, which equals the expectation value of σ^y acting only on an ancillary qubit prepared in the state $|+\rangle$. The eigenstates of σ^y are mapped into the computational basis states by the rotation

$$R_x\left(\frac{\pi}{2}\right) = e^{-i\frac{\theta}{2}X} = \frac{\sqrt{2}}{2}\begin{pmatrix} 1 & -i \\ -i & 1 \end{pmatrix}, \tag{5.22}$$

in such a way that $R_x(\pi/2)|\sigma^y = 1\rangle = |0\rangle$ and $R_x(\pi/2)|\sigma^y = -1\rangle = |1\rangle$. As a consequence, $\mathrm{Im}\, C(\epsilon)$ will be measured by counting the occurrences of zeroes

and ones in the computational basis:

$$\begin{aligned} \operatorname{Im} C(\epsilon) &= (+1)\, p_\psi(\sigma^y = 1) + (-1)\, p_\psi(\sigma^y = -1) = \\ &= p_{R_x(\pi/2)\,\psi}\,(0) - p_{R_x(\pi/2)\,\psi}\,(1)\,. \end{aligned} \tag{5.23}$$

5.4 Implementation and results

Using the methods described before, we have realized the simulation for the 3×3 lattice with periodic boundary conditions represented in Fig. 5.3. The periodic conditions ensure that the number of sites equals the number of plaquettes, so that we have worked with $N_p = N^2 = 9$ plaquettes and sites, while the number of links is $N_\ell = 2N^2 = 18$, which corresponds to 18 qubits needed to encode the lattice, plus an additional ancilla for the measurements. The simulation has been carried out within the Qiskit framework and using the local `qasm` simulator (see Appendix B), in order to avoid dealing with the additional noise introduced by the large number of gates employed.

The simulation algorithm contains three free parameters: the number of Trotter steps N_s, the duration of each step t_s and the short time ϵ used to approximate the derivatives that give us the expectation values. The parameter ϵ has been chosen as $\epsilon = 20\, t_s$ for all simulations, after several attempts that probed its influence on the measurements. In this context the Trotter step t_s is our "infinitesimal" time and clearly ϵ has to be larger than t_s. On a time scale of the order $\epsilon \sim t_s$ the results were too much unstable, while if ϵ is too large it does not provide anymore a good approximation of the derivative. The other two parameters were chosen to be the ones whose corresponding circuit for the trotterized adiabatic evolution prepares the best approximation of the ground state, while keeping the running time of the program sufficiently short. Each run follows the steps below:

1. choice of the final coupling h;
2. construction of the circuit (with N_s steps, each with duration t_s) that adiabatically prepares the ground state at the coupling h;
3. construction of the circuit that measures the expectation value of one observable (the energy or a Wilson loop);
4. executions on the local simulator and extraction of the output.

The quantum algorithm stops at each extraction of the output, since projective measurements cause the final quantum state to collapse. The executions of the circuit should be many because each measurement tells us if the state

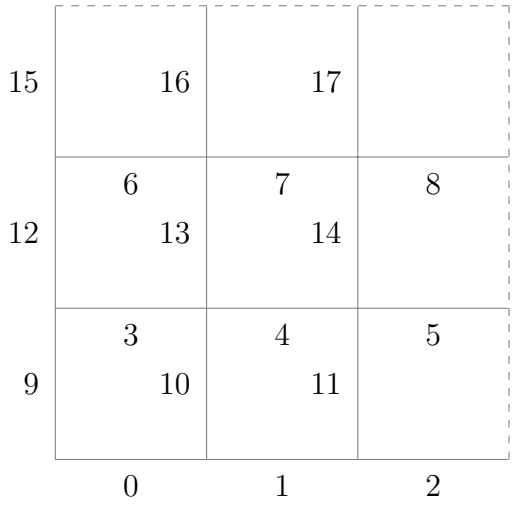

Figure 5.3: The lattice on which the simulation has been implemented, which is composed of 3^2 plaquettes and $2 \cdot 3^2$ links due to the periodic boundary conditions. The links are labelled starting from the horizontal ones and then by enumerating all the vertical ones.

of the ancilla has collapsed into $|0\rangle$ or into $|1\rangle$ and we need to find the probabilities for the two cases, following Eq. (5.23). We have chosen to extract the probabilities with 1000 shots of the quantum circuits and they provide a single measurement of the chosen observable (energy or Wilson loop). The measurements of the output were unstable due to the quantum nature of the final states, so we had to extract some statistics by taking repeated measurements at each value of the coupling. Then, these steps have been iterated for several values of the final coupling, in order to outline a graph of the behaviour of the observable. The range of values that we cover should at least cross the phase transition region, in order to observe interesting physics.

The results for the ground state energy are reproduced in Fig. 5.4, with two different sets of parameters t_s, N_s. Fig. 5.4 (a) has $t_s = 0.005$ and $N_s = 200$, which correspond to the errors

$$\delta_T \approx h\, N_p N_s t_s^2 = 4,5 \cdot 10^{-2} \cdot h$$

$$r = \frac{h}{N_s t_s} = h$$

and Fig. 5.4 (b) has parameters $t_s = 0.0008$ and $N_s = 600$, corresponding to

$$\delta_T \approx h\, N_p N_s t_s^2 \approx 3.45 \cdot 10^{-3} \cdot h$$

$$r = \frac{h}{N_s t_s} = \frac{25}{12}\, h\,.$$

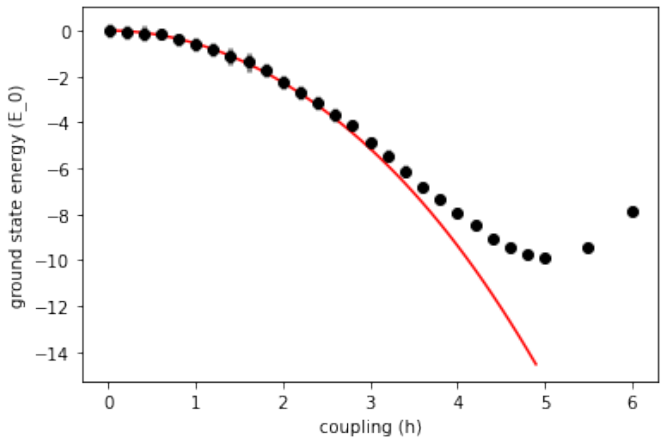

(a) $t_s = 0.005$, $N_s = 200$

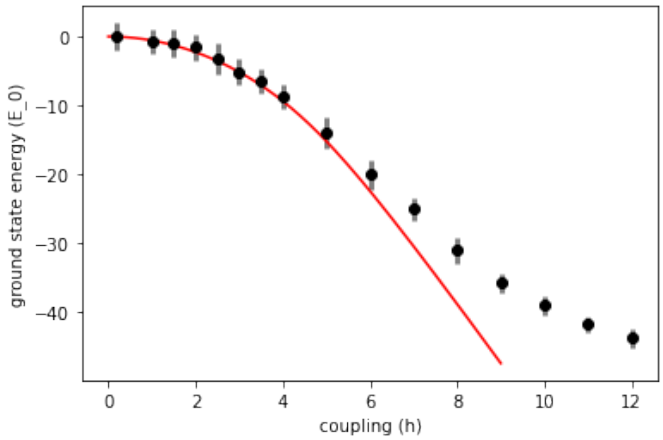

(b) $t_s = 0.0008$, $N_s = 600$

Figure 5.4: Measurements of the expectation value of the energy of the $\mathbb{Z}_2$ LGT on a 3×3 lattice with p.b.c. on the approximate ground states at couplings h. The red line shows the exact values of the ground state energy, computed with an exact diagonalization algorithm. The error bars are discussed in the text.

Both the Trotter error δ_T and the parameter r estimating the adiabaticity are proportional to the final value h at which the evolution stops. This behaviour is reflected in the two pictures: at small values of the coupling, the measured value of the energy coincides with the exact value with great accuracy, while the deviations increase together with the coupling. The exact values of the ground state energy have been independently computed using an exact diagonalization algorithm.

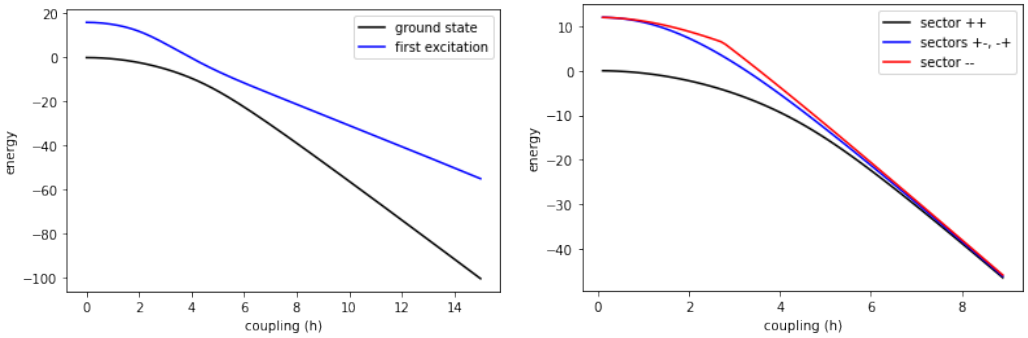

Figure 5.5: The behaviour of the first energy levels of the system, evaluated with an exact diagonalization. The figure of the left has depicted the ground and the first excited state in the topological sector $(+,+)$, which shrink at the phase transition point. The figure on the right represents the ground states of the four topological sectors, that become degenerate in the deconfined phase. The sectors $(+,-)$ and $(-,+)$ are symmetric and their grounds are overlapping on the blue line, while the red line actually is the ground of the $(-,-)$ sector only after the level crossing indicated by the cusp, since at $h = 0$ its energy is $24 > 12$.

The measurements reported in the two pictures correspond to the mean values of a set of 30 measurements taken at each coupling h, while the error bars are the standard deviations of the distributions. Usually the error associated to a mean value is the standard deviation of the mean, but it has been chosen to draw the bare standard deviation to show more clearly that the second choice of the parameters (supposed to improve the Trotter error at the expense of the adiabaticity) entails an enlargement of the overall errors. This second choice $t_s = 0.0008$, $N_s = 200$, however, results also in an improvement of the mean values. With $t_s = 0.005$, $N_s = 200$, the energies were compatible with the actual ground level until $h \approx 3$. This means that the state which has been prepared by our adiabatic evolution is a very good approximation of the true ground until $h \approx 3$, while after that value the errors become macroscopic, they produce larger deviations in the prepared state which, in turn, result in an increasing number of collapses in the first excited states instead of the ground. Instead, with $t_s = 0.0008$, $N_s = 600$, the results are in agreement until $h \approx 6$, which is a notable improvement, and even above that value the deviations accumulate more slowly. This behaviour is not unexpected. To explain it, let us consider more in detail the adiabatic condition, recalling that the parameter r should be compared to the square of the gap with the first excited state. There is a slight difference with

what we have explained in the fourth chapter due to small dimension of the lattice. When $h = 0$ the overall ground state corresponds to all links in the electric ground $|\rho_0\rangle = |\sigma^y = 1\rangle$. With a large lattice, the first excited states have a single plaquette whose links are switched on into $|\rho_1\rangle = |\sigma^y = -1\rangle$, corresponding to the energy $4 \cdot 4 = 16$. Since this is a 3×3 lattice, the states with a single non-contractible electric loop now have energy $4 \cdot 3 = 12$, which is smaller and, at least when $h = 0$, they are the first excited states. However, like we have already argued, this is a symmetry protected process and the transitions to these states belonging to different topological sectors are forbidden. Therefore we have to consider the gap with the first excited state in the $(+, +)$ sector, that is the plaquette with energy 16 mentioned above. If $h = 0$ in both cases we have

$$r = h \ll 16^2 \ , \quad r = \frac{25}{12}\, h \ll 16^2$$

and the adiabatic condition is satisfied. The behaviour of the true values of the ground and the first excited states is depicted in 5.5. In the thermodynamic limit, this gap should close at the phase transition point, thus making the adiabatic approximation inapplicable. But we are far from the thermodynamic limit, since this is only a 3×3 lattice, so the two levels get only slightly closer. Therefore, when h is increased, the deviations to the ground start close to the phase transition point, where there is a sudden (although small) shrinking of the gap, but after the critical point the gap starts to increase again, since when the coupling h is large the magnetic term dominates the hamiltonian and the gap becomes proportional to h. Consequently, the adiabatic error becomes more and more irrelevant with larger values of h, at which $r \propto h \ll const \cdot h^2$. In the end, our observation is that the Trotter error is dominating over the adiabatic error, apart from the small phase transition region. One could try to improve further the Trotter error at the expense of the adiabatic one: the results would get even closer to the actual ground level, until a point is reached where the adiabatic error has become too large and it becomes the dominating one, worsening instead the results. The increasing of the adiabatic error can be mitigated by using a larger number of Trotter steps N_s, but that in turn results in a longer running time of the program. This is also why when passing from $N_s = 200$ to $N_s = 600$ we have decreased the number of points of the graph, since each execution of the code takes three times longer.

Using the same values of t_s, N_s we have measured the expectation values of four Wilson loops, that form a maximal set of loops that does not wrap around the lattice, which due to the boundary conditions has the topology of a torus. The loops considered are the ones represented in Fig. 5.6:

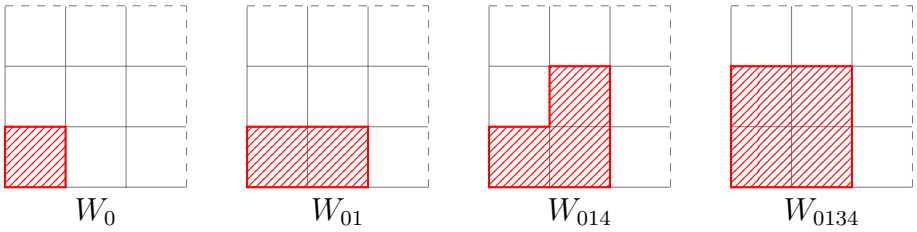

Figure 5.6: The Wilson loops whose ground expectation values have been measured in our simulation. Their orientation is irrelevant in the $\mathbb{Z}_2$ case.

- W_0, along the links 0-10-3-9:
- W_{01}, along the links 0-1-11-4-3-9;
- W_{014}, along the links 0-1-11-14-7-13-3-9;
- W_{0143}, along the links 0-1-11-7-6-12-9.

The plaquettes of the lattice in Fig. 5.3 can be enumerated from 0 to 9 starting from the bottom left corner to the top right one. The subscripts in the names of the loops represent the plaquettes that they cover with the labelling above. The results of the measurements have been reported in Fig. 5.7 and in Fig. 5.8. Due to the small range of values that these observables cover (which should be the interval $[0, 1]$, as explained in the fourth chapter), the width of final mixture of states induces on the Wilson loops relative errors that are larger than the ones for the energy. In these graphs the error bars are the standard deviations of the means, which have been estimated by taking additional repeated set of measurements.

Let us consider first the case with $t_s = 0.0008$ and $N_s = 600$ (see Fig. 5.7), which was the one producing more accurate ground states. Despite the large dispersion, we see an overall behaviour of the mean values that fulfills our expectations: in the deconfined phase the Wilson loops tend to flatten towards 0, whereas in the confined phase their values are close to 1. Moreover one can observe a tendency of the larger loop W_{0143} (made of 4 plaquettes) to be smaller than W_0 (made of a single plaquette), at least in the region with smaller couplings, where the preparation of the ground state is more reliable. At larger couplings the deviations become more consistent and the expectation value becomes significantly lower than 1. The stronger suppression of the loop W_{0143} is expected: the area and perimeter laws, respectively for the confined and deconfined phases, predict exponential suppressions proportional to sizes of the loop. One could try to check these laws numerically by computing ratios of the logarithms of the mean values, but the results would

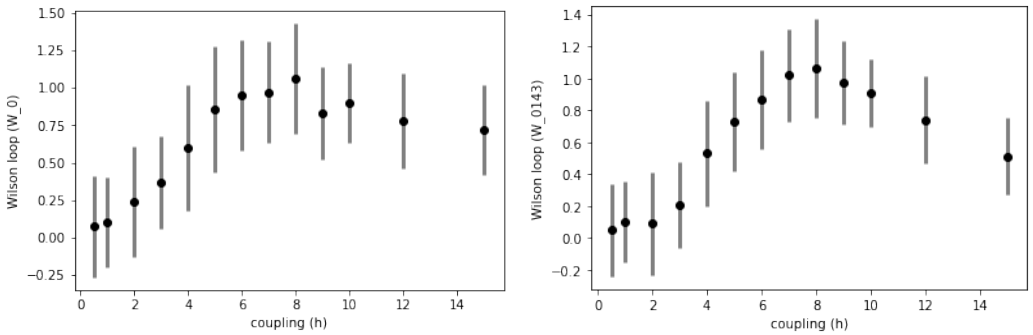

Figure 5.7: Expectation values of the Wilson loops W_0 and W_{0143} on the approximate ground states at several couplings h prepared with $t_s = 0.0008$, $N_s = 600$.

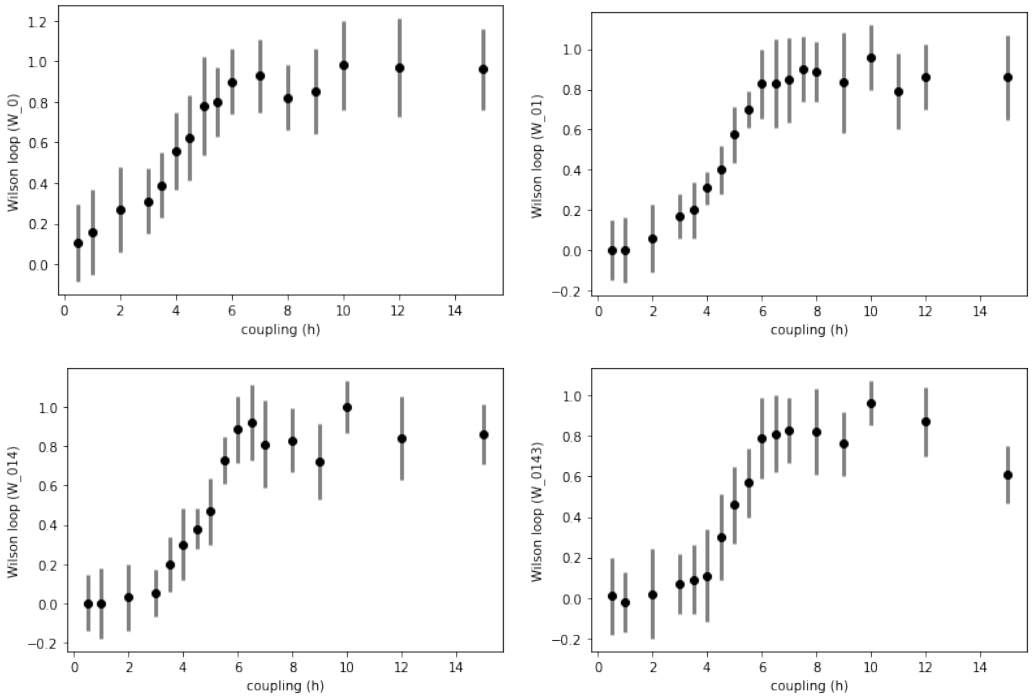

Figure 5.8: Expectation values of the Wilson loops W_0, W_{01}, W_{014} and W_{0143} on the approximate ground states at several couplings h prepared with $t_s = 0.005$, $N_s = 200$.

not be significant because of the large error bars. The strong fluctuations of this measurement and the fact that we are far away from the thermodynamic limit prevent us from validating quantitatively the two laws, even though the

qualitative behaviour is correct. The only numerical value that is reproduced is the quantum critical point: the behaviour of the Wilson loop changes at $h_c \approx 4$, which is the same value predicted by Fig. 5.5. The location of the phase transition is in agreement to what we could have naively expected: the Ising gauge theory with coupling g attached to the electric term is dual to the 2D quantum Ising model and its critical point is known to be at $g_c \approx 0.3$; our model has the coupling on the magnetic term and the electric eigenvalues are modified (but kept at the same order of magnitude), so it is sensible to get a critical point that is close to $1/3$. We expect, however, that the position of the critical point will move when considering larger lattices and it should stabilize towards the TD limit.

The remaining measurements of the Wilson loops were made at $t_s = 0.005$, $N_s = 200$. These values provided worse approximation of the ground state at the couplings above the quantum critical point, however, in comparison to the energies, Wilson loops appear to be less influenced by the deviations from the actual ground of the state that has been prepared. This behaviour does not come as a surprise: a measurement of the energy "feels" the state of all the links simultaneously, while Wilson loops depend only on the links where the loop lies and a flip of the state of a random link is less likely to modify the value of a Wilson loop. Furthermore, coherently with what we have already observed in the measurement of the energy, these parameters provide smaller dispersions of the measurements about their means. Apart from these comments, there is not much that can be added to the previous observations. The qualitative behaviour of the measurements corroborates our expectations: the loops are close to 0 in the confined phase and close to 1 in the deconfined phase, plus there is a tendency to flatten towards 0 in a more evident way the loops that are larger, but the strong dispersions prevent us from verifying quantitatively the area law and the perimeter law. The quantum phase transition point appears again at $h_c \approx 4$. These large errors are a consequence of our initial choice to place the coupling attached to the magnetic term, which results in a larger value critical coupling and forces us to span a larger region of couplings h in order to see the phase transition. If we had placed h on the electric term, we would have found $h_c \approx 1/4$ and in that shorter adiabatic evolution the Trotter errors would not have ended up accumulating that much.

Conclusions and perspectives

In the present thesis we have analyzed how lattice gauge theories with a general gauge group can be simulated on a digital quantum computer and we have implemented a full simulation for the $\mathbb{Z}_2$ model within the Qiskit environment to test the methods discussed.

We started our discussion with a quick review of continuum gauge theories, in order to underline the role of the objects playing a major role when the model is placed on a lattice. Then we explained how to construct a general lattice gauge theory with continuous gauge group both in the path integral formalism, which is used to prove many important results for lattice gauge theories, and in the hamiltonian formalism, that was the one employed for the rest of the thesis. Afterwards we outlined the typical phase structure of these theories, discussing how confined and deconfined phases may arise and their relations with topological properties of the system. After this general introduction, we set up the problem of simulating the theory by illustrating the typical structure of a quantum simulation and the issues that have to be overcome, focusing in particular on the problem of the infinite dimension of the Hilbert space associated with the gauge bosons associated to a Lie gauge group. Then we reviewed the most common approaches in the physics literature used to circumvent this issue, before focusing on the finite group approximation for the rest of the thesis. To devise our simulation model, we had to adapt the construction of the hamiltonian of a lattice gauge theory to the case of a finite gauge group. Our discussion, highlighting the algebraic and geometric structures involved, allowed us to formulate an algorithm able to implement the corresponding the time evolution for any finite gauge group and to prove its correctness. In order to both discretize the gauge group and implement the time evolution, we had to generalize the Fourier transform on functions acting on any group. This object is well known in the mathematical literature and we only had to reformulate the results in more physical terms. After having described how to proceed in general, we focused on a simple case to realize our own full simulation. We chose to implement a simple model, since the aim were not to solve a new theory but rather to start a systematic

analysis of the advantages and drawbacks of our approach. We discussed the structure of $\mathbb{Z}_n$ lattice gauge theories and in particular the Hilbert space and the phases in the $\mathbb{Z}_2$ case, for which we have written and executed a quantum code. Our algorithm prepares the an approximation of the ground state at an arbitrary value of the coupling at measures the behaviour of the ground state energy and of the expectation value of some Wilson loops, finding clear signs of the phase transition involved. The large fluctuations involved, however, prevent us from making a quantitatively accurate analysis of the transition, even though the qualitative behaviour is correct. We have identified two systematic errors and described their influence.

One way to improve our results could be to modify the Trotter approximation of the time evolution operator [21]: had we employed $e^{-i(H_E+H_B)t} \approx e^{-iH_Et/2}e^{-iH_Bt}e^{-iH_Et/2}$, instead of $e^{-i(H_E+H_B)t} \approx e^{-iH_Et}e^{-iH_Bt}$, the trotterized evolution would have been characterized by a better scaling of the errors, at least in a classical simulator of a quantum computer. In an actual quantum computer, the increased number of gates would require some further attention due to the noise that they introduce. Overall, we can expect that the fluctuations would still be relevant even with the improvement of the Trotter decomposition, because the large accumulation of the errors is caused by our evolution that has to cover a wide range of values of the coupling. We had a large range to span because we chose to put the coupling on the magnetic term, in order to get an initial state that was simple to formulate and to prepare with our methods for any gauge group. With the current technology, our completely general methods struggle to provide a quantitatively accurate simulation and some specific optimization probably is required. Another issue that can be considered is the implementation on other platforms apart from than Qiskit which may have better performances, such as running our algorithm on the QuEST GPU simulator.

Apart from the possible optimization of the results, this work can be extended in many directions. Our analysis can be deepened by studying the behaviour of additional observables, such as 't Hooft strings, that can be used also to detect the confinement-deconfinement transition. The method presented in Section 5.3 can be adapted straightforwardly to measure them, since the time evolution they generate is diagonal in the representation basis. Other observables that can be measured are time-like Wilson loops, whose behaviour can be interesting to compare with spatial Wilson loops. Another direction that should be followed is the realization of the model on larger lattices, which should be used to study the scaling properties of our measurements and to extract a sensible continuum limit. In this case the main issue that should be overcome is the shrinking of the gap between the ground and the first excited state in the $(+,+)$ sector, which would inhibit

the adiabatic approximation. A possible way out could be to implement the time evolution of the coupling using instead of $h(t) = \Delta h/t_s \cdot t$ a non linear functions whose growth becomes slower close to the transition point. Our methods can be adapted to simulate any other finite gauge group, both abelian and non-abelian, provided that a suitable realization of the $\mathfrak{U}$ gates is found. The $\mathbb{Z}_4$ case should be the easiest one, since the corresponding quantum Fourier transform is simply realized and the internal operation is isomorphic to the sum modulo 4 [61]. Other possible interesting groups are the dihedral groups, which are among the smallest non abelian groups. When considering more complicated gauge groups, one should keep in mind that the number of qubits required for each link is proportional to the order of the group, so that the dimension of the largest lattice that can be simulated decreases. Matter may also be added, allowing to reproduce interesting dynamical phenomena such as the string breaking effect or pair production from the vacuum.

APPENDIX I.

The mathematical toolbox: groups and representations

This appendix gathers the main results on group theory and representation theory that needed throughout the thesis. We start from the case of finite groups and later we shall extend it for compact Lie groups, for whom very similar statements hold. Some useful references are [31, 36, 71, 76, 79, 83].

A.1 Fourier analysis on finite groups

Given any group G, two representations $\rho, \pi \in \mathrm{Hom}(G \to \mathrm{GL(V)})$ on the same vector space V are equivalent if they have the same action up to a change of basis, i.e. if there exists $A \in \mathrm{Aut(V)}$ such that $\rho(g) = A\,\pi(g)\,A^{-1}$ $\forall\, g \in G$. The equivalence of representations is an equivalence relation, which creates a partition of the set of all representations of a group. If we choose a representative element from each class, we get a quotient set made of all inequivalent representations of the group.

Theorem A.1. *Let G be a finite group acting on a vector space endowed with an inner product. Then any representation can be chosen to be unitary.*

Definition A.1. Given a finite group G, $\hat{G}$ is the set of all unitary irreducible inequivalent representations of G.

Theorem A.2. *Let G be a finite group. Then it has a finite number of irreducible inequivalent representations, i.e. $\hat{G}$ is finite. Furthermore, if $d_\alpha \equiv dim\,\rho_\alpha$ for all representations ρ_α belonging to $\hat{G}$, then*

$$\sum_{\alpha \in \hat{G}} d_\alpha^2 = |G|\,.$$

In general, all irreducible representations of a finite group are finite dimensional. If G is abelian, by the Schur's Lemma all irreducible representations are one-dimensional. It follows that an abelian group always has exactly $|G|$ inequivalent irreducible representations (which can be made unitary).

Theorem A.3. *(Orthogonality relation) Let ρ_α, ρ_β be two irreducible representations belonging to $\hat{G}$ and consider their matrix elements. Then*

$$\frac{1}{|G|}\sum_{g\in G}[\rho_\alpha(g)]^*_{ij}[\rho_\beta(g)]_{kl} = \frac{1}{d_\alpha}\,\delta_{\alpha\beta}\delta_{ik}\delta_{jl}\,.$$

The group algebra is the set of all functions from the finite group G to the field of complex numbers and it can be endowed with a natural inner product.

Definition A.2. (Group algebra) $\mathbb{C}[G] = \{f : G \to \mathbb{C}\}$.

Definition A.3. (Inner product) Consider two functions f, $g \in \mathbb{C}[G]$. Then

$$\langle f, g\rangle = \frac{1}{|G|}\sum_{h\in G} f(h)^* g(h)\,.$$

In a quantum-mechanical context it is more natural to remove the normalization $1/|G|$, in order to mimic completely the L^2 inner product, as it is done in the main text. For all $g \in G$, we can define the function $e_g : G \to \mathbb{C}$ s.t. $e_g(h) = \delta_{g,h}$. Then any function $f \in \mathbb{C}[G]$ can be expanded as

$$f(g) = \sum_{h\in G} f(g)e_g(h)\,,$$

showing that $\{e_g\}_{g\in G}$ is a basis for $\mathbb{C}[G]$. Notice that it will be a finite dimensional vector space, as long as $|G|$ is finite. The Dirac notation can be introduced by identifying $|g\rangle \equiv e_g$, so that the group algebra can be seen as the free vector space generated by the elements of the group

$$\mathbb{C}[G] \cong \text{span}\,\{|g\rangle \,|\, g \in G\}\,.$$

$\mathbb{C}[G]$ is an algebra with respect to an internal operation that respects the structure of the group. If we define it in such a way that $e_g * e_h = e_{gh}$, then

$$\left(\sum_g a(g)e_g\right) * \left(\sum_h b(h)e_h\right) = \sum_{g,h} a(g)b(h)\,e_{gh} = \sum_{g'}\left(\sum_h a(g'h^{-1})b(h)\right)e_{g'}$$

and we see that the internal operation on $\mathbb{C}[G]$ is the convolution

$$(a * b)(g) = \sum_h a(gh^{-1})b(h)\,.$$

Basically an element g of the group is acting on its algebra $\mathbb{C}[G]$. We can define similarly the (left) regular representation of the group.

Definition A.4. (Regular representation) The left regular representation of G is the homomorphism $\rho_L : G \to \mathrm{GL}(\mathbb{C}[G])$ such that $\rho_L(g)\, e_h = e_{gh}$. Similarly, the right regular representation satisfies $\rho_R(g)\, e_h = e_{hg^{-1}}$.

A simple computation shows that the actions on $f(g) = \sum_h f(g)e_g(h)$ are

$$[\rho_L(g)f](h) = f(g^{-1}h)$$
$$[\rho_R(g)f](h) = f(hg)\,.$$

The regular representations share analogous properties, which are particularly interesting because they are not irreducible and their decomposition contains all the other irreducible representations of G. Consider for instance the character of the left regular representation, that is the function

$$\chi_L : G \to \mathbb{C}\ , \quad \chi_L(g) = \mathrm{tr}(\rho_L(g))\,,$$

so it is an element of the group algebra. Clearly $\rho_L(e) = \mathbb{I}$, then $\chi_L(e) = |G|$ since $\dim\mathbb{C}[G] = |G|$. When $g \neq e$, $\rho_L(g)\, e_h = e_{gh} \neq e_g$, therefore $\rho_L(g)$ is a permutation matrix of the basis vectors e_g and it is always 0 along its principal diagonal. This implies $\chi_L(g) = 0$ whenever $g \neq e$. Any representation ρ of a finite group can be reduced using the inner product [76]

$$\rho = \bigoplus_{\alpha\in\hat{G}} a_\alpha \rho_\alpha\ , \qquad a_\alpha = (\chi_\alpha, \chi_\rho) = \frac{1}{|G|}\sum_g \chi_\alpha(g)^*\chi_\rho(g)$$

For our case $\chi_L(g) = 0\ \forall\, g \neq e$ implies $(\chi_\alpha, \chi_L) = d_\alpha$. Then it follows

Theorem A.4. *The regular representation can be reduced as* $\rho_L = \bigoplus_{\alpha\in\hat{G}} d_\alpha\, \rho_\alpha$ *and it holds the vector space isomorphism* $\mathbb{C}[G] \cong \bigoplus_{\alpha\in\hat{G}} \big(V_\alpha^{\oplus\, d_\alpha}\big)$.

Notice that $\dim\big(V_\alpha^{\oplus\, d_\alpha}\big) = (\dim V_\alpha)^2 = \dim\,\mathrm{End}(V_\alpha)$, implying also that

$$\mathbb{C}[G] \ \cong \bigoplus_{\alpha\,\in\,\hat{G}} \mathrm{End}(V_\alpha)\,.$$

This is even an isomorphism of algebras, as it can be seen by linearly extending all the irreps. In particular, we extend $\rho_\alpha : G \to \mathrm{GL}(V_\alpha)$ to $\mathcal{F}_\alpha : \mathbb{C}[G] \to \mathrm{End}(V_\alpha)$, using the chain of identifications

$$\begin{array}{ccccc} G & \longrightarrow & \mathbb{C}[G] & \longrightarrow & \mathrm{End}(V_\alpha) \\ g & \longmapsto & e_g & \longmapsto & \rho_\alpha(g) \end{array}$$

where the linearity we assume is $\lambda\, e_g + \mu\, e_h \mapsto \lambda\, \rho_\alpha(g) + \mu\, \rho_\alpha(h) \in \mathrm{End}(V_\alpha)$. In general it does not belong to $\mathrm{GL}(V_\alpha)$ because the sum of invertible matrices may not be invertible. It is an algebra homomorphism since $e_g * e_h = e_{gh} \mapsto \rho_\alpha(g)\rho_\alpha(h) = \rho_\alpha(gh)$, which implies that

$$\mathcal{F}_\alpha(a * b) = \mathcal{F}_\alpha(a)\, \mathcal{F}_\alpha(b)\,.$$

The usual Fourier series is related to the representation theory of U(1). This procedure applied on a generic element $f \in \mathbb{C}[G]$ yields the generalized Fourier components on a finite group.

Definition A.5. (Fourier transform) The Fourier transform on a finite group is the mapping $\mathcal{F}_\alpha : \mathbb{C}[G] \to \mathrm{End}(V_\alpha)$ defined by the relation

$$\mathcal{F}_\alpha[f] \equiv \hat{f}(\rho_\alpha) = \sum_{g \in G} f(g)\rho_\alpha(g)\,.$$

Explicitly, the correspondence that realizes this isomorphism of algebras is

$$\varphi : \mathbb{C}[G] \to \bigoplus_{\alpha \in \hat{G}} \mathrm{End}(V_\alpha) \ , \quad \varphi[f] = \bigoplus_{\alpha \in \hat{G}} \hat{f}(\rho_\alpha).$$

Notice that a function has a Fourier component for any irreducible representation ρ_α of G and the components $\hat{f}(\rho_\alpha)$ are, in general, matrices. When G is abelian its irreducible representations are all one dimensional by the Schur lemma, so that the Fourier components get back to being numbers. φ is an isomorphism and maps bases into bases. Using it, we could try to build an alternative basis for $\mathbb{C}[G]$ sending back the canonical basis for $\mathrm{End}(V_\alpha)$ (i.e. the elementary matrices). Consider the functions

$$\bar{\rho}_\alpha(\cdot)_{ij} : G \longmapsto \mathbb{C} \ , \quad \bar{\rho}_\alpha(g)_{ij} = \rho_\alpha(g)^*_{ij}\,.$$

Now let us compute its Fourier component on a representation β. We get

$$\bar{\rho}_\alpha(\cdot)_{ij} = \sum_g \rho_\alpha(g)^*_{ij}\, e_g \mapsto \sum_g \rho_\alpha(g)^*_{ij}\, \mathcal{F}_\beta[e_g] = \sum_g \rho_\alpha(g)^*_{ij}\, \rho_\beta(e_g)$$

and by the orthogonality formula we immediately find its matrix elements

$$\left(\mathcal{F}_\beta[\bar{\rho}_\alpha(\cdot)_{ij}]\right)_{kl} = \frac{|G|}{d_\alpha}\,\delta_{\alpha\beta}\,\delta_{ik}\,\delta_{jl}\,,$$

which are exactly the element of the elementary matrices of the canonical basis of $\mathrm{End}(V_\alpha)$ apart from the normalization factor. Therefore $\bar{\rho}_\alpha(\cdot)_{ij}$ is a basis of $\mathbb{C}[G]$ and we can express any function $f \in \mathbb{C}[G]$ as

$$f(g) = \sum_\alpha \sum_{ij} c^\alpha_{ij}\,\rho_\alpha(g)^*_{ij}\,.$$

To find the components c^α_{ij}, we can employ again the isomorphism φ. It maps

$$f \;\mapsto\; \hat{f}(\rho_\alpha)_{ij} = \sum_g f(g)\,\rho_\alpha(g)_{ij}$$

and we can compare this expression to what we get after having expanded f

$$f = \sum_{\beta,kl} c^\beta_{kl}\,\bar{\rho}_\beta(\cdot)_{kl} \;\mapsto\; \hat{f}(\rho_\alpha)_{ij} = \sum_{\beta,kl} c^\beta_{kl}\,\frac{|G|}{d_\beta}\,\delta_{\beta\alpha}\,\delta_{ki}\,\delta_{lj} = \frac{|G|}{d_\alpha}\,c^\alpha_{ij}\,.$$

In both cases we have computed $\hat{f}(\rho_\alpha)_{ij}$, so this provides us an expression for the components. The following theorem holds.

Theorem A.5. *The set* $\{\sqrt{d_\alpha}\bar{\rho}_\alpha(\cdot)_{ij}\}_{\alpha\in\hat{G},\,ij=1\ldots d_\alpha}$ *is an orthonormal basis for* $\mathbb{C}[G]$ *w.r.t. the inner product given in definition A.3. Moreover,* $\forall\, f \in \mathbb{C}[G]$

$$f = \sum_{\alpha\in\hat{G}} \sum_{i,j=1}^{d_\alpha} \frac{d_\alpha}{|G|}\,\hat{f}(\rho_\alpha)_{ij}\,\bar{\rho}_\alpha(\cdot)_{ij}\,.$$

This expansion is the generalization to a finite group of the Fourier series of f. It relates the components $f(g)$ with respect to the basis e_g, called *group element basis*, to the components $\hat{f}_{\alpha,ij}$ corresponding to the *representation basis* $\bar{\rho}_\alpha(\cdot)_{ij}$. This theorem is the finite-dimensional analog of the Peter-Weyl theorem for compact Lie groups. The Fourier transform is exactly the transformation that reduces the regular representation. Notice that

$$[\rho_L(h)\,\bar{\rho}_\alpha(\cdot)_{ij}](g) = \rho_\alpha(h^{-1}g)^*_{ij} = c_{ik}\,\rho_\alpha(g)^*_{kj}\;,\;\; c_{ik} = \rho_\alpha(h^{-1})_{ik}\,.$$

The action of the left regular representation on an element of the representation basis shuffles only the elements within the same representation α: the block-diagonal structure is clear. Furthermore, the sum is only on one index k, so that it contains $\#k = d_\alpha$ elements and each block will appear d_α times.

A.2 Fourier analysis on compact Lie groups

We start by stating the statements similar to those of finite groups that hold for compact Lie groups.

Theorem A.6. *Let G be a compact Lie group acting on a Hilbert space. Then any representation can be chosen to be unitary.*

Definition A.6. Given a compact Lie group G, $\hat{G}$ is the set of all unitary irreducible inequivalent representations of G.

Theorem A.7. *Let G be a compact Lie group acting on a Hilbert space. Then any irreducible representation is finite dimensional and the the set of all irreducible inequivalent representations of G is countable.*

Theorem A.8. *(Orthogonality relation) Let ρ_α, ρ_β be two irreducible representations belonging to $\hat{G}$ and consider their matrix elements. Then*

$$\frac{1}{Vol(G)} \int_G dg\, [\rho_\alpha(g)]^*_{ij} [\rho_\beta(g)]_{kl} = \frac{1}{d_\alpha}\, \delta_{\alpha\beta}\delta_{ik}\delta_{jl}\,.$$

As always dg is the Haar measure on G and by $Vol(G)$ we mean the volume of G w.r.t. dg. In this case, the group algebra has to be defined differently. We cannot consider all functions on G because there may be convergence problems with the inner product and we want to work on a Hilbert space. Therefore we restrict our attention to the square integrable functions (with respect to the Haar measure) on the compact Lie group.

Definition A.7. (Group algebra) $\mathbb{C}[G] = (L^2(G), dg)$

Definition A.8. (Inner product) Consider two functions $f,\, g \in L^2(G)$. Then

$$\langle f, g\rangle = \frac{1}{Vol(G)} \int_G dh\, f(h)^* g(h)\,.$$

The regular representations can be defined likewise to what we did for finite groups and their basic properties carry on to this case. The most important result is the Peter-Weyl theorem, which lies at the core of harmonic analysis on Lie groups. Consider again the matrix elements $\bar{\rho}_\alpha(\cdot)_{ij}$ in the (countable) set of unitary irreducible representations of G. The theorem then states

Theorem A.9. *(Peter-Weyl) The set* $\{\sqrt{d_\alpha}\bar{\rho}_\alpha(\cdot)_{ij}\}_{\alpha\in\hat{G},\, ij=1\dots d_\alpha}$ *is an orthonormal basis for* $L^2(G)$ *w.r.t. the inner product given in definition A.8.*

Again, the representation basis is dual to the group element basis via a generalization of the Fourier transform. Given any $f \in L^2(G)$ it is defined as

$$\mathcal{F}_\alpha[f] \equiv \hat{f}(\rho_\alpha) = \int_G dg\, f(g)\rho_\alpha(g)$$

and it yields the Fourier coefficients of the series expressing the function f

$$f = \sum_{\alpha\,\in\,\hat{G}} \sum_{i,j=1}^{d_\alpha} \frac{d_\alpha}{Vol(G)}\, \hat{f}(\rho_\alpha)_{ij}\, \bar{\rho}_\alpha(\cdot)_{ij}\,.$$

Like it happens for the finite group case, the left regular representation is block-diagonal on the representation basis and it establishes the isomorphism

$$L^2(G) = \bigoplus_{\alpha\,\in\,\hat{G}} \mathrm{End}(V_\alpha)\,.$$

Notice that there is a sum only because we have chosen to work with a compact group, whose irreducible representations are countable. If we worked for instance with $\mathbb{R}$, we would have found $\hat{\mathbb{R}} \cong \mathbb{R}$, it has infinite irreducible representations labelled by the Fourier variable k dual to x.

A.3 Riemannian structure on Lie groups

In this section we gather the main results on Lie groups that allow us to interpret geometrically the electric term of the Kogut-Susskind hamiltonian. A natural laplacian is automatically defined on a manifold when it is endowed with a Riemannian structure, so we shall quickly review here some key definitions about to the standard procedure to introduce a metric on a Lie group. For more details, see e.g. [71]

Let G be the Lie group we are considering and let $\mathfrak{g}$ be its Lie algebra. First, recall the definition of the adjoint representation of $\mathfrak{g}$: it is the Lie algebra homomorphism $ad : \mathfrak{g} \to \mathrm{End}\,\mathfrak{g}$ such that $ad_X Y = [X, Y]$.

Definition A.9. (Killing form) $\kappa : \mathfrak{g} \times \mathfrak{g} \to \mathbb{R}\,,\ \kappa(X, Y) = \mathrm{tr}\,(ad_X \circ ad_Y)$

In general κ is a bilinear form on $\mathfrak{g}$ and it satisfies the following properties:

1. given any triple $X, Y, Z \in \mathfrak{g}$, $\kappa([X, Y], Z) = \kappa(X, [Y, Z])$

2. given any $\varphi \in \mathrm{Aut}\,(\mathfrak{g})\,,\ \kappa(\varphi(X),\varphi(Y)) = \kappa(\varphi(X),\varphi(Y))$
3. $\kappa_{ij} = f^n_{im} f^m_{jn}$, on the basis vectors that satisfy $[E_i, E_j] = f^k_{ij} E_k$

An ideal of a Lie algebra $\mathfrak{g}$ is the subset $I \subset \mathfrak{g}$ s.t. given any $i \in I$ $[i, X] \in I\ \forall\, X \in \mathfrak{g}$. Trivially, $\{0\}$ and $\mathfrak{g}$ itself are always ideals of $\mathfrak{g}$. $\mathfrak{g}$ is a called a *simple* Lie algebra whenever it is non-abelian and it has no trivial ideals. Non-simple Lie algebras may still be *semisimple*, meaning that $\mathfrak{g}$ is a direct sum of simple Lie algebras. It holds the following theorem.

Theorem A.10. *(Cartan's criterion) The Killing form on $\mathfrak{g}$ is non-degenerate if and only if $\mathfrak{g}$ is a semisimple Lie algebra.*

Most of the groups that are interesting for physics are indeed simple or semisimple and in that case the Killing form is nondegenerate, so that the bilinear form defines an inner product on $\mathfrak{g}$. Studying the eigenvalues of the Killing form provides also important informations about the topology of the associated Lie group.

Theorem A.11. *G is a compact Lie group if and only if the Killing form on $\mathfrak{g}$ is negative definite.*

The Lie algebra associated to a group G can be thought as the tangent space on the identity element, or equivalently to the set of left-invariant vector fields on G. This fact can be used to define a (semi-)Riemannian metric on the whole Lie group given an inner product on its Lie algebra such as the Killing form, which is the most relevant one. The left translation on a Lie group is the action $L:\ \mathrm{G} \to \mathrm{Diff(G)}\,,\ L_a b = a \cdot b$, while the right translation is $R : \mathrm{G} \to \mathrm{Diff(G)}\,,\ R_a b = b \cdot a^{-1}$. Then

Definition A.10. Let g be a metric on G and let $u, v \in T_b G$. Then, g is *left-invariant* iff $g_b(u,v) = g_{ab}((dL_a)_b u, (dL_a)_b v)$.

Definition A.11. Let g be a metric on G and let $u, v \in T_b G$. Then, g is *right-invariant* iff $g_b(u,v) = g_{ba^{-1}}((dR_a)_b u, (dR_a)_b v)$.

Definition A.12. Let g be a metric on G and let $u, v \in T_b G$. Then g is *bi-invariant* if it is both left-invariant and right-invariant.

In these definitions e.g. $(dL_a)_b$ is the differential of the diffeomorphism L_a computed at the point b, which yields the push-forward of a vector from $T_b G$ to $T_{ab} G$. An inner product on $T_e G$ can be extended to a metric on the whole group manifold with the following theorem.

Theorem A.12. *Let $\langle\ ,\ \rangle$ be an inner product on $\mathfrak{g} \cong T_eG$. Given $u, v \in T_aG$, define $g_a(u,v) = \langle (dL_{a^{-1}})_a u,\, (dL_{a^{-1}})_a v \rangle$. Then g is a left-invariant metric on G.*

When $\langle\ ,\ \rangle$ is taken to be the Killing form, the resulting metric becomes bi-invariant. Bi-invariant semi-Riemannian metrics on a Lie groups have several important properties, among them there is the fact that the Levi-Civita connection corresponding to the given metric is proportional to the adjoint representation, in particular it holds the relation

$$\nabla_X Y = \frac{1}{2}\,[X, Y]\,.$$

If one defines the corresponding laplacian as the trace of tensor hessian, it results equal to the quadratic Casimir element, seen as a differential operator [36]. This statement can be seen intuitively by looking directly at the definition of the quadratic Casimir. We identify here $\mathfrak{g}$ and its dual space, since they are finite dimensional. Let $\{E_i\}$ be a basis for $\mathfrak{g}$ and let $\{\tilde{E}^i\}$ be its dual basis satisfying $\kappa(\tilde{E}^i,\, E_j) = \delta^i_j$. Its definition is [45]

Definition A.13. (Quadratic Casimir element) $\Omega = \sum_{ij} \kappa(E_i, E_j)\, \tilde{E}^i\, \tilde{E}^j$.

Ω is an element of the *universal enveloping algebra* $U(\mathfrak{g})$, which is the tensor algebra generated by $\mathfrak{g}$ modulo the identification $X \otimes Y - Y \otimes X \sim [X, Y]$. In the definition, the tensor product symbol has been omitted. When the Lie algebra is semisimple and κ is non-degenerate, the quadratic Casimir is unique and independent of the basis. Moreover, it belongs to the center $Z(\mathfrak{g})$ of the universal enveloping algebra, meaning that it commutes with any other element. Using the duality relation, we could have alternatively written it as

$$\Omega = \sum_{ij} \kappa^{ij}\, E_i\, E_j\,,$$

where κ^{ij} is the inverse matrix of κ_{ij}. If we interpret the elements E_i as left-invariant vector fields and we recall that in differential geometry vectors are directional derivatives, it is immediate to identify the universal enveloping algebra as the algebra of all left-invariant differential operators on G [36] and Ω becomes a second order differential operator with exactly the same structure of the laplacian w.r.t the metric κ.

APPENDIX II.

The computational toolbox: quantum codes and Qiskit

Quantum computing is a deloping technology that exploits quantum mechanical effects to handle information differently to what classical computers do. In this thesis we have performed a simulation of a quantum system on the IBM platform *Qiskit*. This appendix gathers a few key facts about quantum computing and Qiskit, in order to provide some context and to fix some notations. We refer to the literature for an introduction on the topics: a standard textbook on quantum computation is [61], while [2] provides a quick introduction on the basics of quantum computation within the Qiskit environment. Furthermore, the site `https://qiskit.org` itself provides an online textbook for Qiskit, in addition to the complete documentation.

Quantum computers perform operations by manipulating quantum systems. A state of a classical computer is expressed by a string of bits '$b_1 b_2 ... b_n$'. On a quantum computer, bits are replaced by qubits $|q\rangle = \alpha|0\rangle + \beta|1\rangle$, so that a state becomes the tensor product $|q_1\rangle|q_2\rangle...|q_n\rangle \equiv |q_1 q_2 ... q_n\rangle$. The operations are represented by *quantum gates*, that replace the classical logic gates. Any operation of a quantum computer can be thought as a time evolution e^{-iKt} generated by some effective hamiltonian K applied on a subset of the qubits of the computer. Consequently, quantum gates can be any unitary operator acting on a subset of qubits. An important quantum gate that acts on a single qubit is the *Hadamard gate* H, that acts on the computational basis $|0\rangle = (1,0)^T$, $|1\rangle = (0,1)^T$ as

$$H = \frac{1}{\sqrt{2}} \begin{pmatrix} 1 & 1 \\ 1 & -1 \end{pmatrix} \quad \Rightarrow \quad H|0\rangle = \frac{|0\rangle + |1\rangle}{\sqrt{2}} \ , \quad H|1\rangle = \frac{|0\rangle - |1\rangle}{\sqrt{2}} \ .$$

The Hadamard gate can be used to produce the superposition states that are one of the main tools that quantum computers have and that classical

computers do not. Other relevant single-qubit gates the Pauli matrices, the phase gate $U(\phi)$, and the single-qubit rotations $R_\alpha(\theta)$:

$$X = \begin{pmatrix} 0 & 1 \\ 1 & 0 \end{pmatrix} \ , \quad Y = \begin{pmatrix} 0 & -i \\ i & 0 \end{pmatrix} \ , \quad Z = \begin{pmatrix} 1 & 0 \\ 0 & -1 \end{pmatrix}$$
$$U(\phi) = \begin{pmatrix} 1 & 0 \\ 0 & e^{i\phi} \end{pmatrix} \ , \quad R_\alpha(\theta) = \exp\left(-i\frac{\theta}{2} X_\alpha\right) .$$

The other new tool of quantum computing is that we can take advantage of is entanglement. The Hilbert space of a many-component system is the tensor product of the single Hilbert spaces, so the Hilbert space associated with a quantum computer is the product of the spaces associated to the single qubits. For simplicity, let us consider a two qubit Hilbert space. If $|q_1\rangle \in \mathcal{H}_1$ and $|q_2\rangle \in \mathcal{H}_2$, their direct product $|q_1\rangle|q_2\rangle \equiv |q_1 q_2\rangle$ is an element of $\mathcal{H}_1 \otimes \mathcal{H}_2$, but not all elements of $\mathcal{H}_1 \otimes \mathcal{H}_2$ can be written as $|q_1\rangle|q_2\rangle$ for some $|q_1\rangle$ and $|q_2\rangle$. In mathematical terms, these states are called "non-decomposable tensors" and they correspond to entangled states. The most important two-qubit gate probably is the controlled-NOT, or CNOT gate

$$CNOT = \begin{pmatrix} 1 & 0 & 0 & 0 \\ 0 & 1 & 0 & 0 \\ 0 & 0 & 0 & 1 \\ 0 & 0 & 1 & 0 \end{pmatrix} ,$$

which acts as a NOT gate on the second qubit controlled by the state of the first one. If the first qubit is in the state $|0\rangle$ it leaves the second qubit unchanged, while if the first one is in $|1\rangle$ it flips the second qubit. It is a simple exercise to show that

$$CNOT\left(\, H|0\rangle \otimes |0\rangle \,\right) = \frac{|00\rangle + |11\rangle}{\sqrt{2}},$$

that is an entangled state: if we make a measurement of first qubit, the procedure will automatically cause a collapse also of the state of the second qubit and vice-versa. Here the tensor product has been made explicit for clarity. A typical quantum algorithm consists of a sequence of quantum gates applied to the set of input qubits and after them some appropriate measurements are performed on the final state that the gates have prepared. Measurements make the states collapse and we measure what is the eigenstate into which the state has collapsed, so that the outputs typically are classical bits. Today we know few efficient quantum algorithms, such as the algorithm developed by Shor computing quantum Fourier transforms or Grover's search algorithm.

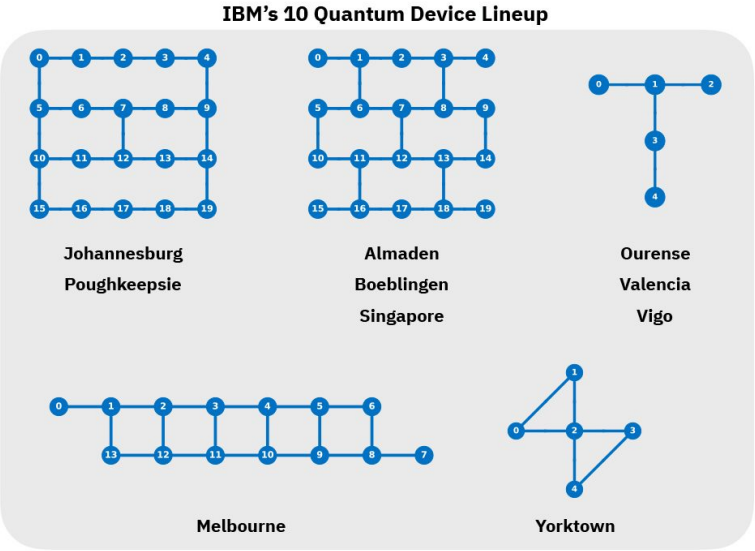

Figure B.1: The topologies of some of the quantum computers made available by IBM. Two qubits are connected by an edge if it is possible to apply a physical CNOT gate between them. The picture is taken from the site `https://quantum-computing.ibm.com`

Quantum algorithms are difficult to find because the more intuitive classical problem should be rethought in terms of a quantum evolution and the computation has to be decomposed into a sequence of unitary operations, which in general may be a very difficult task. However, these few "fundamental" quantum procedures can be used as building blocks to devise other algorithms that tackle other specific tasks. For instance the quantum Fourier transform can be used to improve factoring algorithms, while, of course, Grover's algorithm improves all problems whose best solution would otherwise be a straightforward binary search. These improvements are remarkable: the quantum Fourier transform grants an exponential speedup in comparison to the classical case, while the quantum search a quadratic one. As a consequence, despite knowing only a small class of fundamental quantum algorithms that outspeed the classical counterparts, the applications that these algorithms have found stimulated the construction of the first actual quantum computers, which are being built by leading technology companies and research institutes. Among them, some of the quantum computers provided by IBM are publicly available through the online cloud system *IBM Quantum Experience*. Quantum algorithms are written using the open-source frame-

work Qiskit, that, in practice, can be used as python library. Within Qiskit, the characteristic objects of quantum computing are realized as instances of classes. Qubits are element of the `QuantumRegister` class, for the classical bits there is the class `ClassicalRegister` and quantum circuits belong to the class `QuantumCircuit`, whose standard constructor takes as arguments both qubits and classical bits (necessary when the circuits includes measurements). The methods belonging to the `QuantumCircuit` class allow to add gates and measurement operations to the qubits that initialize the circuit object. Consequently, these quantum computers can be programmed by writing familiar python codes, which can be executed on the actual quantum computers as well as on a local classical computer, that becomes a classical simulator of a quantum computer. When working on a real quantum computer, one has to take into account the connectivity of its qubits, also known as the topology of the device. Some examples are reported in Fig. B.1. Typically, the physical realizations of the quantum computers do not allow to entangle directly a qubit with any other one. If it is possible to physically realize a CNOT gate between the qubits j and k and the qubits k and l, a CNOT between j and l can be effectively realized as

$$CNOT_{jl} = CNOT_{kl}\, CNOT_{jk}\, CNOT_{kl}\, CNOT_{jk}\,.$$

Other simulators are freely available, such as QuEST or Microsoft's Q#.

Bibliography

[1] G. Aarts, *Introductory lectures on lattice QCD at nonzero baryon number*, Journal of Physics: Conference Series, vol. 706, p. 022004, (2016). [Online] Available: `http://dx.doi.org/10.1088/1742-6596/706/2/022004`

[2] J. Abhijith et al., *Quantum algorithm implementation for beginners* (2020). [Online]. Available: https://arxiv.org/abs/1804.03719

[3] Y. Aharonov, D. Bohm, *Significance of electromagnetic potentials in the quantum theory*, Phys. Rev. 115(3), 485 (1959).

[4] T. Albash and D. A. Lidar, *Adiabatic quantum computing*, Rev. Mod. Phys. vol. 90, p. 015002 (2018).

[5] J. P. Aubin, *Applied functional analysis*, Wiley-Interscience (2000).

[6] J. Baez and I. Munian, *Gauge fields, knots and gravity*, World Scientific Publishing Co Pte Ltd (1994).

[7] D. Banerjee, M. Dalmonte, M. Müller, E. Rico, P. Stebler, U.-J. Wiese and P. Zoller, *Atomic quantum simulation of dynamical gauge fields coupled to fermionic matter: from string breaking to evolution after a quench*, Phys. Rev. Lett. vol. 109, p. 175302 (2012).

[8] M. C. Bañuls, R. Blatt, J. Catani, A. Celi, J. I. Cirac, M. Dalmonte, L. Fallani, K. Jansen, M. Lewenstein, S. Montangero, C. A. Muschik, B. Reznik, E. Rico, L. Tagliacozzo, K. V. Acoleyen, F. Verstraete, U. J. Wiese, M. Wingate, J. Zakrzewski, and P. Zoller, *Simulating Lattice Gauge Theories within Quantum Technologies*, The European Physical Journal, D vol. 74, no. 165 (2020).

[9] J. Bender, E. Zohar, A. Farace, and J. I. Cirac, *Digital quantum simulation of lattice gauge theories in three spatial dimensions*, New Journal of Physics, vol. 20, no. 9, p. 093001 (2018).

[10] A. Bermudez, L. Mazza, M. Rizzi, N. Goldman and M. Lewenstein, *Wilson fermions and axion electrodynamics in Optical Lattices*, Phys.Rev. Lett., vol. 105, p.190404 (2010).

[11] M. Blagojević and F. W. Hehl, *Gauge theories of gravitation*, World Scientific Publishing Co Pte Ltd (2013).

[12] C. Borgs and E. Seiler, *Lattice Yang-Mills theory at nonzero temperature and the confinement problem*, Comm. Math. Phys., vol. 91, 329–380 (1983).

[13] C. Borgs, *Confinement, deconfinement and freezing in lattice Yang-Mills theories with continuous time*, Comm. Math. Phys., vol. 116, 309-342 (1988).

[14] R. Brower, S. Chandrasekharan, U.-J. Wiese, *QCD as a quantum link model*, Phys. Rev. D 60, 094502 (1999).

[15] H. P. Büchler, M. Hermele, S. D. Huber, Matthew P. A. Fisher and P. Zoller, *Atomic quantum simulator for lattice gauge theories and ring exchange models*, Phys. Rev. Lett., vol. 95, p. 040402 (2005).

[16] T. Byrnes and Y. Yamamoto, *Simulating lattice gauge theories on a quantum computer*, Phys. Rev. A, vol 73, p. 022328 (2006).

[17] S. Chandrasekharan and U.-J. Wiese, *Quantum link models: A discrete approach to gauge theories*, Nuclear Physics B, vol. 492, pp. 455–471 (1997).

[18] A. Childs, *Lecture notes on quantum algorithms* (2017). [Online] Available: https://www.cs.umd.edu/ amchilds/qa/

[19] M. Creutz, *Quarks, gluons and lattices*, Cambridge Univ. Press (1985).

[20] M. Creutz, L. Jacobs, and C. Rebbi, *Monte Carlo computations in lattice gauge theories*, Physics Reports, vol. 95, no. 4, 201 – 282, (1983). [Online] Available: http://www.sciencedirect.com/science/article/pii/0370157383900169

[21] X. Cui, Y. Shi and J.-C. Yang, *Circuit-based digital adiabatic quantum simulation and pseudoquantum simulation as new approaches to lattice gauge theory*, J. High Energ. Phys. 2020, 160 (2020).

[22] M. C. Diamantini, C.A. Trugenberger and V.M. Vinokur, *Quantum magnetic monopole condensate* (2020). [Online] Available: https://arxiv.org/abs/2007.02356

[23] E. Ercolessi, P. Facchi, G. Magnifico, S. Pascazio, and F. Pepe, *Phase Transitions in Zn Gauge Models: Towards Quantum Simulations of the Schwinger-Weyl QED*, Physical Review D, vol. 98 (2018).

[24] R. P. Feynman, *Simulating physics with computers* Int. J. Theor. Phys., vol. 21, pp. 467–488 (1982).

[25] C. Fitzgerald, *Cayley graphs and representation theory* (2015). [Online]. Available: https://osf.io/d24js/

[26] E. Fradkin, S. H. Schenker, *Phase diagrams of lattice gauge theories with Higgs fields*, Phys. Rev. D, vol. 19, n.12 (1979).

[27] E. Fradkin, *General field theory* (2020). [Online] Available: http://eduardo.physics.illinois.edu/homepage/

[28] E. Fradkin, *Advanced field theory* (2020). [Online] Available: http://eduardo.physics.illinois.edu/homepage/

[29] E. Fradkin, *Field theories of condensed matter physics*, Cambridge University Press (2013).

[30] E. Fradkin and D. Susskind, *Order and disorder in gauge systems and magnets*, Phys. Rev. D 17, 2637 (1978).

[31] W. Fulton and J. Harris, *Representation Theory*, Springer (2004).

[32] C. Gattringer and C. B. Lang, *Quantum chromodynamics on the lattice*, Springer (2010).

[33] J. Greensite, *The confinement problem in lattice gauge theory* Progress in Particle and Nuclear Physics, vol. 51, no. 1, p. 1–83, Jan 2003. [Online]. Available: http://dx.doi.org/10.1016/S0146-6410(03)90012-3

[34] L. R. Hales, *The Quantum Fourier Transform and Extensions of the Abelian Hidden Subgroup Problem*, PhD Thesis, University of California, Berkeley. [Online] Available: https://arxiv.org/abs/quant-ph/0212002.

[35] P. Hauke, O. Tieleman, A. Celi, C. Ölschläger, J. Simonet, J. Struck, M-Weinberg, P. Windpassinger, K. Sengstock, M. Lewenstein and André Eckardt, *Non-Abelian gauge fields and topological insulators in shaken optical lattices*, Phys. Rev. Lett., vol. 109, p. 145301 (2012).

[36] S. Helgason, *Groups and geometric analysis*, American Mathematical Society (2000).

[37] M. Henneaux and C. Teitelboim, *Quantization of gauge systems*, Princeton University Press (1992).

[38] G. 't Hooft. *On the phase transition towards permanent quark confinement*. Nucl. Phys. B, vol.138, is.1, pp.1-25 (1978).

[39] D. Horn, M. Weinstein, and S. Yankielowicz. *Hamiltonian approach to Z (N) lattice gauge theories*, Phys. Rev. D 19, 3715–3731 (1979).

[40] P. Høyer, *Efficient quantum Fourier transforms* (1997). [Online] Available arXiv:quant-ph/9702028

[41] A.C. Irving, J.F. Owens(Florida State U.), C.J. Hamer*Compact U(1) in 2+1 dimensions: The finite-lattice Hamiltonian approach*, Phys. Rev. D, vol. 28, p. 2059 (1983).

[42] T. Johnson, S. Clark, and D. Jaksch. *What is a quantum simulator?*, EPJ Quantum Technology, 1 (2014).

[43] S. P. Jordan, Keith S. M. Lee and John Preskill, *Quantum algorithms for quantum field theories*, Science 336, 1130-1133 (2012).

[44] A. Y. Kitaev, *Fault tolerant quantum computation by anyons*, Annals Phys., vol. 303, p. 2 (2003).

[45] A. W. Knapp, *Lie Groups: Beyond an Introduction*, Boston: Birkhäuser, 1996.

[46] J. B. Kogut, *An introduction to lattice gauge theory and spin systems*, Rev. Mod. Phys., vol. 51, pp. 659–713 (1979).

[47] J. Kogut and L. Susskind, *Hamiltonian formulation of Wilson's lattice gauge theories* Phys. Rev. D, vol. 11, pp. 395–408 (1975).

[48] H. Lamm, S. Lawrence and Y. Yamauchi, *General methods for digital quantum simulation of gauge theories*, Phys. Rev. D, vol. 100, p. 034518 (2019).

[49] N.E. Ligterink, N.R. Walet, R.F. Bishop, *Towards a Many-Body Treatment of Hamiltonian Lattice SU(N) Gauge Theory*, Annals Phys., 284, 215-262 (2000).

[50] S. Lloyd, *Universal quantum simulators*, Science, vol. 273, issue 5278, pp. 1073-1078 (1996).

[51] G. Magnifico, *Quantum Simulation of (1 + 1)D QED via a Zn Lattice Gauge Theory*, Master thesis, Università di Bologna (2015).

[52] A. Mariani, *Finite-group Yang-Mills lattice gauge theories in the Hamiltonian formalism*, Master Thesis, Università di Bologna (2020).

[53] A. Maroncelli, *QED and Abelian lattice gauge theories in 2 + 1 dimensions*, Master thesis, Università di Bologna (2019).

[54] E. A. Martinez, C. A. Muschik, P. Schindler, D. Nigg, A. Erhard, M. Heyl, P. Hauke, M. Dalmonte, T. Monz, P. Zoller, and et al., *Real-time dynamics of lattice gauge theories with a few-qubit quantum computer* Nature, vol. 534, no. 7608, 516–519 (2016).

[55] A. Messiah, *Quantum Mechanics, Vol. II*, North-Holland Publishing Company (1962).

[56] A. Mezzacapo, E. Rico, C. Sabín, I.L. Egusquiza and L. Lamata, *Non-abelian SU(2) lattice gauge theories in superconducting circuits*, Phys. Rev. Lett., vol. 115, p. 240502 (2015).

[57] A. Milsted and T. J. Osborne, *Quantum Yang-Mills theory: An overview of a program*, vol. 98, Phys. Rev. D1, Jul 2018. [Online] Available: http://dx.doi.org/10.1103/PhysRevD.98.014505

[58] I. Monvay and G. Münster, *Quantum fields on a lattice*, Cambridge University Press (1994).

[59] C. Moore, *Generic quantum Fourier transforms*, SODA '04: Proceedings of the fifteenth annual ACM-SIAM symposium on Discrete algorithms-January, pp. 778–787 (2004)

[60] G. Münster, *On the Characterization of the Higgs Phase in Lattice Gauge Theories*, Zeitschrift für Physik C Particles and Fields, vol. 6, pp. 175–185 (1980).

[61] M. A. Nielsen and I. L. Chuang, *Quantum computation and quantum information*, Cambridge University Press (2010).

[62] H. Nielsen and M. Ninomiya. *A no-go theorem for regularizing chiral fermions*. In: Physics Letters B 105.2, pp. 219–223 (1981).

[63] S. Notarnicola, E. Ercolessi, P. Facchi, G. Marmo, S. Pascazio, and F. Pepe, *Discrete Abelian gauge theories for quantum simulations of QED* Journal of Physics A, vol. 48 (2015).

[64] G. Ortiz, J.E. Gubernatis, E. Knill and R. Laflamme, *Quantum algorithms for fermionic simulations*, Phys. Rev. A, vol. 64, p. 022319 (2001).

[65] M. Peskin and D. V. Schroeder, *An introduction to quantum field theory*, Westview Press (1993).

[66] A. M. Polyakov, *Gauge fields and strings*, Harwood-Academic Publishers (1987).

[67] A. M. Polyakov, *Compact gauge fields and the infrared catastrophe*, Physics Letters B vol. 59, issue 1, pp. 82-84 (1975).

[68] A.M. Polyakov, *Quark confinement and topology of gauge theories*, Nuclear Physics B vol. 120, issue 3, pp. 429-458 (1977).

[69] J. Preskill, *Quantum computing in the NISQ era and beyond*, Quantum 2, 79 (2018).

[70] M. Püschel, M. Roettler and T. Beth, *Fast quantum Fourier transforms for a class of non-abelian groups*, Proceedings 13th International Symposium on Applied Algebra, Algebraic Algorithms and Error-Correcting Codes (AAECC'99), Honolulu, Hawaii, Springer LNCS, pp. 148-159 (1999).

[71] J. Quaintance and J. Gallier *Differential geometry and Lie groups*, Springer (2020).

[72] F. Rennecke, *The chiral phase transition of QCD* (2015). [Online] Available: https://www.researchgate.net/publication/280846230 _The_Chiral_Phase_Transition_of_QCD.

[73] H. J. Rothe, *Lattice gauge theories: an introduction*, World Scientific Publishing Co Pte Ltd (2012).

[74] W. Rudin, *Fourier analysis on groups*, Wiley-Interscience, (1990).

[75] S. Sachdev, *Quantum phase transitions*, Cambridge University Press (1999).

[76] B. Simon, *Representation theory of finite and compact Lie groups*, American Mathematical Society (1995).

[77] A. Smith, M. S. Kim, F. Pollmann and J. Knolle, *Simulating quantum many-body dynamics on a current digital quantum computer*, npj Quantum Information, vol.5, n. 106 (2019).

[78] R. Somma, G. Ortiz, J. E. Gubernatis, E. Knill and R. Laflamme, *Simulating physical phenomena by quantum networks*, Phys. Rev. A, vol. 65, p. 042323 (2002).

[79] M. Sugiura, *Fourier series of smooth functions on compact Lie groups*, Osaka J. Math., vol. 8, no. 1, 33-47 (1971).

[80] L. Susskind, *Lattice fermions*, Phys. Rev. D16, 3031–3039 (1977).

[81] F. Tacchino, A. Chiesa, S. Carretta and D. Gerace, *Quantum computers as universal quantum simulators: state of art and perspectives*, Advanced Quantum Technologies 3, 1900052 (2020).

[82] L. Tagliacozzo and G. Vidal. *Entanglement renormalization and gauge symmetry*, Physical Review B 83, p. 115127 (2011).

[83] T. Tao, *The Peter-Weyl theorem, and non-abelian Fourier analysis on compact groups*, (2011). [Online]. Available: https://terrytao.wordpress.com/2011/01/23/the-peter-weyl-theorem-and- non-abelian-fourier-analysis-on-compact-groups

[84] A. Terras, *Fourier analysis on finite groups and applications*, Cambridge University Press (1999).

[85] A. Terras, *Harmonic analysis on symmetric spaces and applications /*, Springer (1984).

[86] D. Tong, *Gauge theory* 2018. [Online]. Available: http://www.damtp.cam.ac.uk/user/tong/gaugetheory.html

[87] M. Troyer, U.-J. Wiese, *Computational complexity and fundamental limitations to fermionic quantum Monte Carlo simulations*, Phys. Rev. Lett. 94 170201 (2004).

[88] A. Turing, *Finite Approximations to Lie Groups*, Annals of Mathematics, vol. 39, pp. 105–111 (1938).

[89] F. J. Wegner, *Duality in generalized Ising models and phase transitions without local order parameters*, Journal of Mathematical Physics, vol. 12, no. 10, pp. 2259–2272 (1971).

[90] K. G. Wilson, *Confinement of Quarks*, Phys. Rev. D, vol. 10, p. 2445 (1974).

[91] C. N. Yang and R. L. Mills *Conservation of Isotopic Spin and Isotopic Gauge Invariance*, Phys. Rev. vol. 96, p. 191 (1954).

[92] M. Zhuang, J. Huang, Y. Ke, and C. Lee, *Symmetry-protected quantum adiabatic evolution in spontaneous symmetry breaking transitions*, Ann. Phys., vol. 532, p. 1900471 (2020).

[93] E. Zohar, J. I. Cirac and B. Reznik, *Quantum simulations of gauge theories with ultra-cold atoms: local gauge invariance from angular momentum conservation*, Phys. Rev. A, vol. 88, p. 023617 (2013).

[94] E. Zohar, J. I. Cirac and B. Reznik, *Simulating compact quantum electrodynamics with ultracold atoms: Probing Confinement and Nonperturbative Effects* Phys. Rev. Lett., 109, 125302 (2012).